PHOTOCHEMISTRY OF THE CHLOROPENTAKIS(ALKYLAMINE)CHROMIUM(III) COMPLEXES

by

CARL WONG

B.Sc., University of Victoria, 1971

A THESIS SUBMITTED IN PARTIAL FULFILLMENT
OF THE REQUIREMENTS FOR THE DEGREE OF

MASTER OF SCIENCE

in the Department

of

Chemistry

ACCEPTED
FACULTY OF GRADUATE STUDIES

[redacted]

DEAN

DATE 7 Sept/73

We accept this thesis as conforming
to the required standard

[redacted]

UNIVERSITY OF VICTORIA

August 1973

Supervisor: Professor A. D. Kirk.

Abstract

The photochemistry of the series of complexes $Cr(RNH_2)_5Cl^{2+}$, R= H, CH_3, CH_3CH_2, $CH_3(CH_2)_2$, $CH_3(CH_2)_3$, has been investigated in water and acetone-based acidic solutions at various temperatures and irradiating wavelengths.

For photolysis in water and in 33 w/w % acetone/water, photoaquation of amine to give predominantly cis-$Cr(RNH_2)_4(H_2O)Cl^{2+}$ (estimated >90% cis) was found to be the predominant reaction mode for all the alkylamine complexes. The quantum yields (Φ) are practically solvent independent (R= H, Me and Et) and, in 33% acetone/water, 20°C, pH 3 and 565 nm, they are 0.41_4 (NH_3), 0.39_3 ($MeNH_2$), 0.24_8 ($EtNH_2$), 0.21_2 (n-$PrNH_2$) and 0.17_6 (n-$BuNH_2$). Slight wavelength and temperature dependences were observed for the amine quantum yields. Apparent activation energies, obtained by an Arrhenius-type treatment of Φ_{amine} are generally about 1.5 kcal/mole.

Photolysis of $Cr(MeNH_2)_5Cl^{2+}$ in practically 100% acetone yielded $Cr(MeNH_2)_4(S)Cl^{2+}$, where S is a solvent molecule. The extent of substitution by acetone, or whether this occurred at all, was not unambiguously established, but the product is predominantly in the cis-configuration. The quantum yield at 565 nm, 20°C was found to be 0.4_1.

The quantum yields for photoaquation of chloride were determined in water and/or in 33% acetone/water at 13°C. The upper limits at 565 nm (less than 10^{-3} for all the complexes) are much

smaller than those reported earlier for $Cr(NH_3)_5Cl^{2+}$. At 401 nm, the quantum yields are generally larger and show a substantial decrease upon changing the solvent from water to 33% acetone/water.

The results are discussed in terms of the empirical observations and proposals made by earlier workers.

It is noted that the photochemical results of $Cr(MeNH_2)_5Cl^{2+}$ in practically 100% acetone are consistent with substitution of the strong field ligand on the weak field axis and thus represent an extension of the validity of Adamson's rules, which were proposed for photoreactions in water.

Treatment of the temperature dependence of Φ_{amine} assuming that reaction occurs from the lowest excited quartet and Chen's proposals that essentially all excited states are deactivated either through chemical reaction or internal conversion ($^4T_2 \longrightarrow {}^4A_2$), gave the difference between the activation energies of these two processes, $E_r - E_{ic}$. For all the $Cr(RNH_2)_5Cl^{2+}$ ions, $E_r - E_{ic}$ is about 2 kcal/mole. E_r is apparently positive and thus suggests that reaction occurs via an activated intermediate.

For the series of complexes, the trend of Φ_{amine} is consistent with Adamson's proposal that Φ should vary as the average ligand field strength. Following Chen's proposals, the observed trend of Φ_{amine} was also rationalized in terms of the competition between internal conversion and chemical reaction as the dominant deactivation processes for the eventual deactivation of both the quartet and doublet states.

A comparison of the magnitude of the chloride quantum yields with the Co(III) systems (where photoreduction of Co(III) to Co(II)

apparently occurs via charge transfer states) indicates that the smaller quantum yields found for the series of complexes are more reasonable than those reported earlier for $Cr(NH_3)_5Cl^{2+}$ and give support to the earlier suggestion that chloride aquation occurs through charge transfer states. The solvent dependence of Φ_{Cl^-} is rationalized in terms of the ability of the solvent molecules to effectively solvate the chloride in the excited molecule.

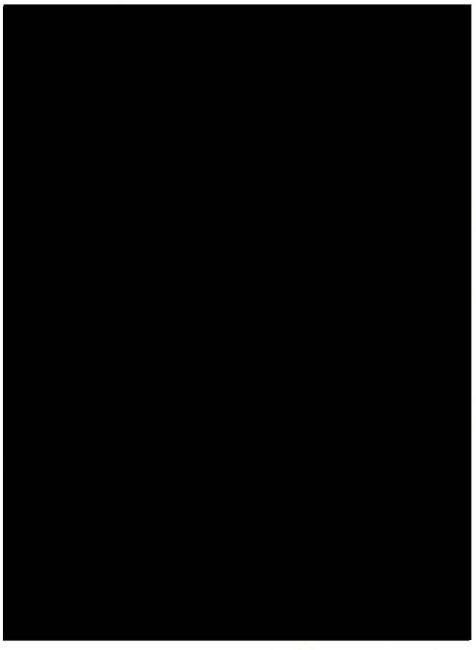

TABLE OF CONTENTS

Page

Page

Page

LIST OF TABLES

LIST OF FIGURES

Figure Page

ACKNOWLEDGEMENTS

The author wishes to express his sincere thanks to Dr. A. D. Kirk for advice, criticism and patient guidance throughout the course of this work.

To father

I. INTRODUCTION

The photosensitivity of transition metal complexes has long been known and some scattered studies date back more than a century. But although organic photochemistry has been thriving for some decades, serious investigations of photochemical reactions of transition metal complexes prior to 1960 are rare. However, the development of ligand field theory and subsequent advances in the understanding of the excited states and excited state deactivation processes of transition metal complexes has generated increased interest in transition metal photochemistry.

The photochemistry of many transition metal systems is difficult to study because their ground state chemistry is not well known and/or their spectroscopy is not well established; many other systems are impossible to study because of their thermal kinetic instability. These difficulties greatly reduce the number of systems suitable for study and only the chromium(III), cobalt(III) and platinum(II) systems have up to now received extensive investigations.

The photochemistry of chromium(III) complexes is perhaps the best understood, but even for these systems understanding is far from complete. Much of the earlier data has been phenomenological and more systematic studies-- and these are important--are just becoming common. Also, better understanding of some aspects of the photochemical reactions must necessarily await further theoretical and/or

experimental developments concerning the various deactivation processes of excited states.

Much of the understanding of Cr(III) photochemistry has been developed through the consideration of the bonding and spectroscopy of Cr(III) complexes as well as the study of the photoreactions. These important aspects, together with some of the more recent developments in the photochemistry of Cr(III) complexes will be briefly considered in the following sections. More detailed discussions may be found in the references cited.

A. Bonding

A large number of Cr(III) hexacoordinate complexes have been prepared, most of these having approximate octahedral symmetry. Figure 1 shows the molecular orbital energy level diagram for the simplest case of an octahedral (O_h) complex with six identical ligands which are capable only of σ-bonding. The orbitals of appropriate symmetry for σ-bonding are the $3d_{z^2}$, $3d_{x^2-y^2}$, 4s and $4p^3$. The t_{2g} set of atomic orbitals, consisting of the d_{xy}, d_{xz} and d_{yz}, are so oriented that only π-bonding is possible so that, for this particular case, they are non-bonding. The energy difference between the t_{2g} and e_g^* orbitals is known as the ligand field parameter Δ (or 10 Dq).

When π-bonding ligands are present π-interaction results in a splitting of the energies of the t_{2g} set. Depending on the orientation and number of π-bonding ligands, one or more of the t_{2g} orbitals may be split into a bonding/antibonding pair. In the case of π-donating ligands, the antibonding orbitals will be centered on the metal and the effect of the π-interaction is to destabilize the t_{2g} orbitals involved,

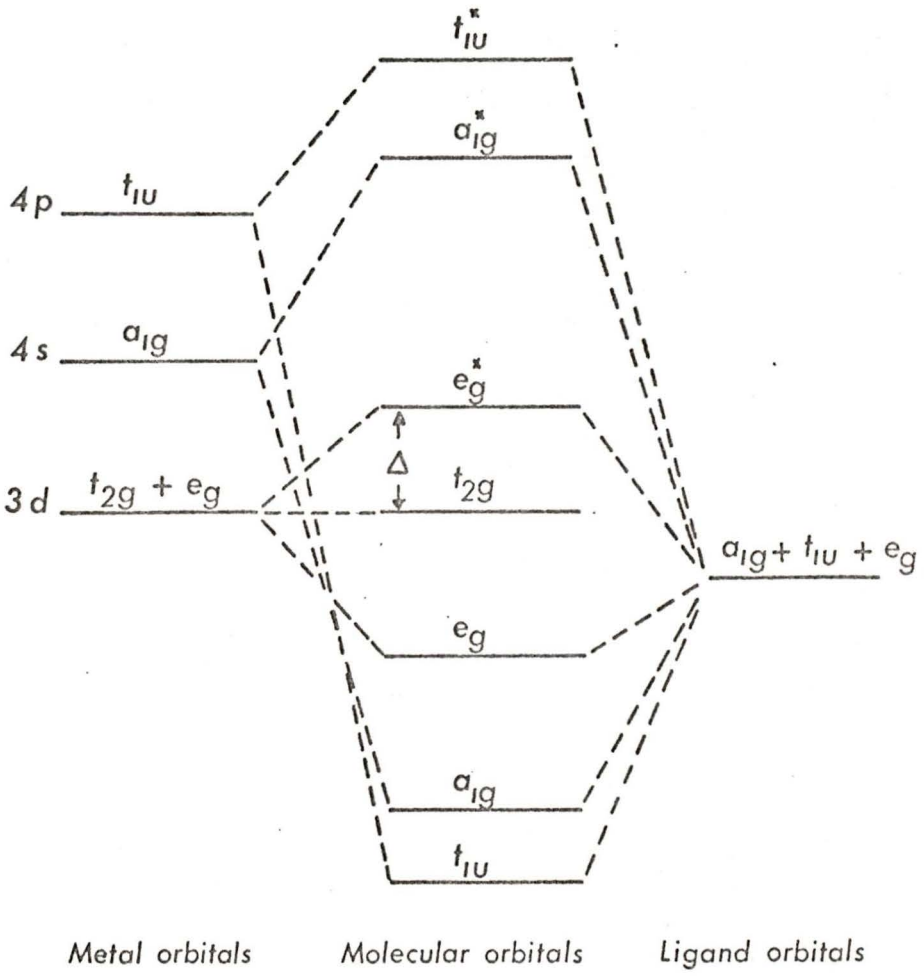

Figure 1. Molecular orbital energy level diagram for an octahedral complex containing ligands which have orbitals available only for σ-bonding.

thus lowering the value of Δ. On the other hand, π-acceptor ligands will tend to lower the electron density of the t_{2g} orbitals, thus lowering the energy of this set and increasing the value of Δ where all three t_{2g} orbitals interact with π-acceptor ligands; where only one π-acceptor ligand is present, one of the t_{2g} orbitals (d_{xy} if the ligand is on the z-axis) does not interact with this ligand, and the energy of this orbital is not lowered so that the value of Δ is not affected. When both π-donor and π-acceptor ligands are present in the same molecule, the net effect depends on the competition between the interaction of the two types of ligand π-orbitals with the t_{2g} metal orbitals. The magnitude of Δ thus depends on both the σ and π-bonding abilities of the ligands.

In complexes where more than one type of ligand is present, the ligand field is not strictly octahedral and the energies of the metal-centered e_g^* levels are split. In a complex $Cr(A)_5X^{n+}$ where X is a weaker field ligand than A, for example, the splitting would result in the d_{z^2} being lower in energy than the $d_{x^2-y^2}$ (the A-Cr-X axis being taken to be the z-axis). More detailed discussions on the energy level splitting in non-cubic ions are given in Ref. 1.

B. Electronic States and Spectroscopy of Cr(III) Complexes

Chromium(III) belongs to the d^3 electronic configuration and the energy levels of its complexes have been intensively investigated both theoretically and experimentally[2]. The simplified Tanabe-Sugano term diagram (Figure 2) for the d^3 configuration in O_h symmetry shows the splitting and changes in energy of the Russell-Saunders terms due to the ligand field[3]; for Cr(III) octahedral complexes of average ligand

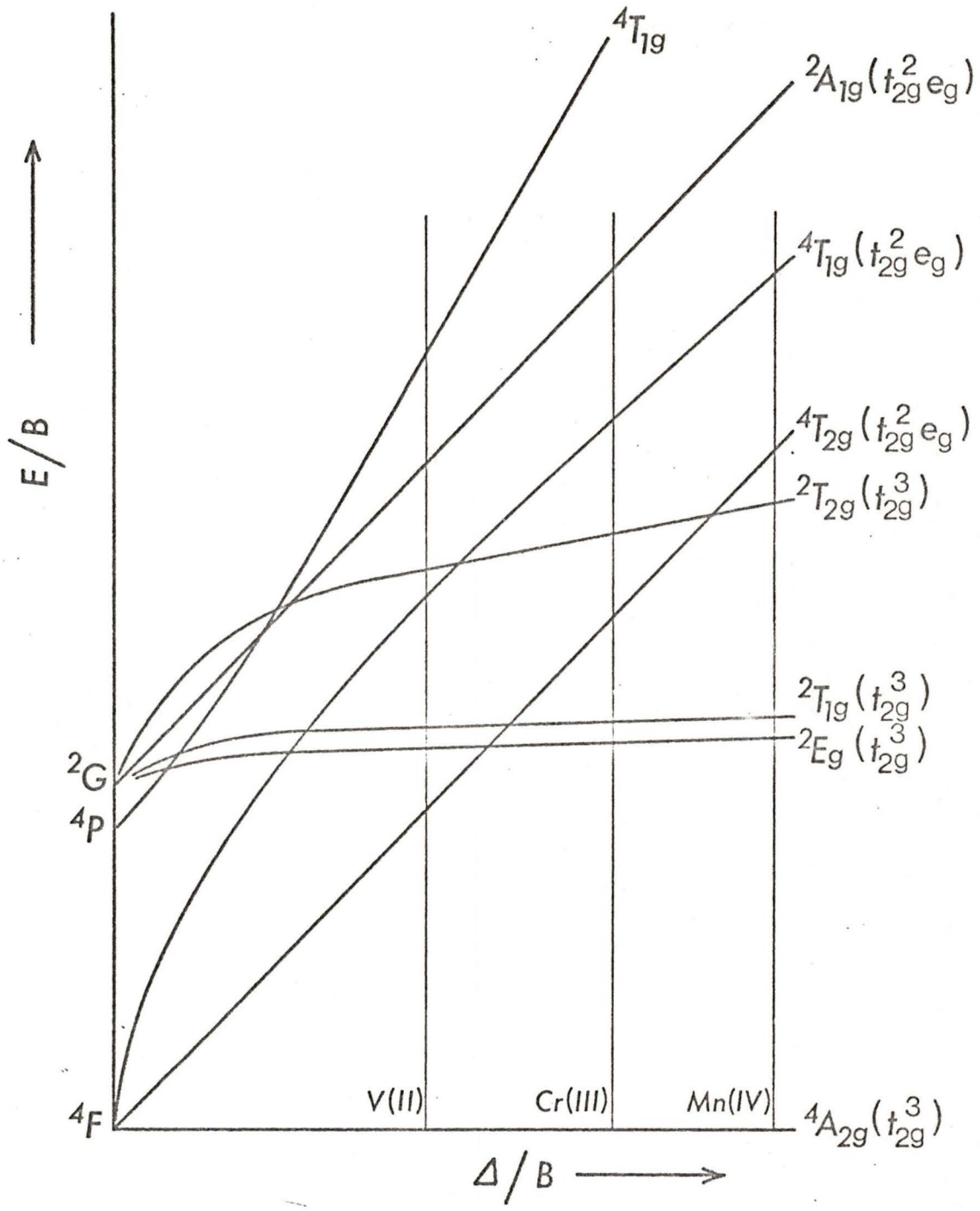

Figure 2. A simplified Tanabe-Sugano term diagram for the d^3 configuration in octahedral field.

field, the ordering of states is as designated in the figure. When the symmetry is lowered to C_{4v} (e.g. $[Cr(A)_5X]^{n+}$, trans-$[Cr(A)_4XY]^{n+}$), D_{4h} (e.g. trans-$[Cr(A)_4X_2]^{n+}$) or C_{2v} (e.g. cis-$[Cr(A)_4XY]^{n+}$), the degeneracy of some of the octahedral states is partially removed. For convenience, complexes of lowered symmetry are generally designated as non-O_h. Figure 3 shows the more important splittings for such complexes where X and Y are weaker field ligands than A.

Figure 4 is a typical uv-visible absorption spectrum for a Cr(III) complex having practically octahedral microsymmetry. The band marked D corresponds to the spin- and parity-forbidden transitions from the ground state $^4A_{2g}$ to the lowest doublet states ^2E_g and $^2T_{1g}$ and generally has an extinction coefficient of 0.1-1.0. (In pure octahedral field and in the absence of spin-orbit interactions, the ^2E_g and $^2T_{1g}$ are degenerate and for convenience are normally jointly designated as ^2E_g.) These transitions consist of spin-pairing of d electrons within the non-bonding t_{2g} sub-shell so that these doublets must have almost the same metal-ligand bond distances as the ground state (as depicted in Figure 5). Where it is observed, the absorption is very sharp and usually shows vibrational structure. The energy difference between the ^2E_g and $^4A_{2g}$ is fairly independent of the ligand field parameter Δ; thus the band energy is relatively insensitive to the type of ligands around the central atom, although some dependence on the π-bonding character of the ligands has been noted[4].

The bands marked Q_1 and Q_2 correspond to the parity-forbidden transitions from the $^4A_{2g}$ to the excited states $^4T_{2g}$ and $^4T_{1g}$ (F) respectively. These transitions involve electron promotion from the t_{2g} to the e_g^* antibonding orbitals so that the metal-ligand equilibrium

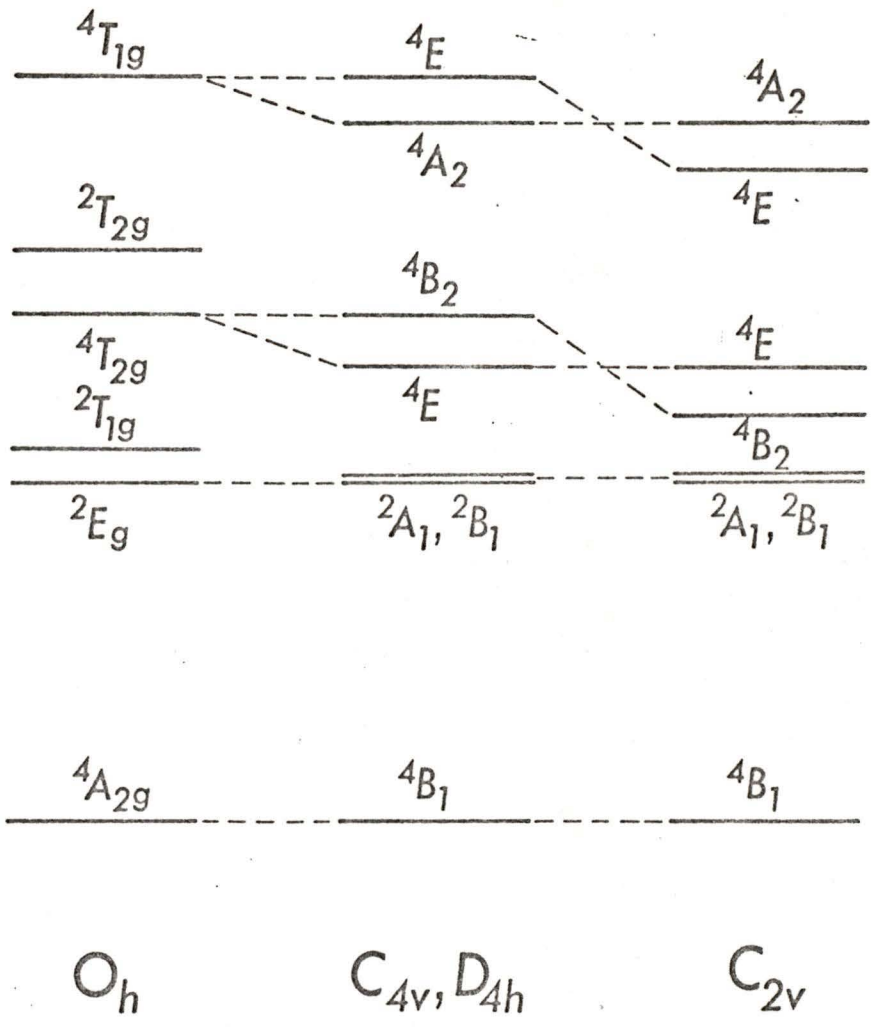

Figure 3. Schematic diagram showing the more important splittings of the octahedral states in fields of lower symmetry.

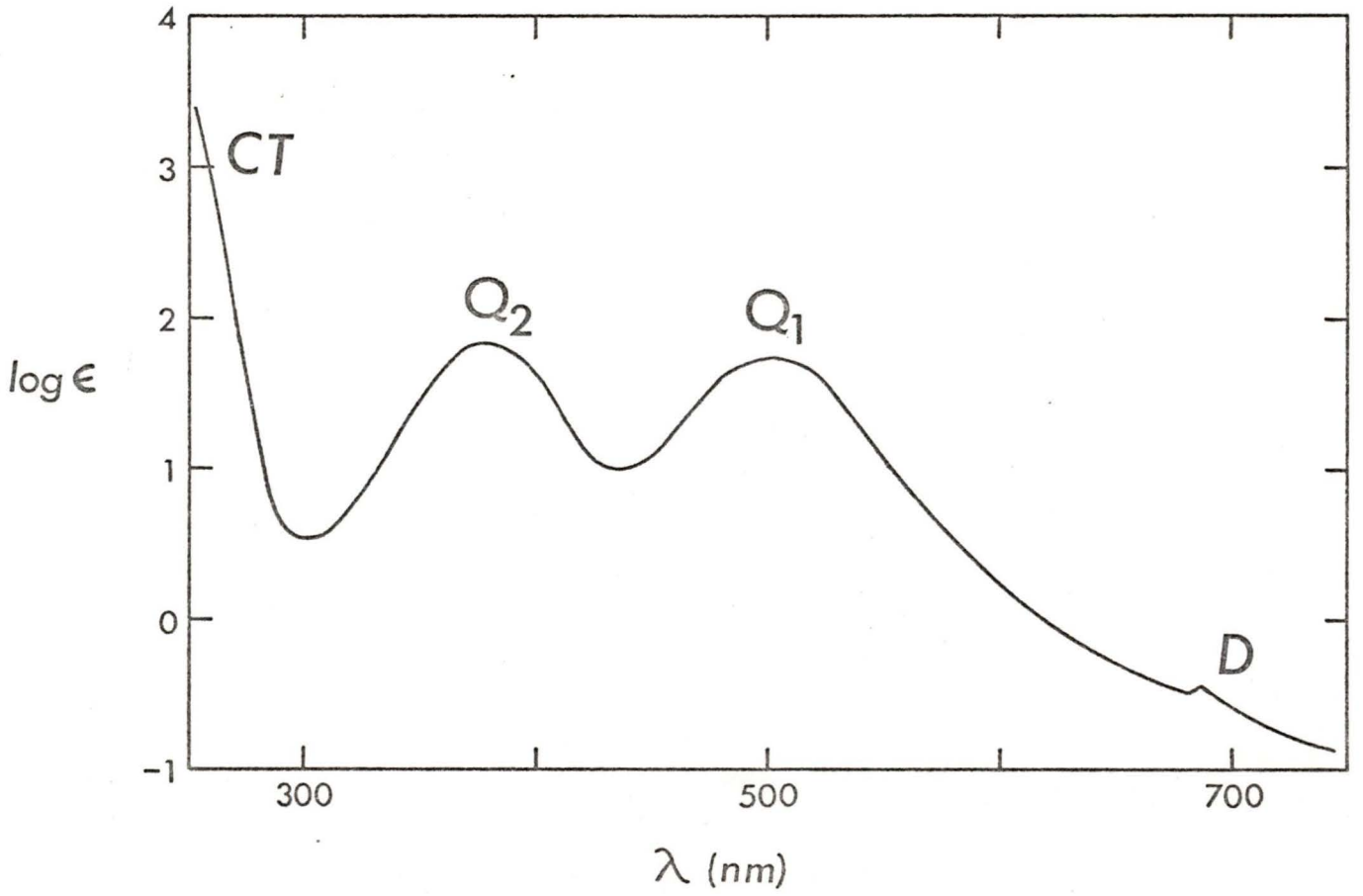

Figure 4. A typical absorption spectrum of a Cr(III) complex having practically octahedral microsymmetry.

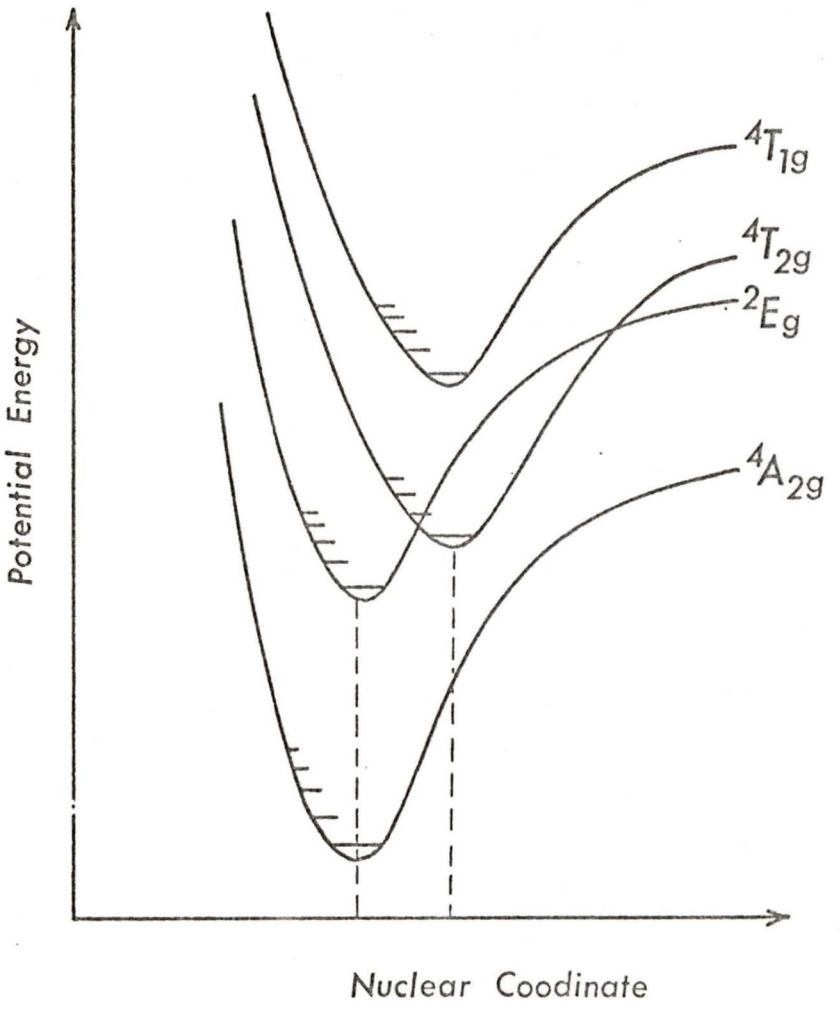

Figure 5. Schematic representation of the potential surfaces of the ground and lowest excited states of octahedral Cr(III) complexes showing the relative metal-ligand internuclear distances.

distances are expected to be larger in the excited states than in the ground state (as shown in Figure 5). Franck-Condon transitions (see Appendix A) thus lead to high vibrational levels of the excited states and the corresponding absorption bands are broad and structureless. The spectral positions of the quartet-quartet bands are expected to depend on the type of ligands since promotion of the electron from the t_{2g} to e_g^* involves the ligand field parameter Δ.

The optical assignment of the low lying ligand field states of O_h complexes is considerably easier than in complexes of lower symmetry. For these latter, the energy splittings are often small and for most complexes, the absorption bands show little or no splitting. Examination of polarized spectra has been generally helpful and where the axial ligands (D_{4h} and C_{4v}) are of lower ligand field strength, as for most of the complexes studied, the assignments are as shown in Figure 3.

The intense band at short wavelengths (Figure 4) is usually a ligand-to-metal charge transfer band. This band, together with other charge transfer bands and internal ligand bands, usually obscures any other d-d bands which might otherwise be observable at short wavelengths.

The luminescence of Cr(III) complexes in low temperature rigid media has been thoroughly studied. Most of these complexes show a phosphorescent emission ($^2E_g \longrightarrow {}^4A_{2g}$), usually with some vibrational structure, in the red part of the visible region. The emission occurs at about the same position as the corresponding absorption ($^2E_g \longrightarrow {}^4A_{2g}$) band, confirming the expectation that the two states have approximately the same geometry. The fluorescent emission ($^4T_{2g} \longrightarrow {}^4A_{2g}$), when

observed, is broad and considerably shifted to the red with respect to the corresponding absorption band, thus confirming that the $^4T_{2g}$ state is strongly distorted. (A correlation between the type of luminescence emission with the ligand field strength has been found[5].) The quantum yields of both emissions decrease as temperature is increased, especially when the glass point is reached, and generally no emission can be observed in aqueous media at room temperature. This inverse temperature dependence of both emission processes strongly suggests that the rates of the competing radiationless deactivation processes, k_3 and k_6 (Figure 6), increase with temperature.

C. Thermal Reactions in Aqueous Solution

The majority of mononuclear hexacoordinate complexes of Cr(III) are moderately kinetically stable, generally having half-lives of several hours in acidic media at room temperature. The thermal reactions are of four general types: solvolysis, ligand substitution, isomerization and racemization. The mechanism of solvolysis and ligand substitution reactions are generally thought to be dissociative[6]. Where the stereochemistry is observable, these reactions generally occur with retention of geometric configuration, for example[7]

$$\underline{cis}\text{-}Cr(NH_3)_4(H_2O)Cl^{2+} + H_2O \longrightarrow \underline{cis}\text{-}Cr(NH_3)_4(H_2O)_2^{3+} + Cl^- \quad (1)$$

$$\underline{trans}\text{-}Cr(NH_3)_4XY^{n+} + H_2O \longrightarrow \underline{trans}\text{-}Cr(NH_3)_4(H_2O)X^{m+} + Y \quad (2)$$

for XY = $(H_2O)Cl$, Cl_2, ClBr. In contrast to the mechanism suggested by experimental observations, a comparison between the observed activation energies and calculated crystal field stabilization energies led to the

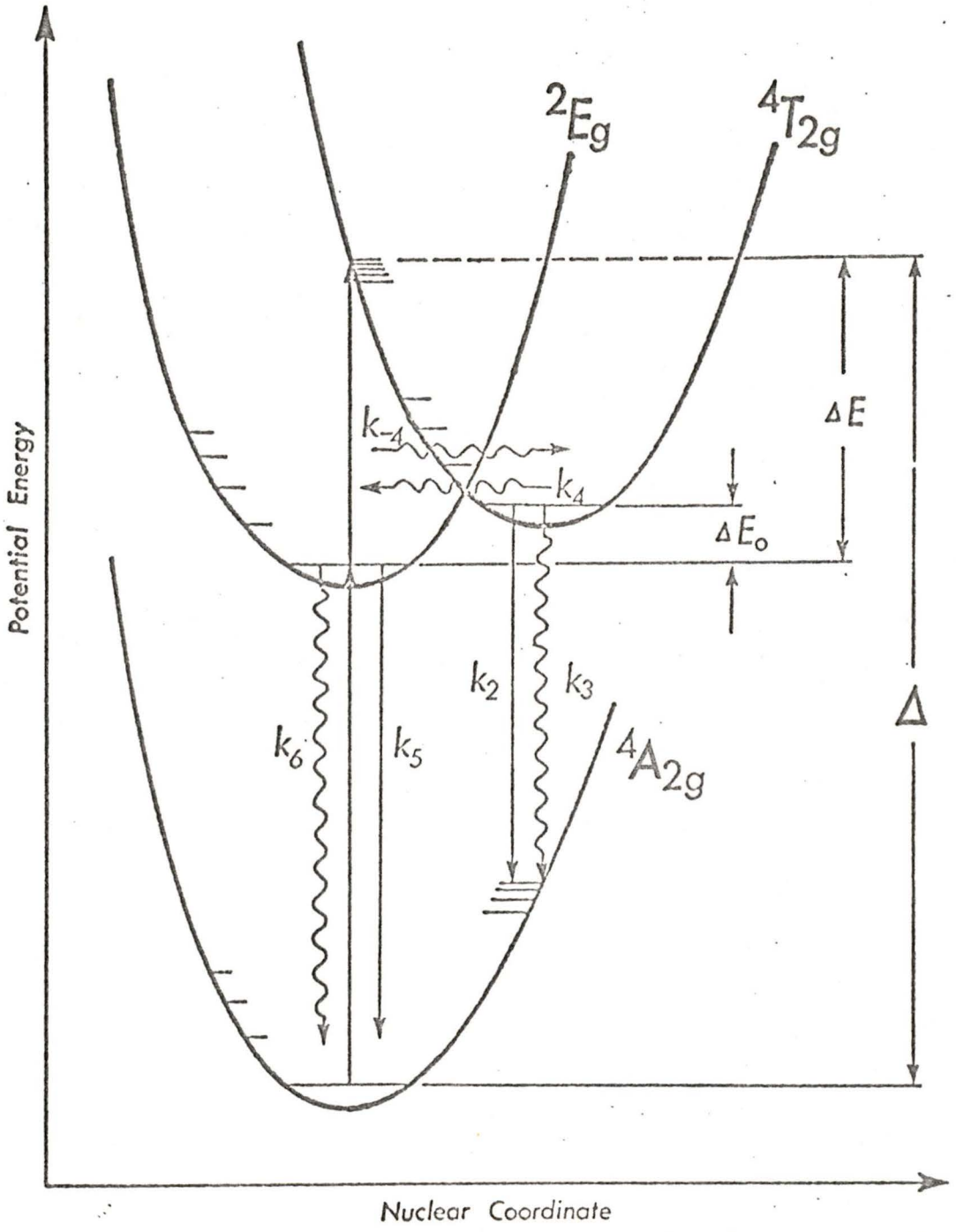

Figure 6. Schematic diagram of the radiative (⟶) and non-radiative (⇝) processes which are of interest in the photochemical behaviour of Cr(III) complexes. The rate constants shown are for radiative transition of $^4T_{2g}$ to the ground state, k_2; internal conversion of $^4T_{2g}$ to $^4A_{2g}$, k_3; intersystem crossing of $^4T_{2g}$ to ^2E_g, k_4; radiative transition of ^2E_g to $^4A_{2g}$, k_5; intersystem crossing of ^2E_g to $^4A_{2g}$, k_6; and return intersystem crossing of ^2E_g to $^4T_{2g}$, k_{-4}.

suggestion that the aquation reactions of Cr(III) complexes proceed via an intermediate of enhanced coordination number (associative mechanism)[8].

D. Photochemistry

1. General Observations

Most experiments in Cr(III) photochemistry have been carried out in aqueous media and for these, aquation has been the most common photochemical reaction, and in addition, it seems to be the only efficient photoreaction route. Reported inefficient photoracemizations[9, 10] and photoanation[11] are thus of secondary importance. Efficient photoisomerizations for such complexes as trans-$Cr(en)_2(H_2O)OH^{2+}$[12] and trans-$Cr(NH_3)_4(H_2O)Cl^{2+}$[13] are likely due to photoexchange of water with concurrent stereochemical change[14] (refer to later discussions on the mode and mechanism of photosubstitution).

Photochemical investigations in non-aqueous media are rare and as yet have received little attention. Some recent studies will be considered in Section I-E-2.

2. The Role of the Excited States in Photoreactions

Upon ligand field irradiation of a solution of a chromium(III) complex, the complex may be excited to the corresponding ligand field state (or a charge transfer state if the corresponding bands overlap). Very fast primary processes, internal conversion and intersystem crossing, both coupled with vibrational relaxation, are believed to quickly deactivate the initially populated ligand field state to the ground vibrational levels of the relatively long-lived lowest excited states of the quartet and doublet manifolds ($^4T_{2g}$ and

^2E_g in O_h symmetry). The processes leading to the subsequent deactivation of these states are schematically illustrated in Figure 6. Photochemical reaction might occur from the $^4T_{2g}$ and/or ^2E_g states.

The identification of the excited state(s) responsible for the photoreaction is central towards gaining an understanding of the photochemistry of Cr(III) complexes. The earlier proposal of the ^2E_g as the immediate precursor to reaction[15, 16] based on lifetime arguments, which suggest that the doublet is very much longer-lived than the quartet, was consistent with the nearly wavelength independence of the quantum yields for the O_h complexes (see for example, tables in Ref. 17 and 18). This proposal has been critically examined[19,20]. The wavelength independence of the quantum yields may be equally well explained on the basis of reverse intersystem crossing ($^4T_{2g} \longleftarrow {}^2E_g$) and subsequent reaction from the quartet. Direct evidence which would point to the ^2E_g as the direct precursor, such as that of increased quantum yield on direct excitation to the ^2E_g is difficult and has yet to be obtained.

On the basis of arguments which suggest that the lifetime of the lowest excited quartet may be much longer than had been previously believed, and indirect evidence from the analysis of the temperature dependence of phosphorescence and photoaquation of reineckate ion[19], Adamson proposed the lowest excited quartet ($^4T_{2g}$ in O_h symmetry) to be the photoreactive state. The direct participation of the lowest excited quartet in photoreaction was first shown by Chen and Porter[21] in their study of the quenching of the phosphorescence and aquation of reineckate ion with

$Cr(CN)_6^{3-}$. About half of the photoaquation was unquenchable and this portion was ascribed to direct reaction from the quartet prior to intersystem crossing to the doublet. The quenchable portion was considered to occur either by direct substitution of the doublet state or by thermal repopulation of the quartet followed by aquation; the second path was supported by the temperature dependence of the phosphorescence lifetime of reineckate ion.

Although recent similar results obtained for $Cr(phen)_3^{3+}$[9], $Cr(NH_3)_6^{3+}$[22] and $Cr(CN)_6^{3-}$[23] leave little doubt that the lowest quartet is the main reactive state for these complexes, the wavelength dependence of both the aquation mode and the quantum yields observed for many non-O_h complexes[18, 24] seems to require reaction from more than one excited state. Participation of charge transfer states on direct charge transfer excitation is clearly important[25,26] but because of lack of substantiation, their participation upon ligand field excitation has been questioned[18]. That a second excited quartet is also reactive has been suggested in the study of trans-$Cr(en)_2(NCS)Cl^+$ [24], where the $^4B_2$ state is presumably responsible for ethylenediamine aquation while the lowest quartet, ^4E, is responsible for Cl^- and NCS^- aquation. In addition, although direct evidence for reaction from the doublet has not been obtained, the wavelength dependence of the ratio of the quantum yields for NH_3 and NCS^- aquation for $Cr(NH_3)_5NCS^{2+}$[27], which led the authors to suggest that NCS^- aquation results from the doublet, makes it difficult to eliminate the possibility of reaction from doublet states. At least one of the lower doublet states is π-antibonding[28] and this state may promote aquation of the π-bonding ligand. That

the lowest excited state of a manifold need not be the only one (of that manifold) which may be reactive is suggested by the results of the trans-$Cr(en)_2(NCS)Cl^+$ study[24].

3. Photolysis Mode and Stereochemistry

The photochemical studies of O_h complexes can give no information on photolysis mode or stereochemistry since the primary photoreaction gives only one product. The studies of non-O_h complexes are much more interesting in this respect since more than one reaction mode is possible and the stereochemistry of the reactions becomes observable. Early studies indicated that frequently the predominant photochemical reaction is different from the thermal reaction.

Attempting to systemize the existing data, Adamson proposed the following rules for predicting the mode of aquation and the ligand field strength dependence of the quantum yield[19]:

"(1) Consider the six ligands to lie in pairs at the ends of three mutually perpendicular axes. That axis having the smallest average crystal field will be the one labilized, and the total quantum yield will be about that for an O_h complex of the same average field.

(2) If the labilized axis contains two different ligands, then the ligand of greater field strength preferentially aquates. This may be a type of trans effect.

(3) The discrimination implied by rules 1 and 2 will occur to a greater extent if it is the L_1 rather than the L_2 band that is irradiated."

(L_1 and L_2 correspond to the Q_1 and Q_2 bands discussed earlier.)

Stereochemical implications, namely that the main photoreaction should occur with retention of configuration, are later implied in the study of $Cr(NH_3)_5NCS^{2+}$[27] where the configuration of the $Cr(NH_3)_4(H_2O)NCS^{2+}$ product was apparently trans.

However, the photochemical studies of $Cr(NH_3)_5X^{2+}$(X=Cl,Br)[25, 26, 29] where the aquation products, $Cr(NH_3)_4(H_2O)X^{2+}$, were predominantly in the cis-configuration, indicated that if the stereochemistry was as suggested by Adamson[27], then aquation centered on the weakest-field axis was apparently not followed[18]. The photochemical results for cis- and trans-$Cr(en)_2Cl_2^{+}$[30], mainly ethylenediamine aquation (Φ=.12) for the cis-complex, and Cl^- aquation (Φ=.32) to yield cis-$Cr(en)_2(H_2O)Cl^{2+}$ (at least 70% cis) for the trans-complex, were consistent with aquation of the strong-field ligand on the weakest-field axis, but not consistent with either expectation for the relative quantum yields or the stereochemistry (at least for the trans-complex). On the latter point, Kirk has suggested that photoaquation occurs with stereochemical change and that the stereomobility may be interpreted as showing that the transition state was associative, with the water entering trans to the leaving ligand, in contrast to the dissociative nature of transition states in thermal reactions (see for example, Ref. 6). The photoinertness of trans-$Cr(cyclam)_2Cl_2^{+}$[31], where the constraining ligands which prevent stereochemical change also prevent reaction, is apparently consistent with Kirk's interpretation[14].

Assuming that stereomobility is a general phenomenon for the photoaquations, the predominance of the cis-products found for the

photolysis of $Cr(NH_3)_5X^{2+}$(X=Cl,Br)[25, 26, 29] may now be interpreted as being consistent with the preferential aquation of the strong field ligand on the weak field axis, but that aquation occurs with stereochemical change. In this view, the photochemical results reported by Adamson, et al, for $Cr(NH_3)_5NCS^{2+}$[27] are anomalous. However, a recent re-examination of $Cr(NH_3)_5NCS^{2+}$[32], which placed a lower limit of 95% for the predominance of the cis-product, removed this unique exception. Thus all the photochemical results cited to this point, and in addition, those of trans-$Cr(en)_2(NCS)Cl^{+}$[24] and trans-$Cr(NH_3)_4XY^{n+}$(XY=Cl_2, $(H_2O)Cl$, (NCS)Cl, $(H_2O)NCS$, $(H_2O)_2$)[13] are consistent with this new interpretation, and the extent to which stereochemical change occurs for the last series of complexes (generally close to 100%)[13] is consistent with the associative nature of the transition state[14].

The theoretical basis for the preferential labilization of the weakest field axis, first suggested by Adamson[19, 20], has been clarified by Linck[33] and is now generally accepted. The lowest excited quartet state, which is the main reactive one, involves an electron promotion to the e_g^* σ-antibonding levels, which are split in non-O_h symmetry so that the d_{z^2} (which, for most cases, is the weakest-field axis) is lower in energy than the $d_{x^2-y^2}$. The promoted electron thus occupies the d_{z^2} orbital and will labilize the z-axis. As experimental support for this σ-bonding theory, Linck has shown that the photolysis mode of trans-$Cr(en)_2F_2^{+}$ is mainly ethylenediamine aquation[33], consistent with the exceptional ordering of the σ-antibonding orbitals in this complex, where $d_{x^2-y^2}$ lies below d_{z^2}. (The reversal of the "normal" ordering of

the e_g^* orbitals occurs in this complex because of the good π-donating ability of fluoride which makes it a weak-field ligand despite its strong σ-donating ability.) Where the predictions of the labilized axis based on the σ-bonding ability and the ligand field strength differ, that based on σ-bonding is apparently superior.

Where the labilized axis contains two different ligands, the preferential aquation of the stronger-field ligand (or more appropriately, the stronger σ-bonding ligand) has recently been explained quantum mechanically by Zink[28]. The model used, however, implicitly assumes a dissociative mechanism for reaction and no attempt was made to consider medium effects. Some of Zink's assertions have been recently criticized by Linck and Wirth[34] and the success of Zink's model is questioned. The recent photochemical investigation of trans-$Cr(en)_2FCl^{+}$[34] showed that contrary to expectations (assuming F^- is stronger σ-bonding than Cl^-), the predominant photoreaction mode is Cl^- aquation, yielding both trans- (~10% at 3°C) as well as cis-$Cr(en)_2(H_2O)F^{2+}$. Chloride aquation clearly does not follow Adamson's second rule and Linck and Firth[34] have suggested the following order of groups in a rough order of photoaquation leaving ability:

$$NH_3 > H_2O > Cl^- \simeq NCS^- > F^-,$$
$$NH_3 > Br^- > F^-$$

Also presented was the alternative suggestion that the failure of observing F^- aquation may be due to the exceptional stability of the Cr-F bond. The strength of the Cr-ox bond has also been invoked to

explain the rather low quantum yield for oxalate aquation in $Cr(en)(ox)_2^-$[35].

The question of stereospecifity of photoaquations was also opened[34]. The authors argued that the determinations of the extent of isomer predominance for the reactions studied are subject to relatively large (5-10%) uncertainties and that these are large enough to make elimination of reaction through a five-coordinate trigonal bipyramidal intermediate difficult.

4. Relative Quantum Yield

The implication in Adamson's first rule of the dependence of the relative quantum yield on the ligand field strength of the labilized axis has been criticized on the basis that it is ambiguous[18, 35]. Although there are notable exceptions (for example $Cr(CN)_6^{3-}$[36] and $Cr(NH_3)_5H_2O^{3+}$[37] in addition to the photoinert complexes such as $Cr(phen)_3^{3+}$[9] and $Cr(cyclam)Cl_2^+$[31], the available data are generally consistent with the interpretation of this rule[35], that the total quantum yield for all reaction modes should vary as the average ligand field of the complex (see also Section I-E-2).

Of historical importance is that a similar rule for predicting the magnitude of the quantum yield, Φ, notably that Φ should increase with increasing ΔE (ΔE as illustrated in Figure 6), was considered by Edelson and Plane[37]. Since the zeroth vibrational level of the ^2E_g is relatively insensitive to the ligand field strength, ΔE generally varies as Δ, which in turn roughly varies as the average ligand strength. Thus the ΔE rule and Adamson's rule, as interpreted above, are roughly equivalent.

For illustration of the ΔE rule, Edelson and Plane[37] used the amine complexes shown below.

complex	Φ for amine release
$Cr(NH_3)_6^{3+}$	.29
$Cr(NH_3)_5H_2O^{3+}$	.17
$Cr(NH_3)_4(H_2O)_2^{3+}$	.15
$Cr(NH_3)_3(H_2O)_3^{3+}$	.02
$Cr(NH_3)_2(H_2O)_4^{3+}$	.002

Since NH_3 is stronger-field than H_2O, the amine complexes, as listed, are in order of decreasing ligand field strength, or equivalently, decreasing ΔE. Although the quantum yields are qualitatively consistent with the ΔE rule, the correlation suffers because, except for $Cr(NH_3)_4(H_2O)_2^{3+}$ (which is probably the cis-isomer since the trans-isomer had not been prepared), there is no isomer distinction for the other polyaquo-substituted complexes, and no attempt was made to consider water exchange. In view of the present empirical observations, water exchange is expected to be especially important for those complexes with water ligands on the same axis. As a further comment, $Cr(H_2O)_6^{3+}$, which would have the smallest ΔE, has a water exchange quantum yield of about 0.1[38]. The importance of considering all reaction modes has been emphasized in a similar attempt to correlate Φ using the series $[Cr(en)_{3-n}(ox)_n]^{(3-2n)+}$, n=0, 1, 2, 3[39].

Since much of the earlier quantum yield data is either incomplete and/or probably not too reliable, correlations should be made with critically chosen data (see Section I-E-2).

Theoretical verification of Adamson's rule is difficult and more reliable data are needed to test this rule, at least qualitatively.

E. Considerations in this Work

1. Thermal Reactions

The possibility of study of the photochemical reactions often hinges on the thermal stability of the complex(es). For the complexes chosen for this study, the chloropentakis(alkylamine)chromium(III) ions, $Cr(RNH_2)_5Cl^{2+}$ (R= proton, methyl, ethyl, n-propyl and n-butyl, hereafter abbreviated to H, Me, Et, n-Pr and n-Bu, respectively), the thermal chemistry has been reasonably well investigated[40, 41]. All the complexes thermally aquate chloride with pseudo first-order constants which are pH independent at pH<6. At 25°C, the least kinetically stable of these, $Cr(NH_3)_5Cl^{2+}$, has a first-order rate constant which corresponds to about 3% decomposition in one hour (about 1.5% per hour at 20°C). The activation parameters for both acid and base hydrolysis are consistent with a dissociative mechanism for the rate determining step[41].

Since only chloride aquation occurs thermally, and this only very slowly, the extent of thermal decomposition during the period of a photolysis experiment is negligible when considering photosubstitution of amine (which is expected to be the main photoreaction mode for the series of complexes to be studied). When determining the photolytic aquation of chloride, corrections for the thermal decomposition must be made since the quantum yield for chloride release is expected to be small and the rate of thermal chloride release is expected to be greater or at least comparable to

that for photolytic release. More detailed discussions pertaining to these corrections appear in the experimental sections.

2. Objectives of this Work

a. Relative Quantum Yields

As noted before, the relation between the magnitude of the quantum yield and the average ligand field strength noted in Adamson's rules is crudely followed. This relation may be better seen in closely related series of complexes where all photoreaction modes have been considered and where the data are reasonably reliable (see Table I).

The series of complexes chosen for this work are well-suited for comparisons of quantum yield with the ligand field strength. For the series, the ligand field parameter Δ decreases going from R=H to R=n-Bu (see Section III-A), but other factors, such as the type of Cr-ligand bonds, are the same.

b. Photochemistry in Non-aqueous Solvents

Adamson's rules, though they seem to apply (but not rigidly, and with the exception of trans-$Cr(en)_2FCl^+$ as noted in Section I-D) in aqueous solutions to most of the complexes studied, have not been adequately tested for photolysis in non-aqueous solvents. Studies of photochemical reactions in non-aqueous solutions to establish whether these rules are general would be important. Especially interesting would be photochemical investigations in strong field solvents; since, as is apparent, the preferential solvation of the strong field ligand, even in water, is not a "good" rule, the photochemical

Table I

Some critically selected quantum yield data for chromium(III) complexes[a].

Complex[b]	Φ(aquation mode)	Remarks	Reference
O_h complexes			
$Cr(NH_3)_6^{3+}$	0.29[c]		37
$Cr(en)_3^{3+}$	0.37	10°C, pH 2	42
$Cr(NCS)_6^{3-}$	0.26	23°C, pH 1.2	43
$Cr(urea)_6^{3+}$	0.10	22°C, natural pH	43
C_{4v}, D_{4h} complexes			
$Cr(NH_3)_5NCS^{2+}$	0.48 (NH_3)	25°C, pH 1	27
	0.02 (NCS^-)	25°C, pH 1	27
$Cr(NH_3)_5Cl^{2+}$ [d]	0.37 (NH_3)	1°C, pH 3	25
	0.005 (Cl^-)	1°C, pH 3	25
	0.36 (NH_3)	15°C, pH 3	18
	0.04 (Cl^-)	15°C, pH 7	18
	0.42 (NH_3)	20°C, pH 3	This work
	0.36 (NH_3)	8°C, pH 3	This work
	$<3\times10^{-4}$ (Cl^-)	13°C, pH 3	This work
$Cr(NH_3)_5Br^{2+}$	0.35 (NH_3)	5°C, pH 3	26
	0.009 (Br^-)	3°C, pH 3	26

(cont.)

trans-$Cr(en)_2F_2^+$	0.46 (en)	21°C, pH 1	33
trans-$Cr(en)_2(NCS)Cl^+$	0.18 (NCS^-)	1°C, pH 3	24
	0.06 (Cl^-)	1°C, pH 3	24
	0.009 (en)	15°C, pH 3	24
trans-$Cr(en)_2FCl^+$	0.33 (Cl^-)	23°C, pH 2	34
trans-$Cr(en)_2Cl_2$	0.32 (Cl^-)	0°C, pH 3	30
trans-$Cr(NH_3)_2(NCS)_4^-$	0.27 (NCS^-)	23°C, natural pH	43
C_{2v} *complexes*			
$Cr(en)_2(ox)^+$	0.15 (en)	23°C, pH 3	35
cis-$Cr(en)_2(NCS)Cl^+$	0.14 (en)	0°C, pH 3	44
cis-$Cr(en)_2Cl_2^+$	0.12 (en)	0°C, pH 3	30
$Cr(en)(ox)_2$	0.02 (en)	15°C, pH 3	35

[a] Quantum yields are for irradiation of the lowest energy spin-allowed ligand field band and reaction in aqueous solution.

[b] For each group of complexes, these are listed roughly in order of decreasing average ligand field strength.

[c] This value has also been reported to be 0.5[22].

[d] Several quantum yield sets are given here for comparison purposes.

mode in strong field solvents, and in general, in non-aqueous solutions, would be even more uncertain.

So far, studies of thermal reactions of Cr(III) ions in non-aqueous or mixed solvents have not been extensive. As examples, King, et al[45], have investigated the equilibrium aspects of the solvation of Cr(III) in methanol/water and ethanol/water, and Palmer and Watts[46] have studied the isomerism and solvation of $Cr(en)_2Cl_2^+$ ions in N,N-dimethylformamide (DMF) and dimethylsulfoxide (DMSO). In the latter cases, solvolysis of the cis-isomer to give cis-$Cr(en)_2(S)Cl^{2+}$, S=DMF or DMSO and the reverse chloride anation are both thought to be dissociative in nature; removal or production of trans-$Cr(en)_2Cl_2^+$ is due to cis-trans isomerism. Thus, at least for the cases cited, thermal substitution reactions are similar to those in water in that the transition state is dissociative and substitution occurs with stereochemical retention. In addition, it should be noted that the rates of thermal solvent substitution reactions are generally solvent dependent.

Photochemical studies in non-aqueous or mixed water solvents are even rarer than the thermal studies. Investigations involving O_h complexes, for example, $Cr(CN)_6^{3-}$[23] and $Cr(NCS)_6^{3-}$[47], obviously contribute little to testing Adamson's rules and the modifications discussed earlier. Only Langford and Tipping's investigation of $Cr(RNH_2)_5Cl^{2+}$, R=H, Me, Et, in DMSO[22], where amine release was found to be the dominant photochemical reaction, gives some insight into the reaction mechanism. However, also of interest are the stereochemistry and the

relative quantum yields in non-aqueous solvents.

The study of photochemistry in strong-field solvents such as ammonia pose obvious difficulties such as rapid solvolysis. In view of this, the present intent is to investigate the reaction mode, stereochemistry and quantum yields in a solvent where analytical and other practical problems are less severe.

c. Wavelength and Temperature Dependence of Quantum Yields

In addition to the main themes of this study, systematic studies of the wavelength and temperature dependence of quantum yields may be made. Many early photochemical investigations have been phenomenological and the data are suitable only for qualitative purposes. The present state of Cr(III) photochemistry requires more systematic and more reliable data.

In view of the earlier discussion on the possibility of reaction from states other than the lowest excited quartet, the wavelength dependence of quantum yields should be considered. Of main concern is the dependence of the chloride Φ since the corresponding reactions for $Cr(NH_3)_5X^{2+}$, X=Cl, Br[25, 26], have been postulated to occur via charge transfer states, even upon irradiation in the ligand field region; the amine Φ is expected to be practically wavelength independent since the major portion of the reaction is expected to occur via the thermally equilibrated ^4E (which is the lowest quartet in C_{4v} symmetry).

The temperature dependence of quantum yields has generally been difficult to interpret because of the lack of data on the

rates of the processes leading to deactivation of the excited states[18]. The apparent activation energy, E_{app}, obtained from an Arrhenius-type equation or plot of log Φ versus 1/T cannot be unambiguously interpreted[18]. However Chen's analysis of the temperature dependence, drawn from results for the reineckate system in methanol/glycol/water[48], suggests that a more meaningful treatment of the temperature dependence is possible. A brief description of the analysis is given below for convenience.

For complex solutions near room temperature, k_2 and k_5 (Figure 6), the rates of the radiative transitions, must be much smaller than k_3 and k_6 since emission is seldom observed. The main pathway for deactivation of the doublet seems to occur via thermal repopulation of the quartet, k_{-4}. This implies that deactivation of the ^2E_g through k_6 is inefficient compared with deactivation through k_{-4} followed by internal conversion or reaction. Therefore essentially all deactivation of the doublet and quartet occurs through the two routes, k_3 and k_r. Thus the reaction quantum yield may be approximately expressed by

$$\Phi_r = \frac{k_r}{k_3 + k_r} \qquad \text{(I-1)}$$

$$\text{or} \qquad \frac{1}{\Phi_r} - 1 = \frac{k_3}{k_r} \ , \qquad \text{(I-2)}$$

and the Arrhenius plot of $\ln [(1/\Phi_r) - 1]$ vs 1/T will yield the difference between the activation energies of the photochemical

reaction and internal conversion, $E_r - E_3$. Although the activation energies, E_r and E_3, cannot at present be separated, the temperature dependence becomes more meaningful.

In order to look at the wavelength and temperature dependence of quantum yields, precise and accurate measurements are essential. Throughout this work, considerable emphasis is made to obtain such measurements.

II. EXPERIMENTAL

A. Preparation of Compounds and Solvents

1. Compounds

a. $[Cr(NH_3)_5Cl]Cl_2$ was obtained as a by-product from the preparation of μ-hydroxo-bis{pentaaminechromium(III)} chloride as described by Linhard and Weigel[49].

b. $[Cr(NH_3)_5Cl](ClO_4)_2$ was obtained by dissolving the chloride salt in a minimum volume of water and adding excess solid sodium perchlorate. The pinkish-red precipitate was twice recrystallized from warm (35-40°C) acidified water. The purity of the product was confirmed spectrophotometrically[50] as well as chromatographically (Section II-D).

c. The chloropentakis(alkylamine)chromium(III) chlorides, $[Cr(RNH_2)_5Cl]Cl_2$, R= Me, Et, n-Pr, n-Bu, were prepared by the slow addition of anhydrous chromic chloride to the pure anhydrous (dried over KOH and distilled) amines as described by Rogers and Staples[40]. All the reactions are exothermic and cooling with dry-ice/acetone (R= Me, Et) or ice/water baths was necessary. For each of the preparations, the temperature of the reaction was kept between 5-20°C below the boiling point of the amine. Excess amine was either allowed to evaporate at room temperature (methylamine and ethylamine) or removed by decantation and washing of the product with ether. The crude $[Cr(MeNH_2)_5Cl]Cl_2$ was recrystallized by dropwise addition of

concentrated HCl to an acidified aqueous solution of the complex. The other three complexes were recrystallized by dissolving in acidified methanol and partially evaporating the solvent (near room temperature, using a rotary evaporator).

d. The $Cr(RNH_2)_5Cl(ClO_4)_2$ salts were obtained by dissolving the corresponding chloride salts in a minimum of $HClO_4$-acidified water (R= Me, Et), or aqueous acetone, adding excess $NaClO_4$ and cooling to 0°C. The perchlorate salts were then twice recrystallized from slightly acidified warm (30-40°C) aqueous acetone (R= Me) or aqueous methanol. (Aqueous methanol was used where a warmer solution was desired.)

$Cr(MeNH_2)_5Cl(ClO_4)_2$ was obtained as red crystals.

Anal. Calcd: Cr, 11.77; C, 13.60; H, 5.71; N, 15.86.
Found: Cr, 11.84; C, 13.59; H, 5.62; N, 15.52.

$Cr(EtNH_2)_5Cl(ClO_4)_2$ was obtained as red crystals (slightly purplish in comparison with the methylamine complex).

Anal. Calcd: Cr, 10.16; C, 23.47; H, 6.89; N, 13.68.
Found: Cr, 9.94; C, 23.70; H, 7.00; N, 13.31.

$Cr(n\text{-}PrNH_2)_5Cl(ClO_4)_2$ was obtained as reddish-purple platelets when slightly wet, but these became more powdery when dry.

Anal. Calcd: Cr, 8.94; C, 30.96; H, 7.86; N, 12.04.
Found: Cr, 9.08; C, 31.10; H, 7.87; N, 12.15.

$Cr(n\text{-}BuNH_2)_5Cl(ClO_4)_2$ was obtained as reddish-purple platelets when slightly wet, but on drying became a purplish-pink powder.

Anal. Calcd: Cr, 7.98; C, 36.84; H, 8.50; N, 10.74.
Found: Cr, 7.78; C, 36.78; H, 8.52; N, 10.33.

The purity of the complexes was investigated by ion-exchange chromatography (for R= H, Me; see Section II-D) and/or

by paper chromatography, as well by elemental analysis and inspection of the uv-visible absorption spectra.

2. Solvents

Photolyses were performed in three different solvents: water, 33% acetone/water (by weight), and practically 100% acetone. It was desirable to acidify and, where possible, to add a suitable supporting electrolyte to each solvent. The concentrations of acid and supporting electrolyte, as well as other pertinent details, are given below.

a. Water used as solvent for photolysis runs which involved quantum yield determinations was 10^{-3}M in $HClO_4$ and 0.05 M in $KClO_4$. The perchloric acid added had been standardized.

b. The 33 w/w % acetone/water mixture was prepared by diluting 40 volumes of distilled acetone to 100 volumes with appropriate portions of standardized perchloric acid, potassium perchlorate and water to give 10^{-3}M in $HClO_4$ and 0.02 M in $KClO_4$. Although a knowledge of the exact weight fraction of acetone in the solution is not essential, an approximate determination will be useful. This is possible if one considers the concentrative properties of aqueous acetone solutions[51]. Although data for such solutions are available only for solutions up to 10% acetone by weight, such data for comparable solvents are more extensive. Comparisons of the density of acetone (0.7899 g/ml) with those for methanol and ethanol (0.7914 and 0.7893 respectively), and of the densities of the aqueous solutions of the three organic solvents (Table II) suggest that the profile of the plot of the weight percent

Table II

Density of some mixed aqueous solutions*.

solute	% by weight	density (20°C)
acetone	2.0	0.9971
	4.0	0.9943
	6.0	0.9917
	8.0	0.9891
	10.0	0.9867
methanol	2.0	0.9965
	4.0	0.9931
	6.0	0.9898
	8.0	0.9865
	10.0	0.9834
	20.0	0.9682
	30.0	0.9531
	40.0	0.9364
ethanol	2.0	0.9962
	4.0	0.9928
	6.0	0.9896
	8.0	0.9866
	10.0	0.9837
	20.0	0.9702
	30.0	0.9556
	40.0	0.9371

*Data from Ref. 51.

acetone versus density of the aqueous acetone solution should approximately follow those of the aqueous methanol and aqueous ethanol solutions. Thus the aqueous acetone solution prepared (about 316 g of acetone per liter) should have a density of 0.95 and hence is about 33% acetone by weight.

c. Practically 100% (dry) acetone was obtained by drying spectrograde (Fisher Scientific) acetone over molecular sieves, 4 Å, and distilling over a 40-cm column. The degree of dryness was not analytically determined, but inspection of data (supplied by Union Carbide) for comparable solvents suggested that water might be present in the order of 0.001 - 0.01%. A 0.1 M $HClO_4$ solution was prepared by diluting 2 ml of 35% perchloric acid to 100 ml with dried acetone and a 10^{-3}M $HClO_4$ solution, by appropriate dilution of the 0.1 M solution. The latter solution is thus about 0.02% (or 1×10^{-2}M) in added water.

The $HClO_4$/acetone solution so obtained yellowed visibly over a period of 2-3 hours. It was speculated that this was due to iron impurities from the perchloric acid and the final solutions were made up with perchloric acid which had been passed through a suitably treated strong acid ion exchange column. These final solutions were visibly colourless for at least 3 hours and photolyses were carried out within this interval.

B. Elemental Analysis

Chromium analyses were made using the hot alkaline peroxide oxidation of Cr(III) to chromate ion, CrO_4^{2-}. An excess of hydrogen peroxide was added to an alkaline (aqueous ammonia) solution or slurry of complex. The mixture was then heated on a steam bath, with occasional stirring, until no more oxygen bubbles were evolved (about 30 minutes). The solution was then cooled, diluted to volume (to give about 10^{-4}M in CrO_4^{2-}) and its absorbance at 373 nm was measured. The concentration was determined using a calibration curve.

Carbon, hydrogen and nitrogen analyses were made by Mr. D. McGillivray using a Perkin-Elmer Elemental Analyzer 240.

C. Photolysis Apparatus

The apparatus used for photochemical experiments is shown schematically in Figure 7; the details of the equipment are given in the accompanying legend.

The beam from the light source (A) was focussed with a quartz lens (B) onto a point near the position of the second photolysis cell (H). With the photolysis cells far (~30 cm) from the focussing lens, the light beam was essentially parallel over the short distance across the two cells and this, together with the design of the cell holder (J), which masks the cell edges, eliminated the possibility of the anomalous effects previously observed when the light beam enters the cell walls[52].

The light beam was filtered by a heat reflecting filter (C) and a narrow band interference filter (D). For quantitative runs, it was desirable that the band-widths of the filtered light be small. The widths at half-height of the filters used in this work are given below.

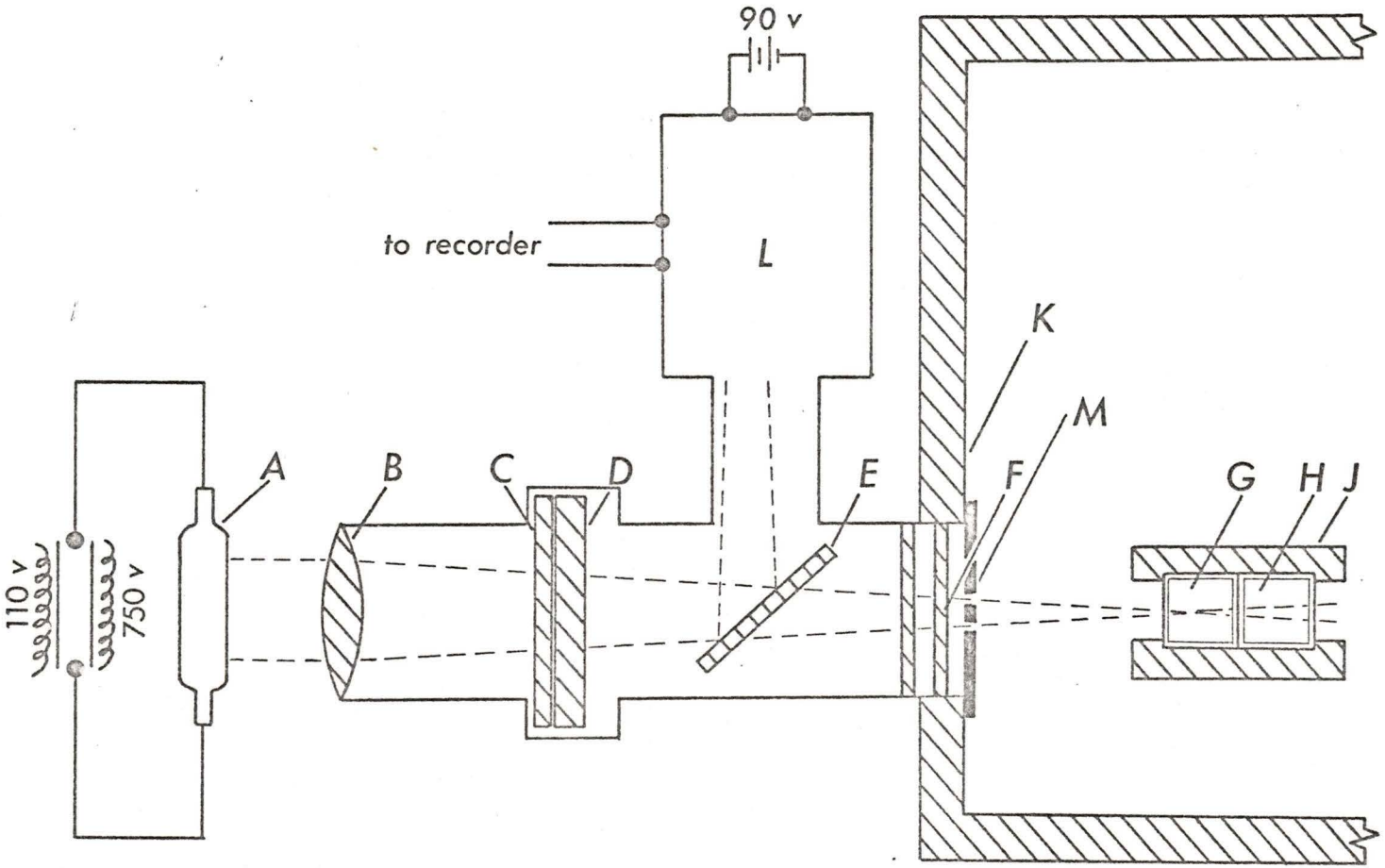

Figure 7. Diagram of the photolysis apparatus (details in Legend).

Legend to Figure 7

A. Light source: AH6-1-B high pressure mercury capillary lamp, P.E.K. Laboratories Inc.; or DXW-120 volt, 1000 watt quartz-iodine lamp, Canadian General Electric.

B. Quartz lens.

C. Heat reflecting filter: Calflex C, Rolyn Corp.

D. Interference filter: Filtraflex B-20, Rolyn Corp.

E. Quartz window.

F. Double quartz window.

G. Position for photolysis cell.

H. Position of cell for the accompanying actinometer solution.

J. Cell holder.

K. Thermostat.

L. Photocell.

M. Shutter.

Nominal wavelength (nm)	Width at half-height (nm)
400	7
478	8
565	6

A constant fraction of the filtered light beam was reflected by the quartz window (E) onto the photocell (J) so that the intensity of the lamp might be continuously monitored. Over a day, the lamp intensity was found to be linear with the photocell output (see Figure 8), but this lamp calibration was found to be relatively unreliable on a long term basis.

The section of the optical train between B and C can become quite hot but may be water-cooled. Since water-cooling led to possible misting of the quartz lens (B), the filters (C and D) and the quartz window (E), the optical train was purged with a stream of dry air.

The thermostat (K) was built of Plexiglass, thermally insulated with thick Neoprene foam and thermally equilibrated with thermostatted water. The double quartz window (F) was purged with a stream of air to eliminate misting of the window surface during runs below room temperature. The shutter (M) fitted into a slot built into the thermostat to permit easy handling.

The cell holder (J) was designed to accommodate two photolysis cells (G and H) which, when wetted and positioned carefully with a spacer behind H, permitted simultaneous photolysis and actinometry runs (see Section II-E-1). The openings in the front and back of the cell holder, which allowed passage of the light beam through the photolysis

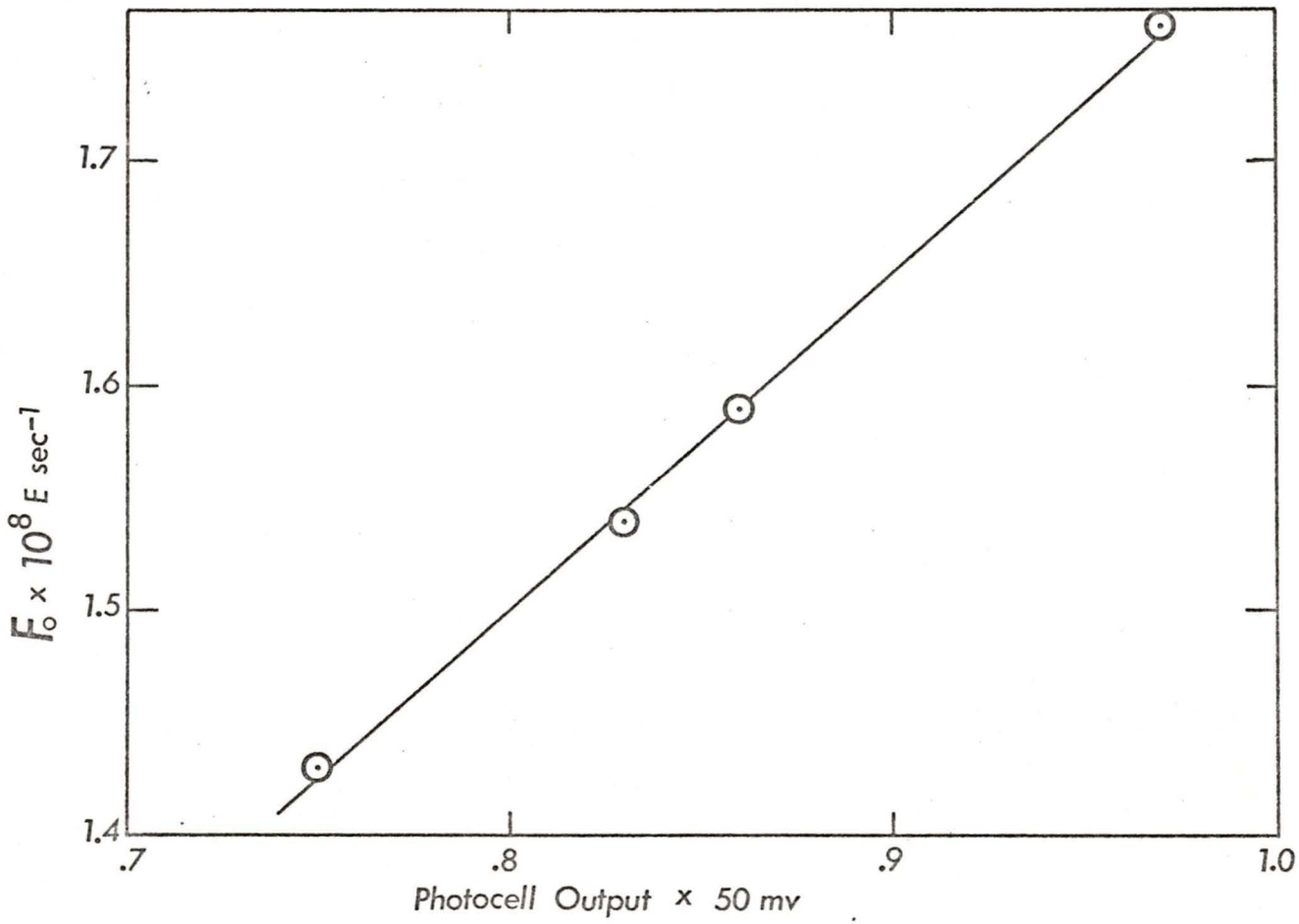

Figure 8. Plot of light flux as a function of the photocell output.

cells, were designed so that the edges of the cells and a small stirring bar, which could be placed in G, were effectively masked. During a photolysis run the cell holder could be covered to eliminate stray light. One of the solutions--in practice, the front one--could be magnetically stirred with a magnetic stirrer placed under the thermostat.

D. Identification of Photolysis Products

1. Chromatography

The chromatography apparatus was a Technicon Auto-Analyzer system. For convenience, a description of the operation of the apparatus is given below; relevant information concerning the ion-exchange column, eluant, pumping rates and solutions used are given in Appendix B.

The solution of complex was pipetted or injected onto the top of the ion-exchange column and eluant of continuously increasing concentration (premixed with a Technicon Autograd) was pumped through the column at a constant rate. While the main portion of the eluant could be collected, a small portion was diverted by the proportioning pump and mixed with constant ratios of hydrogen peroxide and sodium hydroxide solution. The mixture passed, over about twenty minutes, through a hot (95°C) reaction coil where any eluted Cr(III) species was oxidized to CrO_4^{2-}. The solution was then cooled and passed through the colorimeter where the transmittance at ~380 nm (interference filter, half-width about 11 nm), and hence the concentration, was measured and continuously recorded.

If the eluted fractions were collected, the chromatogram could be used to determine the fractions where the concentrations (if the chromatographic bands are well-separated) of eluted complexes were maximal. By converting the transmittance chromatogram to an absorbance one and integrating the band areas, the relative concentrations of complexes in the original mixture could be calculated. Thus, the system could potentially be used for determinations of proportions of photolysis products if more than one photolysis product was possible or for determining the relative purity of a prepared sample of complex.

The system was set up mainly to investigate the possibility of separation of cis and trans-$Cr(NH_3)_4(H_2O)Cl^{2+}$, extension of this to other cis-trans isomers with monodentate amine ligands, and subsequent application of this to investigate the extent of the predominance of the cis-product in the photochemical reactions of $Cr(NH_3)_5X^{n+}$. Although separation of $Cr(NH_3)_4(H_2O)Cl^{2+}$ (cis or trans) from $Cr(NH_3)_5Cl^{2+}$ was relatively easy (see Figure 9a) experimental separation of the cis-trans isomers seemed to be too difficult to accomplish practically (see Figure 9b).

The extreme difficulty of separating the cis-trans isomers just discussed, together with the low water-solubility of some of the complexes used in this investigation, precluded practical use of ion-exchange chromatography for identification and determination of isomer ratios of the photolysis products.

As a result of these investigations, however, it was found that the purity of a particular sample of complex could be quantitatively established. Small quantities of impurities which are invisible on

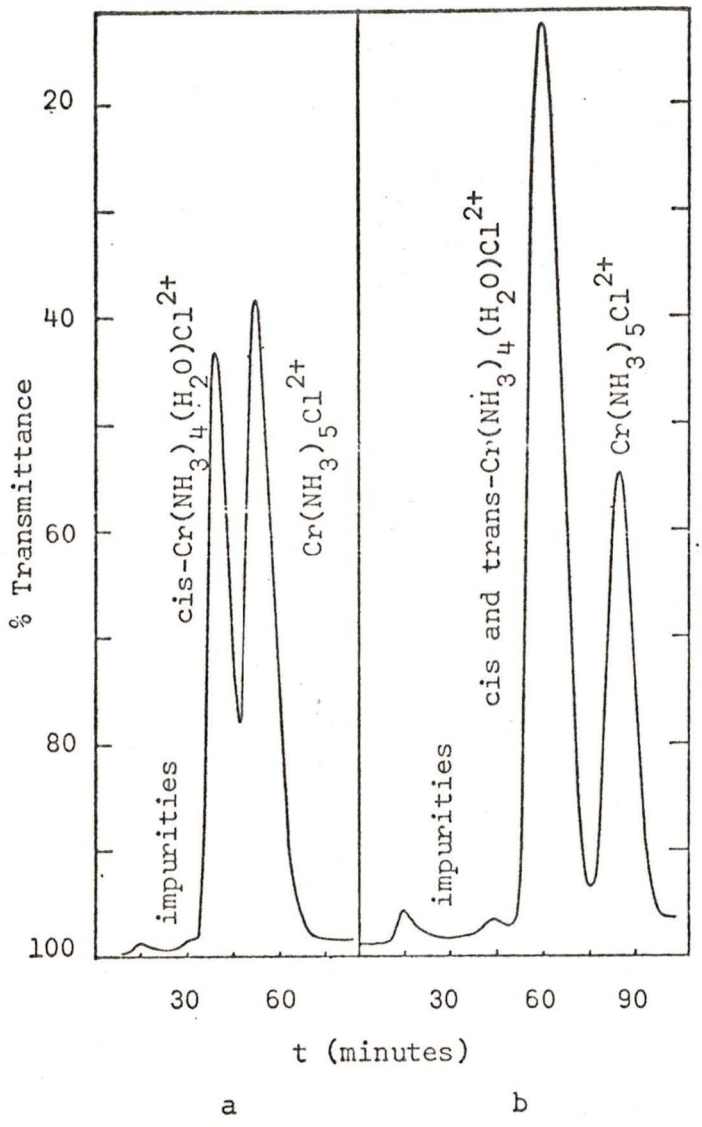

Figure 9. Chromatograms for the separation of

a: cis-$Cr(NH_3)_4(H_2O)Cl^{2+}$ and $Cr(NH_3)_5Cl^{2+}$ using a 6-cm column and 1.0 increasing to 2.0 M NaCl as eluant (19°C)

b: cis and trans-$Cr(NH_3)_4(H_2O)Cl^{2+}$ and $Cr(NH_3)_5Cl^{2+}$ using an 18-cm column and 1.0 increasing to 2.0 M NaCl as eluant (22°C).

the column may be readily observed (see Figure 9). Integration of the absorbance chromatogram can thus give a reasonably precise estimate of purity. In this way the $Cr(MeNH_2)_5Cl(ClO_4)_2$ and $Cr(NH_3)_5Cl(ClO_4)_2$ samples were found to be about 98.5% and >99% pure. Extension to the other complexes was not made since these were either difficult to elute (timewise), or were not water soluble.

2. Difference Spectrophotometry

The experience with the cis-trans isomers of $Cr(NH_3)_4(H_2O)Cl^{2+}$ suggested that attempts at the chromatographic separation of the analogous alkylamine complexes (assuming that both isomers could be formed from ligand field irradiation of the parent $Cr(RNH_2)_5Cl^{2+}$), would be a poor investment of time. The use of difference spectrophotometry, though this can only yield a total spectrum for all products, is more appealing. The experimental details for obtaining the various difference spectra are given below.

$Cr(RNH_2)_5Cl^{2+}$, R= Me, Et, in acidified aqueous solution: Two 3-ml samples of 2.0×10^{-2}M solution of the complex, made up in 3.0×10^{-3}M $HClO_4$, were pipetted into spectrophotometer cells. While keeping one in the dark, the other was photolyzed for about 40 minutes at 20°C with 565-nm light. The photolysis solution was continuously mixed by means of magnetic stirring. The difference spectrum was then obtained by running the spectrum of the photolyzed sample against the dark sample used as reference (Cary 17 spectrophotometer, expanded, 0-0.2, absorbance scale).

$Cr(n\text{-}PrNH_2)_5Cl^{2+}$ and $Cr(n\text{-}BuNH_2)_5Cl^{2+}$: The procedure was the same as for R=Me, Et except that the solutions were made up in 33% acetone/

water and the samples had to be well-stoppered.

$Cr(MeNH_2)_5Cl^{2+}$ in practically 100% acetone: The difference spectrum was obtained as described for the other solutions except that the dark and photolysis solutions were made up in acidified (10^{-3}M $HClO_4$) acetone.

E. Quantum Yield Measurements

The quantum yield (Φ) for the reaction

$$[A] + h\nu \longrightarrow [B]$$

may be defined as

$$\Phi = \frac{\text{molecules of B formed}}{\text{photons absorbed by reactant species A}} \qquad \text{(II-1)}$$

and if A is the only absorbing species, then

$$\text{the number of photons absorbed by A} = F_o(1 - 10^{-\varepsilon_A c \ell})$$

where F_o is the light flux (in photons sec^{-1}) as the light beam enters the reaction medium, ε_A is the extinction coefficient of A at the exciting wavelength, c is the concentration of A, and ℓ is the depth of the solution.

From the definition of Φ, it is apparent that its determination necessitates measuring the number of product molecules formed and the number of photons absorbed by the reactant. The latter may be measured by bolometry, but because of its convenience, chemical actinometry (described below) was used in this work. The number of product molecules formed was determined indirectly.

For the complexes studied in this work, two primary photochemical reaction modes are possible:

$$Cr(RNH_2)_5Cl^{2+} + h\nu + H_2O \rightarrow \begin{cases} Cr(RNH_2)_4(H_2O)Cl^{2+} + RNH_2 & (3) \\ B_1 \\ Cr(RNH_2)_5(H_2O)^{3+} + Cl^- & (4) \\ B_2 \end{cases}$$

A

Thus the number of product molecules B_1 and B_2 formed is equivalent to the number of molecules of RNH_2 and Cl^- released, respectively, and these may be determined by analytical techniques (discussed in later sub-sections).

1. Photolysis and Light Flux Measurements

Since the photolysis experiment was often accompanied by an actinometric run to determine the light intensity during the photolysis run, it is appropriate to combine these two parts.

Because of the nature (described below) of the simultaneous photolysis and actinometric runs, the spectrophotometer cells which were used for photolysis had to be very clean. Cleaning by soaking the cells in warm (~40°C) dilute chromic acid for several hours was found to be effective; the cells were thereafter kept in dilute sulfuric acid when not in use. Dry, clean cells were obtained by copiously rinsing with distilled water, two rinsings with distilled methanol and drying with a stream of filtered air.

For the photolysis experiments, solutions of complex (~1 X 10^{-2}M) were made up in one of the three acidified solutions (Section II-A). To minimize premature photolysis, such solutions were made up in dim, orange-red light. Two samples (2.7 or 3.0 ml) of the solution were pipetted into clean spectrophotometer cells and the cells were stoppered. Keeping one of the samples in the dark,

the other was then photolyzed, either with continuous magnetic stirring or with alternate periods of photolysis and stirring in the dark.

The light flux was measured by reineckate actinometry[43] and during a photolysis run, simultaneous photolysis of a reineckate solution could be performed so that the light flux may be determined directly. The procedure adopted for this is briefly described in what follows. A solution of K[trans-$Cr(NH_3)_2(NCS)_4$] (K-reineckate) (8.0×10^{-3} M) was made up in distilled water. Two samples (2.7 or 3.0 ml) were pipetted into spectrophotometer cells. While one was kept as a dark blank, the other actinometric cell and the front photolysis cell were wetted and carefully coupled face to face so that the film of water between them is free of air bubbles. The cells were then fitted snugly into the cell holder, and after thermal equilibration, the two solutions were photolyzed. Stirring of the actinometric solution was not too critical since the solution is only about 70% absorbing, and the incident light intensity is diminished by the front solution so that conversion was usually very small (<4%). After photolysis, the actinometric solutions were developed with 10 ml of $Fe(III)/HClO_4$ solution and the absorbances at 450 nm were measured, as described by Wegner and Adamson[43].

For simultaneous photolysis/actinometry, it is obvious that the front solution must not be totally absorbing. Practically, it was found that a 30 to 70% absorption by the front solution was desirable. Concentrations of the photolysis solutions were thus chosen with this as one of the criteria.

For all photolysis runs, including actinometric runs, the absorbance and/or transmittance of the initial solutions were measured at, or as near to as possible, the temperature chosen for the photolysis run.

The calculation of the light flux for such simultaneous photolysis/actinometric runs is described in what follows. The light flux entering the actinometer solution may be expressed as

$$F_o = \text{moles } NCS^- \text{ released } \times \frac{1}{f_{aa}} \times \frac{1}{f_{ts}} \times \frac{1}{t} \times \frac{1}{\Phi} \qquad \text{(II-2)}$$

$$f_{aa} = (1-10^{-\varepsilon_a cl})$$

$$f_{ts} = 10^{-\varepsilon_s cl}$$

where f_{ts} is the fraction of light beam transmitted by the front photolysis sample and hence reaching the actinometer solution; f_{aa} is the fraction of the beam subsequently absorbed by the actinometer sample; t is the photolysis time; ε_a and ε_s are the extinction coefficients of the actinometric and sample solutions at the irradiating wavelength; and Φ is the quantum yield of NCS^- release at the photolysis conditions. The moles of NCS^- released is given by

$$\text{moles } NCS^- = \frac{(\alpha_{exp} - \alpha_{dark})_{450}}{\varepsilon_{450}} \times V$$

where α_{exp} and α_{dark} are the absorbances of the Fe(III)-developed exposed and dark solutions, respectively, at 450 nm; ε_{450} is the molar extinction coefficient of the Fe(III)-NCS^- complex(es) per NCS^- ion at 450 nm; and V is the volume of photolyzed reineckate solution. The assumptions and small errors inherent in (Equation II-2) are discussed in Section VI.

Notice from the expression for the lamp flux (Equation II-2), that the accuracy of the numerical values of the transmittance of the solutions at the irradiating wavelength are critical. The light beams used however can not be strictly monochromatic and it was thus necessary to integrate the transmittance of the solutions over the transmission band of the interference filter, or to use an effective wavelength. Some fortunate circumstances in this work enabled relatively easy assignment of effective wavelengths for the interference filters used. The transmittance spectra of the complexes and of reineckate, over better than the half-widths of the transmitted band of the filters, are practically linear. The nominal wavelength can thus be assigned as the mean wavelength, weighted by transmittance, of the transmission band and is found to be close to the specified wavelength of the filters. The effective wavelengths used are 401.2, 479.0 and 565.4 nm for the correspondingly specified filters (Section II-C).

Using the system just described, the problem of variations in light intensity during photolysis was eliminated. The precision of the method was checked by doing several runs with K-reineckate in both front and back cells in the photolysis system, at 479.0 nm. The light flux calculated from the NCS^- released from the front and back solutions generally agreed to within 2% (five runs).

For simultaneous photolysis and actinometry at temperatures other than 23°C, it was necessary to determine the reineckate quantum yields at other temperatures. For this, a DXW-120v, 1000 watt quartz-iodine lamp was used as a potentially steady light source. With the lamp at a nominal power setting (just under 1000 watts) and

the lamp output monitored with the photocell (refer to Figure 7) was carried out at 20°C; small changes (±2%) in light output were compensated for by fine adjustments on the power setting. (This gave light intensities reproducible to better than 1%). With the photolysis system at "equilibrium" running conditions, actinometry was carried out at other temperatures. The quantum yields were later corrected by comparing the quantum yields at 20° and 23°C and are listed in Table III for convenience. A plot of Φ against temperature is nearly linear and for photolysis/actinometry at temperatures other than those shown, the reineckate quantum yield was interpolated.

2. Quantum Yield Measurements for Amine Aquation:

a. In water as solvent.

The photolysis solutions, about 10^{-2}M in complex, were made up in a standard solution of 0.05 M $KClO_4$ 10^{-3}M $HClO_4$. Amine release occurs with consumption of H^+ ions since

$$RNH_2 + H^+ \longrightarrow RNH_3^+ \qquad (5)$$

The quantity of released amine was thus determinable by the ΔpH method outlined by Wasgestian and Schlafer[25]. For low conversions, the ionic strength of the solutions, and hence the H^+ activity coefficient, may be assumed to be constant before and after irradiation. Therefore

$$\Delta pH = pH - pH_o = -\log \frac{c_H}{c_{H_o}} \qquad (II\text{-}3)$$

where pH and pH_o are the measured pH values for the irradiated and initial (or dark) solutions and c_H and c_{H_o} are their

Table III

Reineckate quantum yields at 565.4 nm at various temperatures[a].

T (^{o}C)	Φ
23.0	0.276[b]
20.0	0.273
11.5	0.243
5.5	0.225

[a]For light flux calculations, the quantum yields used for photolysis at 20°C at 401.2 and 479.0 nm were 0.314 and 0.300, respectively. These values were interpolated from wavelength data from Ref. 43 at 23°C, and were found to be practically unchanged (±0.001) at 20°C.

[b]Extrapolated from values in Ref. 43.

corresponding H^+ concentrations. By algebraic manipulation,

$$\Delta c_H = c_{H_o} (10^{-\Delta pH} - 1) \qquad \text{(II-4)}$$

and the quantum yield is

$$\Phi = \frac{-\Delta c_H V}{F_o t (1-10^{-\varepsilon c l})} \qquad \text{(II-5)}$$

where V is the volume of solution, t is the photolysis time and $(1-10^{-\varepsilon c l})$ is the fraction of the light beam absorbed by the solution. When the light intensity is determined with simultaneous photolysis of an actinometer solution for the full photolysis period, $F_o t$ may be combined.

The inner filter effect[53] was negligible (see Section VI) and was not included in the quantum yield calculations.

b. In 33% acetone/water

The photolysis solutions were made up in 0.02 M $KClO_4$ 10^{-3}M $HClO_4$ solution. At the end of the photolysis, the pH of the dark and irradiated samples were measured. A portion of the irradiated sample was pipetted into a container where the solution could be efficiently mixed and then titrated with 0.100 M HCl, using a 10 µl syringe, with the pH monitored, until the pH was lowered below that of the dark solution. A plot of a_{H^+} against the moles of H^+ added (dilution was very small, <1%, and was neglected) was linear so that the moles of H^+ added to reach the pH of the dark solution was easily determined.

The calculated moles H^+, obtained by titration, and that obtained using the ΔpH method were in very good agreement

(several runs). Since the ΔpH method is much more convenient to use, most of the data for quantum yields in 33% acetone was obtained in this way.

c. In practically 100% acetone

The photolysis quantum yields were determined by diluting 2 ml of the photolyzed (or dark) solution with 3 ml of water and measuring the pH. The ΔpH method was then applied even though the assumption that the activity coefficient for H^+ was constant may not be precisely valid. The quantum yields obtained for these runs are not as precise and, probably, not as accurate, as those for the runs in the aqueous solvents.

It should be noted that in the determination of the moles of amine released using the ΔpH method, the volume of solution resulting from dilution of the 2 ml aliquot of acetone solution with 3 ml of water is critical. The total volume is not 5.0 ml, but rather, 4.8 ml, since the total weight is 4.58 g and the density of the solution is about 0.95 (Section II-A).

3. Quantum Yield Measurements for Chloride Aquation

In determinations of the quantum yield of a minor reaction mode, the general practice is to do relatively high conversions so that the concentration of products resulting from this reaction mode becomes measureable[25, 26, 27]. In some cases, where the minor photochemical reaction mode is the same as that of the thermal reaction, corrections for the thermal reaction of the starting material, A, and also of the major primary photoproduct, B_1, may be necessary (see also Section III-B-2). For the purpose of illustration, consider the following example:

$$Cr(NH_3)_5X^{2+} + h\nu + H_2O \rightarrow \begin{cases} Cr(NH_3)_4(H_2O)X^{2+} + NH_3 & (6) \\ \quad B_1 \\ Cr(NH_3)_5(H_2O)^{3+} + X^- & (7) \\ \quad B_2 \end{cases}$$

(A)

$$Cr(NH_3)_5X^{2+} + H_2O \longrightarrow Cr(NH_3)_5(H_2O)^{3+} + X^- \quad (8)$$

$$Cr(NH_3)_4(H_2O)X^{2+} + H_2O \longrightarrow Cr(NH_3)_4(H_2O)_2^{3+} + X^- \quad (9)$$

Reaction 6 is the main photochemical reaction and Reaction 7, the minor photochemical reaction, is the one under investigation. The most convenient method for observing the extent of Reaction 7 is by observing the concentration of X^-. As illustrated here, the thermal reactions, 8 and 9 also release X^-.

Investigations of Reaction 7 have normally been performed at relatively low temperatures and under the assumption that Reaction 9 is negligible. Photolytically released X^- is then determined by considering the X^- concentrations of the photolyzed, dark and initial samples. When the first-order rate constant for Reaction 9 is not bigger than that for Reaction 8 and the conversion of starting material is reasonably low (<10%), the errors incurred should not be objectionably large (<25%).

Preliminary investigations of chloride quantum yields for $Cr(MeNH_2)_5Cl^{2+}$ (see Section III-B) indicated, however, that at 20°C, the first-order rate constant for thermal chloride aquation of the major photoproduct is much larger than that for the starting material so that even at relatively low conversion (~13%) the absolute rate of Reaction 9 is much larger than that of Reaction 8.

The most convenient method for determining qualitatively

whether chloride release is directly due to photolysis or thermal reaction is by monitoring the chloride concentration of the reaction sample before, during and after photolysis. At low conversions, secondary reactions are largely (though never entirely) avoided so that quantitative treatments are obviously simpler and deviations from those of idealized situations are minimized.

The measurement of chloride quantum yields was made with the above considerations in mind.

a. Instrumentation and Measurement of Chloride

Figure 10 shows the photolysis cell set-up for chloride determinations. The chloride measuring cell was a concentration cell without transference. The platinum electrodes were silver-plated by electrolyzing in 0.05 M $NaAg(CN)_2$ and chloridized in 0.10 N HCl under a very small current ($\sim 10^{-3}$ma). With an internal reference of 4.0×10^{-4}M KCl supported by 0.05 M $KClO_4$, the measuring electrode was calibrated for chloride from 1.25×10^{-5}M to 4.0×10^{-4}M (calibration curve is displayed in Figure 11) using KCl solutions made up in 0.05 M $KClO_4$ (to match the photolysis solutions). The lower limit is determined by the purity of the potassium perchlorate and was found by assuming linearity for the E vs -log $[Cl^-]$ plot and iteration of the lower limit until it was consistent. That the lower limit is numerically correct (at least to a good approximation) was confirmed by the linearity of the calibration curve for KCl solutions in 0.02 M $KClO_4$ and 33% acetone (see Figure 12) assuming the lower limit for chloride to be 5.0×10^{-6}M.

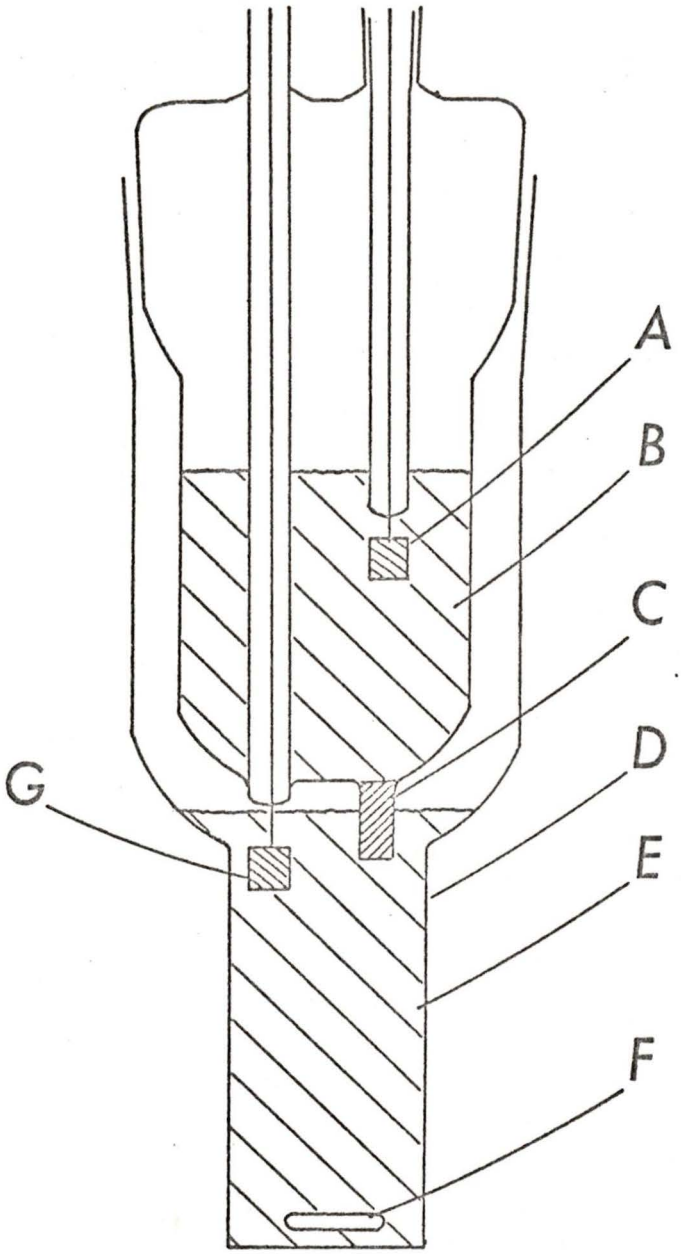

Figure 10. Photolysis cell set-up for chloride measurements. A, 6 x 5 mm Ag/AgCl reference electrode; B, reference electrolyte; C, Agar plug (2% in 2 M NH_4NO_3); D, spectrophotometer cell; E, photolysis solution; F, Teflon-coated magnetic stirring bar; G, 6 x 5 mm Ag/AgCl measuring electrode.

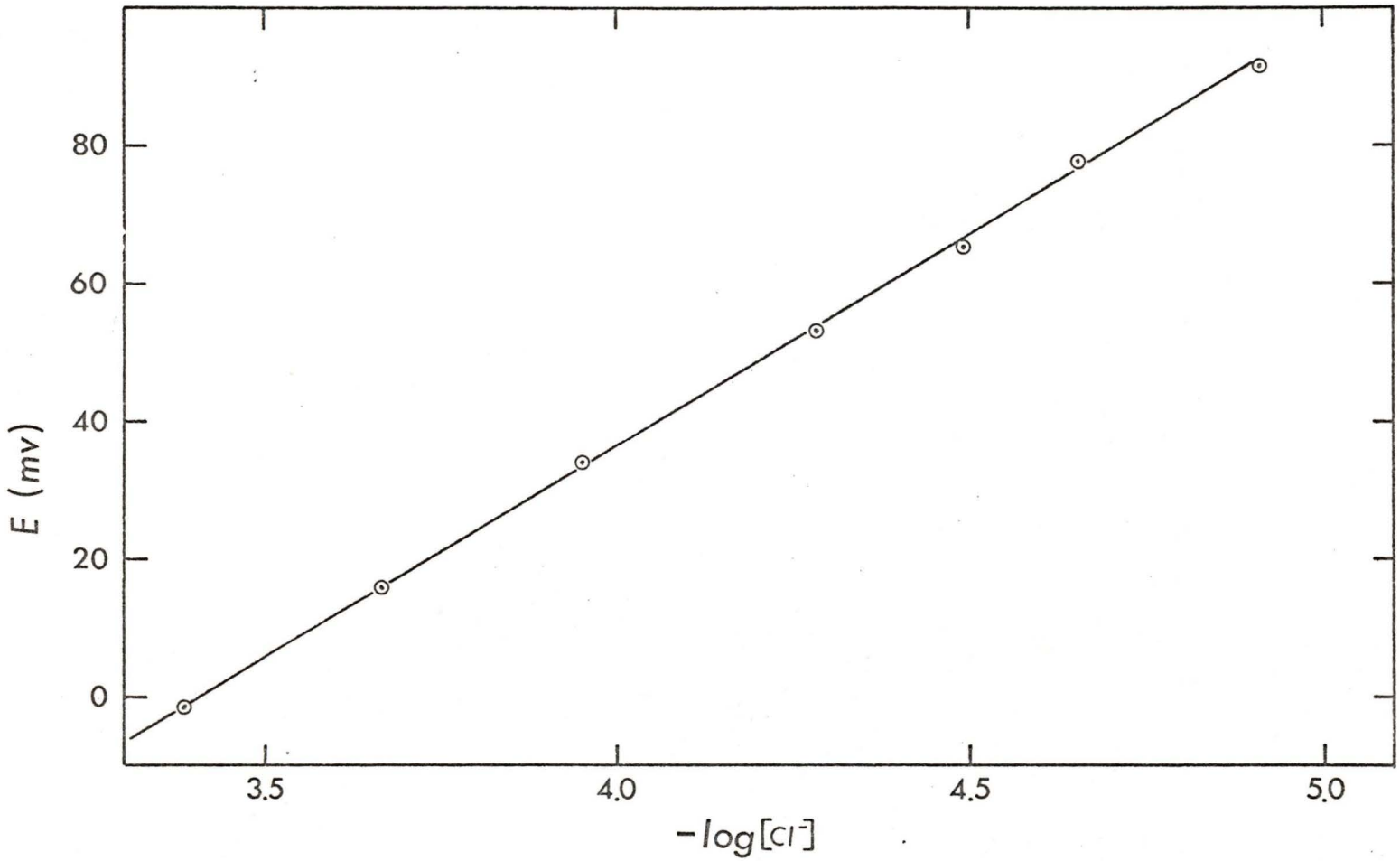

Figure 11. Calibration curve for chloride in 0.05 M $KClO_4$ with 4.0×10^{-4} M KCl in 0.05 M $KClO_4$ as reference.

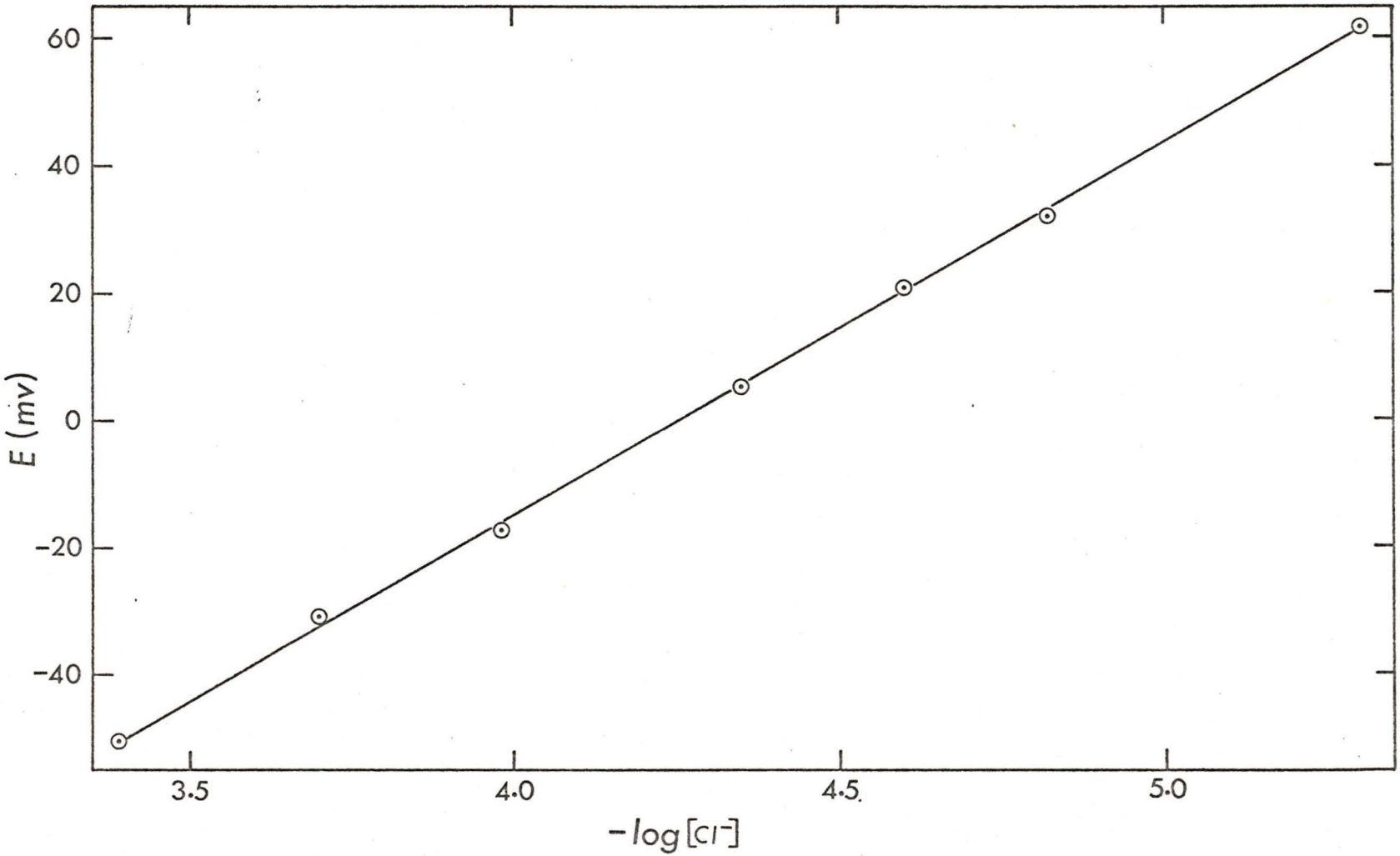

Figure 12. Calibration curve for chloride in 0.02 M $KClO_4$ in 33% acetone/water with 4.0×10^{-4} M KCl in 0.05 M $KClO_4$ as reference.

Although the chloride measuring cell did not give completely reproducible readings from day to day, the bias potential in 0.05 M $KClO_4$-chloride solutions, over a period of several weeks was reasonably constant (-2±2 mv).

A number of experimental details are worth noting. The photolysis cell was masked so that the light beam did not fall directly on the measuring electrode. All measurements for chloride quantum yield were made at 13°C, a somewhat arbitrary temperature chosen from two considerations: minimizing the thermal chloride release and maximizing the reliability of the chloride measurements--the reference solution was not thermostatted and readings became unstable when the temperature difference between the reference and sample solutions became too large[39]. Since the measuring electrode is somewhat separated from the main portion of the solution undergoing direct photolysis, good mixing so that the electrode is truly monitoring the average $[Cl^-]$ is essential. That mixing with the magnetic stirrer is sufficient was confirmed by comparing a photolysis run with magnetic stirring to a run with added mixing from a continuous stream of nitrogen bubbles. The results were virtually the same except that the nitrogen bubbles tended to reflect light onto the measuring electrode and readings were somewhat spurious and showed anamolous jumps at the start and end of photolysis.

b. Procedure

A solution of complex (1-2 X 10^{-2}M), either in 0.05 M $KClO_4$, 10^{-3}M $HClO_4$ or 0.02 M $KClO_4$, 10^{-3}M $HClO_4$, 33% acetone, was made

up. 5.0 ml of the reaction solution was pipetted into the photolysis cell and this cell and the temperature and solvent-equilibrated Ag/AgCl cell were positioned. With the shutter closed, potential readings were noted until the solution and electrode had apparently reached equilibrium. The dark reaction was then followed for a short time. The shutter was then opened and the total photochemical and thermal chloride release was followed. After about 2-7% photolysis, the shutter was closed and the post-photolysis chloride release was followed for a short time. Typical [Cl^-] versus time curves are illustrated in Figures 13 and 14.

c. Calculation of Quantum Yield

The chloride quantum yields encountered were very small so that the rates of the thermal reactions are at least comparable to those for the photolytic chloride release. Because of this and the need to keep the percent conversion relatively low (to give "true" quantum yields), the amounts of photolytically released chloride are often near the limit of sensitivity of the measuring instruments. The relative precision thus can not be high and it was sufficient to estimate the light intensity from the calibrated photocell output.

The calculations used are of two sorts and an example of each are given below.

(i) For $Cr(NH_3)_5Cl^{2+}$, for which even at 13°C, the rate of thermal release of chloride is much larger than that for photolytic release, so that any photochemical chloride release is not easily apparent from the [Cl^-] versus time

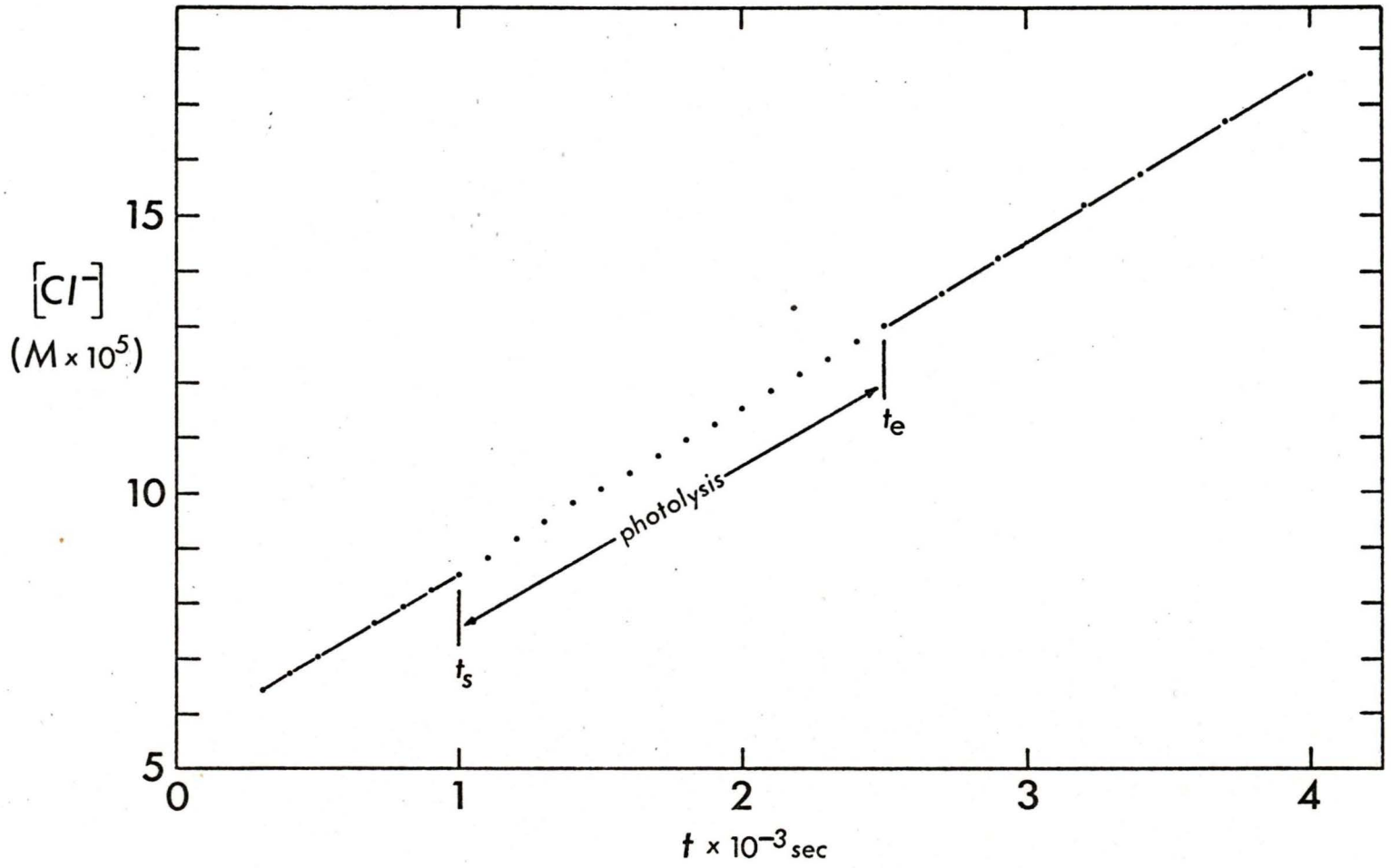

Figure 13. $[Cl^-]$ versus time plot for a photolysis run of $Cr(NH_3)_5Cl^{2+}$ (2.0×10^{-2}M) at 13°C using 565.4-nm light.

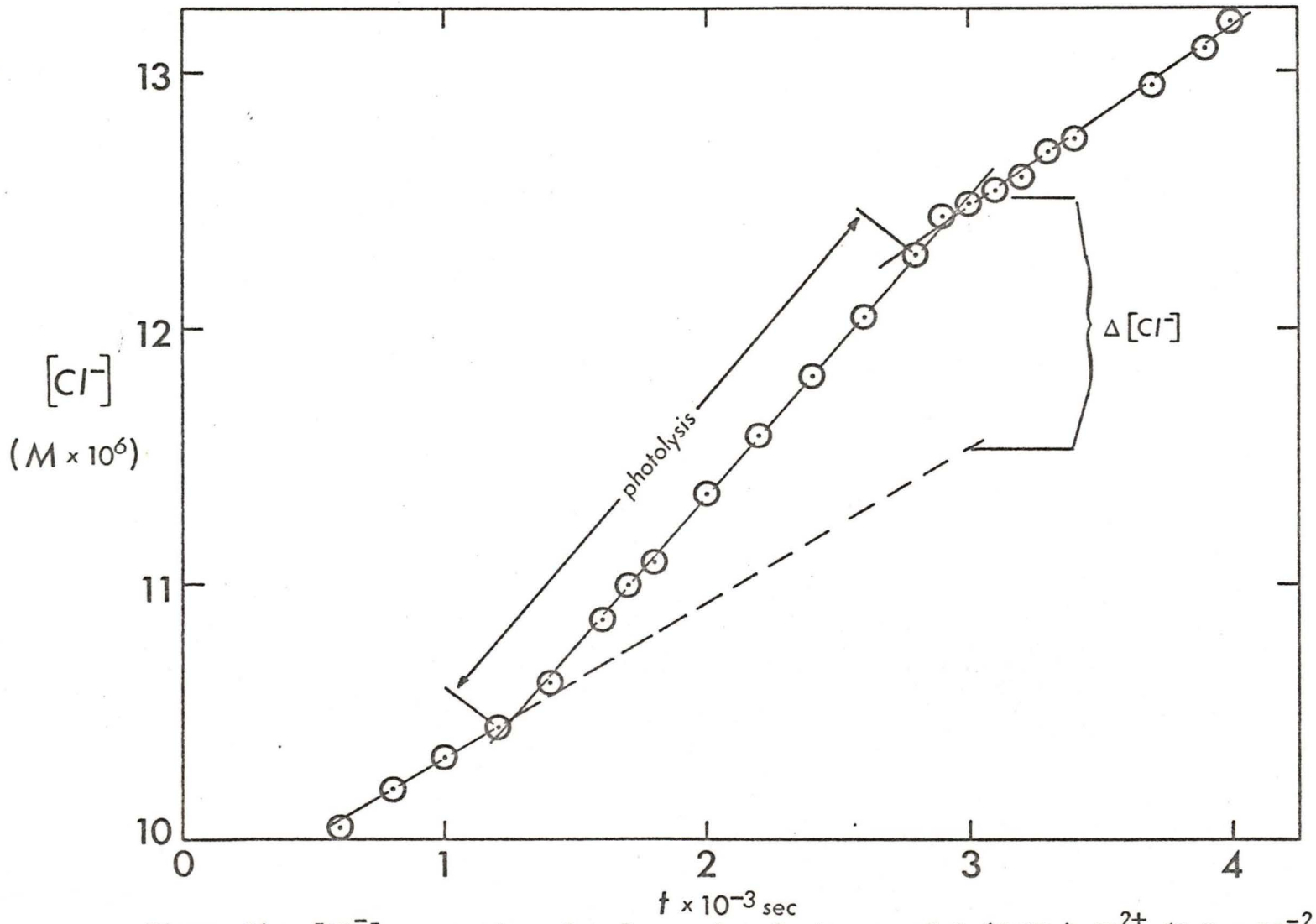

Figure 14. $[Cl^-]$ versus time plot for a photolysis run of $Cr(MeNH_2)_5Cl^{2+}$ (2.0×10^{-2}M) in 33% acetone/water, 13°C, pH 3, and using 401-nm light.

plot (for example, Figure 13), the following method is used to determine the photolytically released chloride:

The average rate of thermal chloride release during photolysis was taken to be the average of the pre- and post- photolysis rates. In principle, this accounted for the thermolysis of the primary photolysis product as well as that of the initial reactant (assuming linear dependence of the concentration of complex with time; see Section VI). In practice, since the rate of thermal chloride aquation is much greater than that of photolytic chloride release, very small variations in temperature and hence in the rates of the thermal reactions would give rise to very large relative errors for the calculated photolytic chloride. Taking the average of the pre- and post-photolysis thermal rates would also tend to cancel the effect of such temperature variations.

For the case shown in Figure 13, the pre- and post-photolysis thermal rates, obtained with a least squares fit, are

$$k_o = 3.017 \times 10^{-8} M \text{ sec}^{-1} \qquad \text{(II-6)}$$

$$\text{and } k_e = 3.049 \times 10^{-8} M \text{ sec}^{-1} \qquad \text{(II-7)}$$

(standard deviation $0.015 \times 10^{-8} M \text{ sec}^{-1}$)

The thermal rate during photolysis is then

$$k_p = \frac{k_o + k_e}{2} \qquad \text{(II-8)}$$

$$= 3.033 \times 10^{-8} M \text{ sec}^{-1}$$

At the start, t_s, and end, t_e, of photolysis, the observed chloride concentrations are

$$[Cl^-]_{t_s} = 8.52\ (\pm.02)\ X\ 10^{-5}M$$

$$[Cl^-]_{t_e} = 13.01\ (\pm.02)\ X\ 10^{-5}M \qquad \text{(II-9)}$$

At the end of photolysis (t=2500 sec), the chloride concentration due to thermal reaction is

$$[Cl^-]_{t_e}^{therm} = k_p(1500\ sec) + [Cl^-]_{t_s} \qquad \text{(II-10)}$$

$$= 13.07\ (\pm.04)\ X\ 10^{-5}M$$

Comparing this value with the observed $[Cl^-]_{t_e}$, it is apparent that, within experimental error, the net photolytic chloride is zero. Thus, the quantum yield is zero. An uncertainty may be estimated by assuming a generous upper limit of $0.05\ X\ 10^{-5}M$ for photolytically released chloride:

$$\Phi = \frac{\Delta[Cl^-]\ X\ V}{I_o(1-10^{-\varepsilon cl})t} = 3\ X\ 10^{-4} \qquad \text{(II-11)}$$

for $V = 5.0\ X\ 10^{-3}\ell$, $I_o = 1.36\ X\ 10^{-8}E\ sec^{-1}$ and $10^{-\varepsilon cl} = 0.550$.

(ii) For $Cr(MeNH_2)_5Cl^{2+}$, the first-order rate constant for chloride release is very small (at 13°C) and although that for the major photoproduct must be much larger (see earlier discussion), the absolute rate is quite small if conversion is kept small. Such a case is illustrated in Figure 14.

For this case an upper limit for the chloride quantum

yield may be determined by assuming that the photoproduct does not thermally lose chloride. The maximum photolytically released chloride, $\Delta[Cl^-]$, may be approximately determined as illustrated in Figure 15. $\Delta[Cl^-]$ was taken at a time about 200 seconds after photolysis since this is the approximate delay due to slightly inefficient mixing. It is apparent, however, that the error incurred from inefficient mixing would not be large since, absolutely, the post-photolysis thermal rate is not much larger than that before photolysis. Also, because of the relatively slow rates of thermal chloride release, the uncertainties in such determinations are relatively much lower than those in case (i).

This method of determining the maximum photolytically released chloride was also applied to the measurements for $Cr(EtNH_2)_5Cl^{2+}$ and $Cr(n\text{-}PrNH_2)_5Cl^{2+}$.

F. General Instrumentation

All absorbance (or transmittance) measurements were made using a Cary 17 spectrophotometer. All pH measurements were made at 20°C with a combination micro glass electrode (Metrohm AG 1900 Herisau) coupled to a Metrohm Compensator E388 potentiometer/pH meter, and chloride measurements, by coupling the Ag/AgCl electrode to the same Metrohm potentiometer.

III. RESULTS

A. Reconstruction of the Spectra of the Photolysis Products

For photolysis runs in water and 33% acetone/water, the concentration of the product was determined using the ΔpH method as described in Section II-E, after the difference spectrum and its corresponding baseline had been obtained. Thus the difference spectrum in absorbance may be converted to one in extinction coefficient. The spectrum of the photoproduct(s) can then be calculated by summing the difference spectrum and the spectrum of the starting material, both in extinction coefficients. For the photolysis of $Cr(MeNH_2)_5Cl^{2+}$ in 100% acetone, the product concentration was calculated assuming a value of 0.41 for the amine quantum yield; the light flux was monitored for the run (photocell).

The quality of such reconstructed spectra should be quite good. For all the complexes in this study, amine solvation to give $Cr(RNH_2)_4(S)Cl^{2+}$ is expected to be the predominant photochemical reaction, and chloride aquation upon ligand field irradiation should be very minor (confirmed by the relative magnitudes of the quantum yields; see Section III-C). If the conversion of the starting material is kept reasonably low (<10%) secondary photolysis is not important. Thermal aquation of the photolysis product is generally reasonably slow and should not be a severe problem for reasonably short (<1 hour) photolysis runs. For example, a first-order rate constant of 1×10^{-5} sec^{-1} (that for the photoproduct of $Cr(MeNH_2)_5Cl^{2+}$ at 20°C) would result in a

3.6% decomposition in the first hour, but since the product is formed continuously over the photolysis period, effectively, thermal decomposition would only be about 1.8% per hour during photolysis. Considering the relative purity which may be attained for isolated samples of comparable complexes, the extent of the thermal decompositions of the primary photoproducts experienced in this work should not be objectionable. More important is that the reproducibility, and hence the precision, of the difference spectra is not as good as would have been desired--the measured absorbances were small (maximum about 0.02). Since the product spectra are sums of the difference spectra and the corresponding spectra of the starting materials, however, an estimated uncertainty perhaps as low as 3% may be placed on the extinction coefficients.

The reconstructed product spectra for R=Me, Et, n-Pr and n-Bu are displayed in Figures 15, 16, 17 and 18, respectively; for comparison, the measured spectrum of the corresponding starting material are also shown. The spectrum of $Cr(MeNH_2)_5Cl^{2+}$ and that of its product of photolysis in 100% acetone are displayed in Figure 19.

B. The Influence of Thermal Reactions on Quantum Yield Measurements

In general, thermal reactions and photochemical reactions occur simultaneously during photolysis. Whereas in thermal kinetic studies, the photochemical reaction is a nuisance, the converse is true in photochemical investigations. The following considerations regarding the thermal reactions relate directly to the consideration of quantum yields in the next few sections and are thus appropriate here.

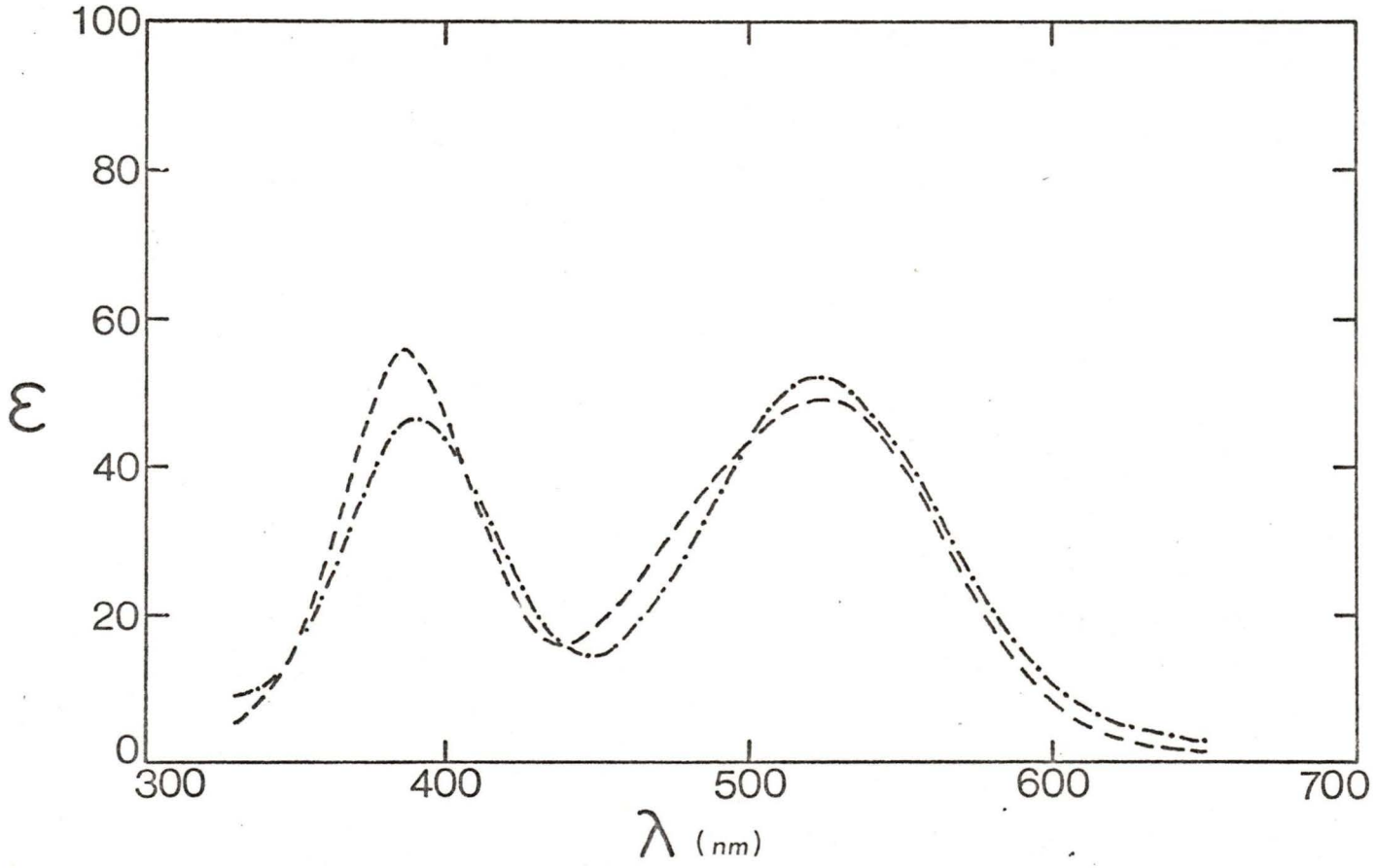

Figure 15. Absorption spectrum of $Cr(MeNH_2)_5Cl^{2+}$ (----) and that of its product of photolysis (-·-·) in water.

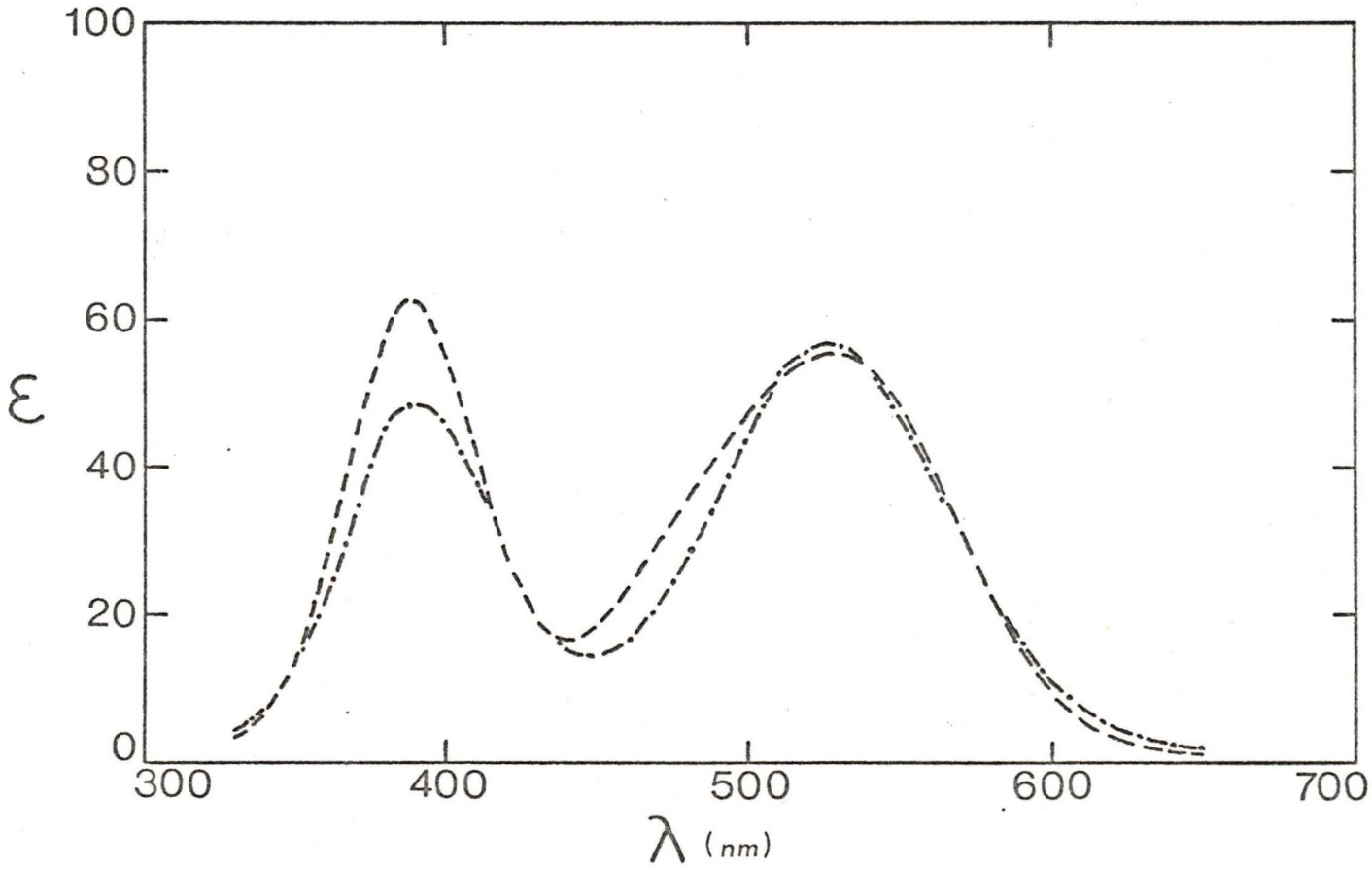

Figure 16. Absorption spectrum of $Cr(EtNH_2)_5Cl^{2+}$ (----) and that of its product of photolysis (-·-·) in water.

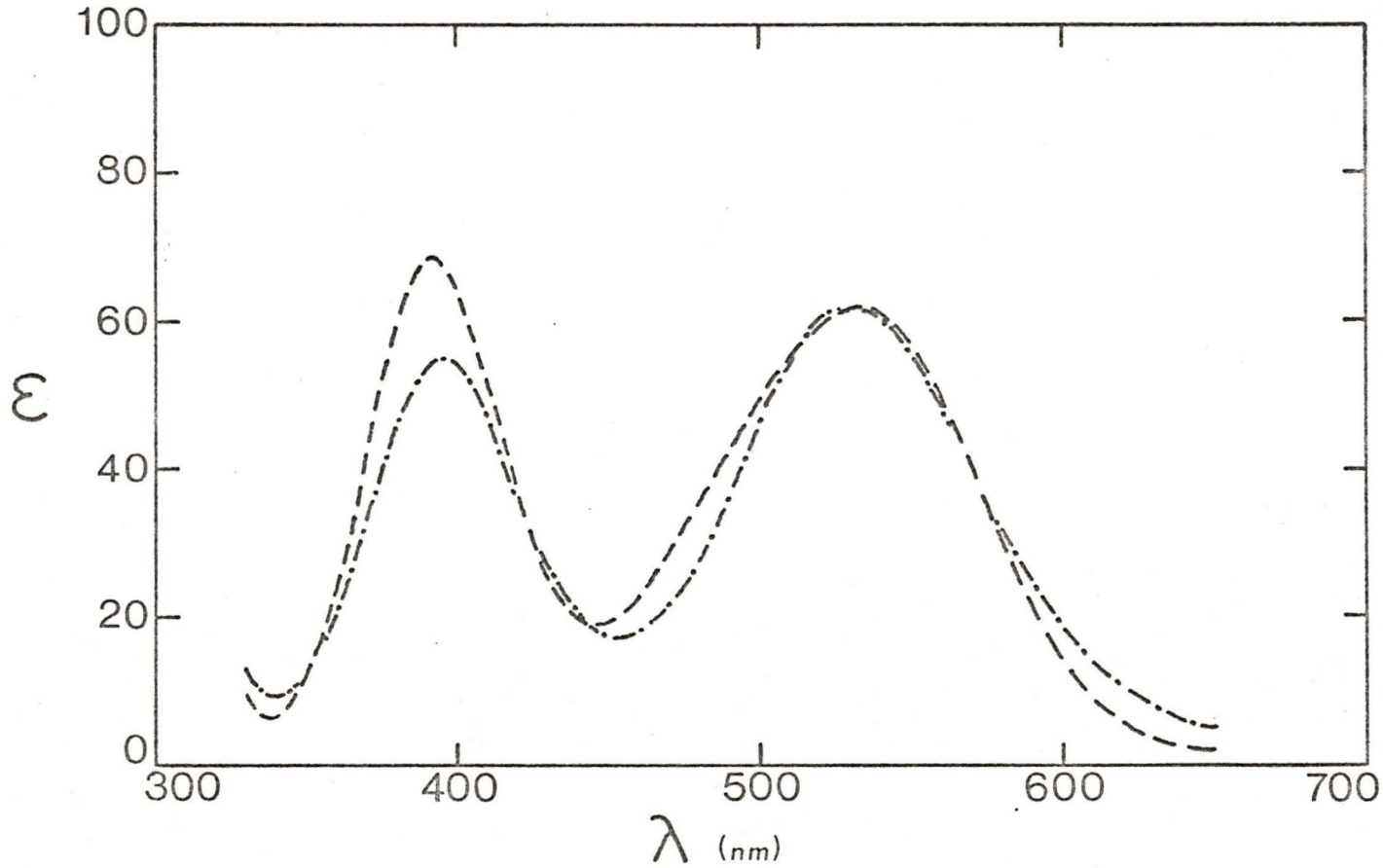

Figure 17. Absorption spectrum of $Cr(n\text{-}PrNH_2)_5Cl^{2+}$ (----) and that of its product of photolysis (-·-·) in 33% acetone/water.

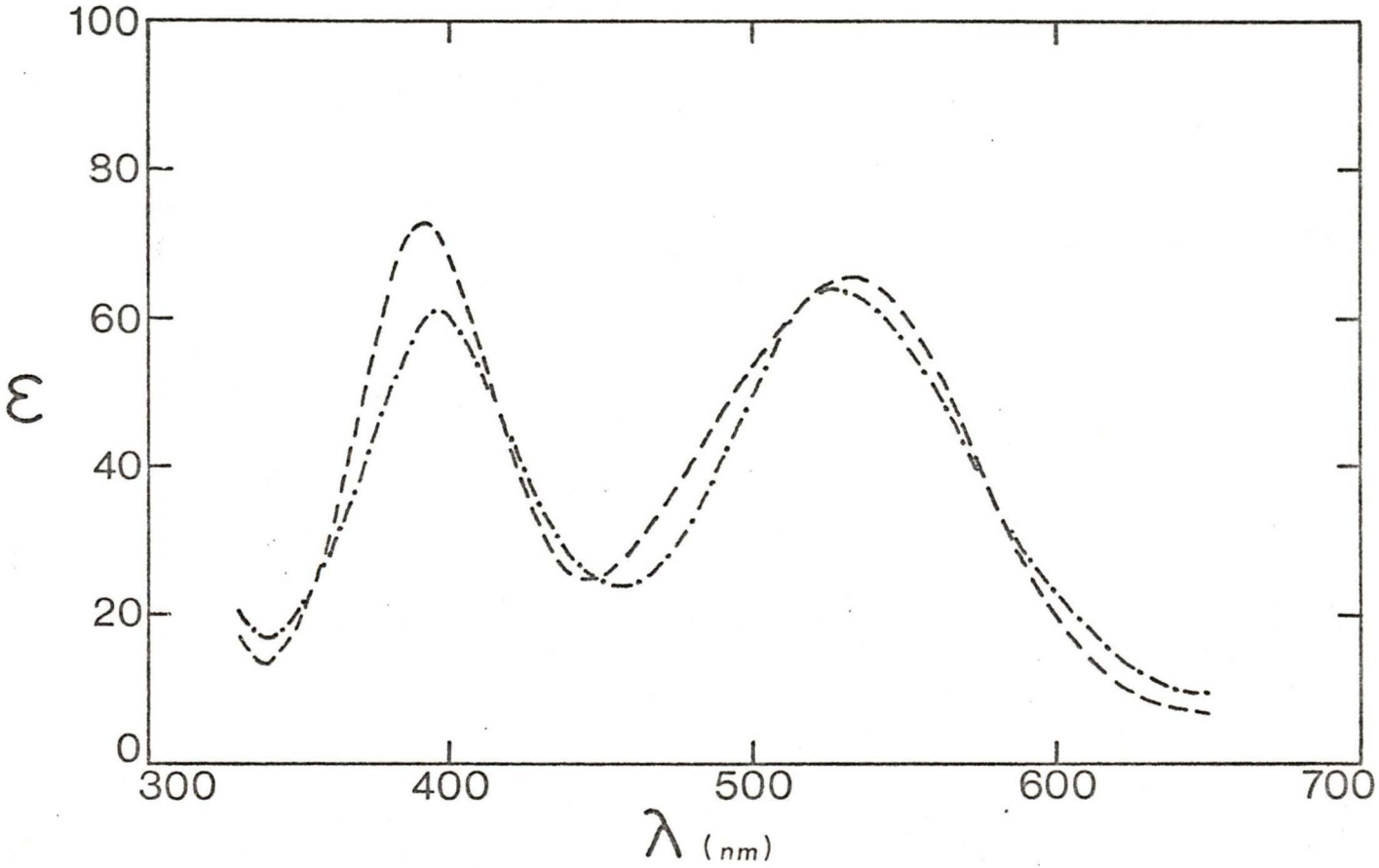

Figure 18. Absorption spectrum of $Cr(n\text{-}BuNH_2)_5Cl^{2+}$ (----) and that of its product of photolysis (-·-·) in 33% acetone/water.

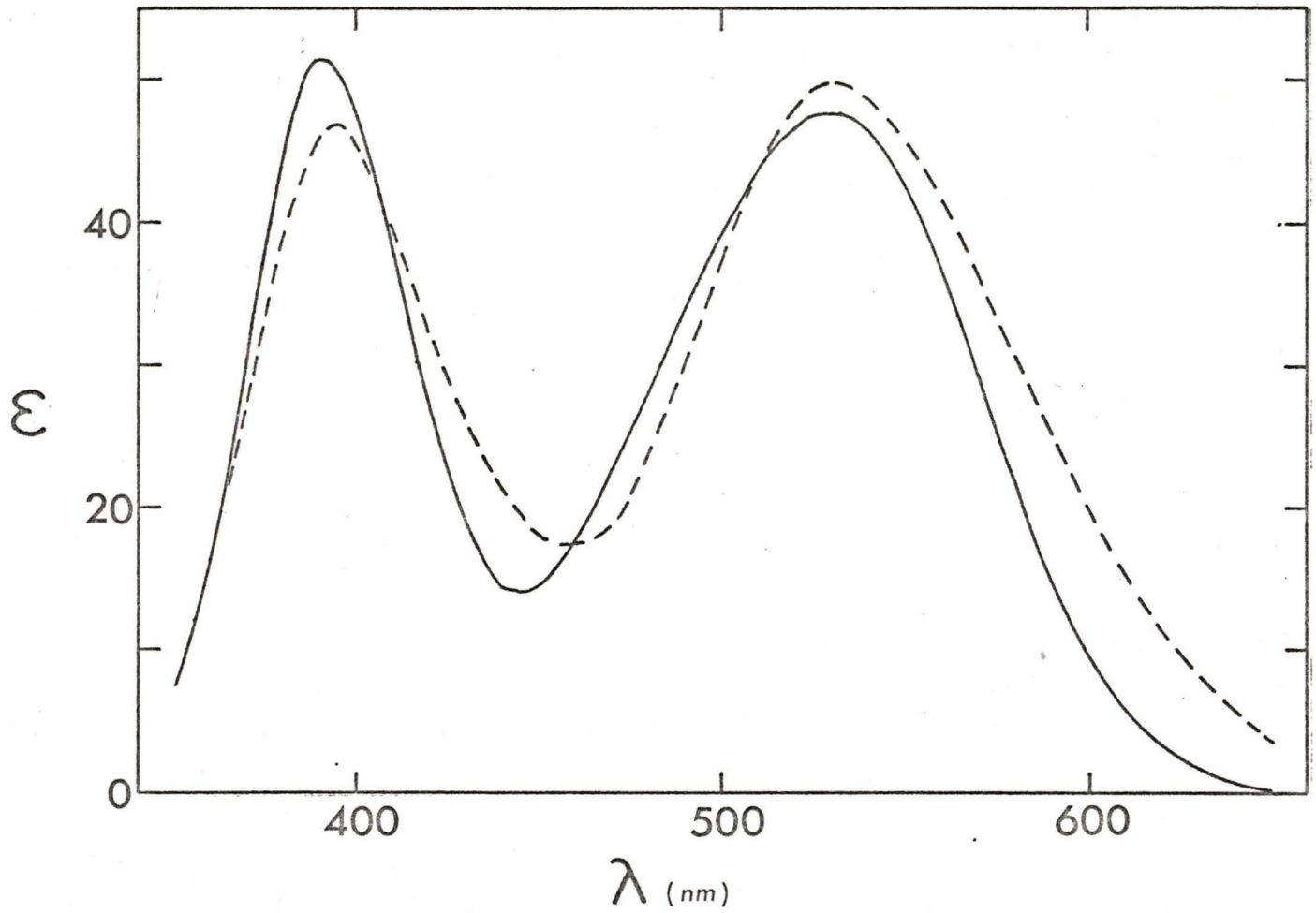

Figure 19. Absorption spectrum of $Cr(MeNH_2)_5Cl^{2+}$ (——) and that of its product of photolysis (----) in practically 100% acetone.

1. Amine Determinations

At pH<7 and near room temperatures, chloride aquation is essentially the only observed thermal reaction for the series of complexes used in this study (see Section I-E). Also, none of the photolyzed solutions showed observable post-photolytic pH changes so that thermal amine aquation is not important for the major photoproducts. Thus determinations of amine release by the ΔpH method are essentially free of any complicating thermal decomposition reactions. However, consideration of the acidity of the complexes is also important. Although the acid dissociation constants of the starting amine complexes, which have no aquo ligands, are expected to be very low ($pK_a \geq 14$)[54], the primary photoproducts, which are aquo complexes, are expected to have pK_a's of 5 to 6 (pK_a for $Cr(NH_3)_5(H_2O)^{3+}$ is about 5.3 at room temperature)[54] so that at pH 4, about 10% of the complex exists in the dissociated form. However, care was taken to photolyze solutions to less than 5% for practically all experiments so that the concentration of aquo product(s) is low and the $[H^+]$ is still reasonably high at the end of photolysis. Assuming a starting $[H^+]$ of 1.0×10^{-3}M and 5% conversion of a 1.0×10^{-2}M solution of complex to give 5×10^{-4}M in the aquo product(s), in the case of $pK_a = 5.0$, the contribution of H^+ from the aquo product(s) is only about 2%. A true correction cannot be applied because the pK_a's are not known, but it should suffice to note that, on a relative basis, the error should be even smaller than the absolute error, and thus may be neglected.

2. Chloride Determinations

As indicated in Sections I-E and II-E, thermal chloride release, due to both the starting material and the product of amine aquation, (?)cis-$Cr(MeNH_2)_4(H_2O)Cl^{2+}$, may complicate measurements of photolytically released chloride. Preliminary investigations of the chloride quantum yield for $Cr(MeNH_2)_5Cl^{2+}$ at 20°C, by considering the $[Cl^-]$ of the photolyzed, dark and initial solutions, and assuming negligible thermal chloride aquation of the photoproduct, showed that the calculated quantum yields increased quite dramatically with photolysis time, percent conversion and the length of time between the end of photolysis and measurement of $[Cl^-]$. Data for four trials, where the $[Cl^-]$ of the exposed solution was measured as quickly as possible are shown below.

photolysis time (sec)	% conversion	apparent Φ_{Cl^-}
1000	7.4	3.0×10^{-3}
1500	11.0	5.0×10^{-3}
1500	11.0	7.0×10^{-3}
2000	15.0	10×10^{-3}

A photolysis run at 20°C with continuous monitoring of $[Cl^-]$ (see Figure 20) indicated that the apparently increasing Φ_{Cl^-} with increasing photolysis time is due to the relatively fast thermal chloride aquation of the major photoproduct (from amine aquation). While the rate constant for $Cr(MeNH_2)_5Cl^{2+}$ is only about 8.8×10^{-8} sec^{-1}, that for (?)cis-$Cr(MeNH_2)_4(H_2O)Cl^{2+}$ is about 100-fold greater, about 1.05×10^{-5} sec^{-1}.

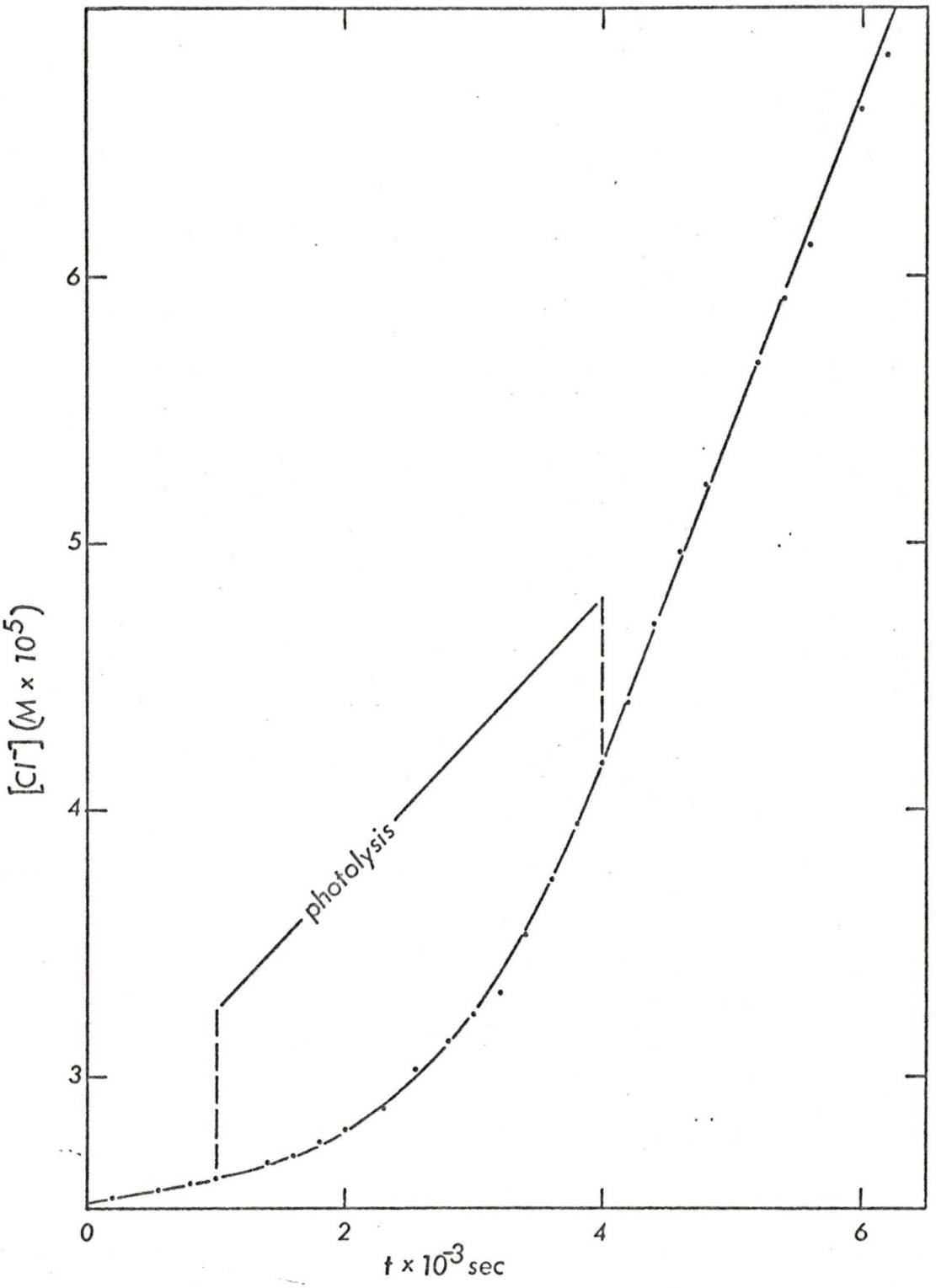

Figure 20. Plot of $[Cl^-]$ versus time for photolysis of $Cr(MeNH_2)_5Cl^{2+}$ at 20°C. The plot shows that the rate of thermal chloride aquation of the major photoproduct, (?)cis-$Cr(MeNH_2)_5(H_2O)Cl^{2+}$, is much larger than that for its starting material.

As a result, the method adopted for chloride determinations in this work (described in Section II-E) emphasized continuous monitoring and low conversions together with reasonably accurate measurements of low chloride concentrations by using the relatively sensitive technique outlined earlier. Coupled with the fact that the use of a relatively unreliable thermal dark run is eliminated, the results obtained, using this method, should be quite reliable.

C. Quantum Yields

1. Amine Quantum Yields

Table IV shows the quantum yields for amine aquation for the series of complexes under various irradiations, solvents and temperatures. The determinations for $Cr(NH_3)_5Cl^{2+}$ in water were carried out to ensure that the photolysis system and techniques used gave results which are absolutely comparable to those obtained by other workers; this complex has been reasonably well studied and there is generally good agreement between the ammonia quantum yields[18, 25] (see Table I).

Since a quantitative comparison of the quantum yields was desirable, photolysis of the series of complexes was performed in at least one common solvent. The mixture of 33 w/w% acetone/water was chosen on the bases of solubility (the complexes with R=n-Pr and n-Bu were not water-soluble) and ease of quantum yield analyses. Photolyses were also carried out in water (R=H, Me and Et) partly to facilitate comparisons between these quantum yields and those for photolysis of other complexes, which have largely been performed in water, and partly to investigate the solvent dependence. The

Table IV

Amine aquation quantum yields for $Cr(RNH_2)_5Cl^{2+}$ ions.

R	irradiation λ (nm)	T°C	Φ_{RNH_2} [a]	Φ_{ave} [b]	[complex] M x 10^2	solvent [c]
H	401.2	20.0	0.376, 0.376	0.37_6	1.0	water
	479.0	20.0	0.395, 0.397 0.404	0.39_9		
	565.4	20.0	0.424, 0.421	0.42_3		
		8.0	0.361, 0.370	0.36_6		
		20.0	0.414, 0.413	0.41_4	1.0	33% acetone
Me	401.2	20.0	0.349, 0.342 0.346, 0.342	0.34_5	1.0	water
	479.0	20.0	0.371, 0.363 0.366	0.36_7		
	565.4	20.0	0.376, 0.371	0.37_4		
			0.384, 0.383	0.38_4 [d]		
			0.382, 0.372	0.37_7 [e]		
		11.5	0.364, 0.356	0.36_0		
		5.5	0.342, 0.335 0.335, 0.341	0.33_8		
	401.2	20.0	0.347, 0.354	0.35_1	1.0	33% acetone
	479.0	20.0	0.396, 0.386	0.39_1		
	565.4	20.0	0.387, 0.400 0.393	0.39_3		
		8.0	0.369, 0.374	0.37_2		
		20.0	0.38 , 0.43	0.41	1.0	100% acetone
Et	401.2	20.0	0.202, 0.204	0.20_3	0.90	water
	479.0	20.0	0.263, 0.266 0.260	0.26_3		

(cont.)

	565.4	20.0	0.245, 0.251	0.24_8		
		13.0	0.230, 0.227	0.22_9		
		8.0	0.223, 0.220	0.22_2		
		6.0	0.220, 0.214	0.21_7		
	401.2	20.0	0.229, 0.228	0.22_9	0.90	33% acetone
	479.0	20.0	0.243, 0.249	0.24_6		
	565.4	20.0	0.236, 0.238	0.23_7		
		8.0	0.205, 0.209	0.20_7		
n-Pr	401.2	20.0	0.201, 0.202	0.20_2	0.80	33% acetone
	479.0	20.0	0.217, 0.214	0.21_6		
	565.4	20.0	0.214, 0.209 0.207, 0.218	0.21_2		
		16.0		0.19_9		
		12.0		0.19_6		
		9.5		0.18_2		
		5.5		0.17_9		
n-Bu	401.2	20.0	0.168, 0.172	0.17_0	0.80	33% acetone
	479.0	20.0	0.197, 0.187	0.19_2		
	565.4	20.0	0.175, 0.174 0.180, 0.174	0.17_6		

[a] Each value represents a separate photolysis run.

[b] Average quantum yield value.

[c] Water= 0.05 M $KClO_4$, 10^{-3}M $HClO_4$; 33% acetone= 0.02 M $KClO_4$, 10^{-3}M $HClO_4$; 100% acetone= 10^{-3}M $HClO_4$, practically dry acetone.

[d] These runs were carried out using a quartz-iodine lamp as light source; a high pressure mercury lamp was used for all other runs.

[e] Δc_H was determined titrimetrically.

experiments with $Cr(MeNH_2)_5Cl^{2+}$ in practically 100% acetone concluded the solvent dependence study for this complex.

The temperature dependence was investigated only at one wavelength, 565 nm. For photolysis runs at constant irradiating wavelength, the relative uncertainties involved in the use of reineckate actinometry for light flux measurements are eliminated. Thus, relatively, the quantum yields are accurate, and their temperature dependence, in a particular solvent, may be quantitatively treated. The apparent activation energies, E_{app}, are listed in the second column of Table V.

2. Chloride Quantum Yields

The chloride quantum yields for the series of complexes are listed in Table VI; determinations for R=n-Bu were omitted because of solubility problems at 13°C. Temperature dependence was not investigated since it was anticipated that uncertainties arising from the instability of the measuring electrode (at lower temperatures) and complications due to thermal reactions (at higher temperatures) would be sufficiently large to mask any real temperature dependence.

Table V

Activation energies for photoaquation of amine for the $Cr(RNH_2)_5Cl^{2+}$ complexes upon irradiation at 565.4 nm[a].

complex	E_{app} (kcal/mole)	$E_r - E_{ic}$[b] (kcal/mole)	solvent
$Cr(NH_3)_5Cl^{2+}$	2.1 ± 0.4[c]	3.5 ± 0.6	water
$Cr(MeNH_2)_5Cl^{2+}$	1.2 ± 0.3	1.9 ± 0.5	water
	0.8 ± 0.4	1.2 ± 0.6	33% acetone
$Cr(EtNH_2)_5Cl^{2+}$	1.5 ± 0.3	2.0 ± 0.4	water
	1.8 ± 0.4	2.4 ± 0.5	33% acetone
$Cr(n\text{-}PrNH_2)_5Cl^{2+}$	1.9 ± 0.4	2.4 ± 0.5	33% acetone

[a] Temperature dependence for R= n-Bu was not studied because of solubility problems at low temperatures.

[b] Difference of activation energies for photochemical reaction and internal conversion ($^4T_2 \longrightarrow {}^4A_2$).

[c] Estimated uncertainties assuming the precision of the measured quantum yields is about 2%.

Table VI

Chloride aquation quantum yields for $Cr(RNH_2)_5Cl^{2+}$ ions at 13°C.

R	irradiation λ (nm)	% conversion/ time (sec)	Φ_{Cl^-} [a]	Φ_{corr} [b]	Remarks [c]
H	401.2	2.4/1500	2×10^{-4} [d]		2×10^{-2} M
	565.4	3.5/1500	$<3 \times 10^{-4}$		in water
Me	401.2	3.2/1500	1.6×10^{-3}	1.4×10^{-3}	2×10^{-2} M
	565.4	6.9/1900	3.4×10^{-4}		in water
	401.2	1.9/1000	8.5×10^{-4} [e]	6×10^{-4}	2×10^{-2} M in
	565.4	4.8/1000	5.9×10^{-4}		33% acetone
Et	401.2	4.4/2000	1.1×10^{-3}	1.0×10^{-3}	9×10^{-3} M in
	565.4	8.7/1500	1.2×10^{-4}		in water
	401.2	2.7/1500	4.7×10^{-4}	4×10^{-4}	1×10^{-2} M in
					33% acetone
n-Pr	401.2	2.2/1000	7.1×10^{-4}	6×10^{-4}	1×10^{-2} M in
	565.4	4.5/1500	1.9×10^{-4}		33% acetone

[a] The quantum yields are upper limits calculated under the assumption that the major photoproduct, (?)cis-$Cr(RNH_2)_4(H_2O)Cl^{2+}$, does not thermally release chloride, except for R= H.

[b] These are corrected quantum yields for photolysis at 401 nm assuming that the true quantum yield at 565 nm is zero. Corrections were made by subtracting an approximately weighted quantity obtained by considering the percent conversions and the photolysis times at 565 and 401 nm.

[c] Water= 0.05 M $KClO_4$, 10^{-3} M $HClO_4$; 33% acetone= 0.02 M $KClO_4$, 10^{-3} M $HClO_4$.

[d] Precision about ± 3×10^{-4}.

[e] Average of two runs; all other values were obtained from one run.

IV. DISCUSSION

A. Solvent Effects on Reaction Mode and Stereochemistry

1. Consideration of Solvent Effects on the Reaction Mode

For each of the complexes, upon irradiation of the Q_1 band, the extent of predominance of the photosubstitution of amine (over that of chloride) is so large (>99%) that in the interpretation of the product spectra, it is not necessary to consider the product of chloride substitution. This is also so for the photoreactions in the mixed solvents, but here, photosubstitution of amine both by acetone and water is possible:

$$Cr(RNH_2)_5Cl^{2+} + h\nu \xrightarrow{+H_2O} Cr(RNH_2)_4(H_2O)Cl^{2+} + RNH_2 \qquad (10)$$

$$Cr(RNH_2)_5Cl^{2+} + h\nu \xrightarrow{+ac} Cr(RNH_2)_4(ac)Cl^{2+} + RNH_2 \qquad (11)$$

Furthermore, thermal equilibration of the two products, if both are formed, is possible.

In 33% acetone/water, Reaction 11 is probably not important. In this solvent, the concentration of acetone and water are approximately 5.5 and 35 molar, respectively. Thus the mole fraction of water is about 0.86. Together with the expectation that water should preferentially solvate the dipositive complex ions of interest, the primary solvent shell should be composed almost exclusively of water molecules. Since photosubstitution reactions are very fast, the predominance of Reaction 10 over Reaction 11

should at least correspond to the statistical distribution of water and acetone in the primary solvent shell. Furthermore, polarity considerations suggest that additional to the large predominance of water in the solvation shell, any acetone molecules in this shell should tend to be oriented away from the side containing the chloride ligand. Therefore essentially all solvent molecules immediately adjacent to the chloride ligand will be water. In terms of the available theory, the amine ligand trans to the chloride should be substituted and the solvent should enter from a position trans to the leaving group, namely a water molecule from the chloride side. Thus, in 33% acetone, photosubstitution by acetone should be very unlikely.

Similar considerations for photolysis in practically 100% acetone would suggest that acetone substitution should be appreciably more likely here than in 33% acetone/water. In this solvent, the added water (in the form of aqueous $HClO_4$) was about 0.02% or roughly 1×10^{-2}M. The total concentration of water may reasonably be two or three times as high. However, since the photolysis solution is 1.0×10^{-2}M in complex, even if one assumes that the acetone solution is about 2 to 3×10^{-2}M in H_2O then, on average, the solvation shell of each complex ion could contain only two to three water molecules. Appreciable photosubstitution by acetone, if such substitution is possible, will thus be likely.

2. Interpretation of the Product Spectra: Identification of the Photolysis Products

a. In water and in 33 w/w% acetone/water

According to the considerations in the previous section, the photoreactions in water and in 33 w/w% acetone/water may be

expected to be identical. Thus for both solvents, the product spectra may be interpreted under the assumption that the sole photoreaction is amine aquation. The aim of the following discussion is to determine the configuration, or the cis-trans ratio of the $Cr(RNH_2)_4(H_2O)Cl^{2+}$ product.

The extent of predominance of one isomer can be estimated by comparing the difference spectrum with difference spectra computed on the basis of various cis-trans ratios of the aquo-product[14] (e.g. Figure 21). However, due to uncertainties in the respective spectra, only a lower limit may be placed on the extent of predominance. A conservative lower limit for $Cr(NH_3)_5Cl^{2+}$ photolysis, based on the comparison made by Kirk[14] (Figure 21), seems to be about 90% for the cis-product.

In this study, direct comparison of the product spectra with those of the cis- and trans-$Cr(RNH_2)_4(H_2O)Cl^{2+}$ isomers is not possible. None of these have been isolated (except for R=H) as solid samples and comparison with the preparations of the ammonia analogues[7] suggests that preparation of solid samples of the above isomers would be extremely difficult. Isolation of samples of the aquo-products via photolysis and ion-exchange chromatography (assuming both isomers may be formed) was not expected to be fruitful. Separation of the isomers of the ammonia analogues by ion-exchange has been shown (Section II-D-1) to be very difficult practically.

However, meaningful interpretation of the product spectra is possible since the spectra of the cis- and trans-$Cr(RNH_2)_4(H_2O)Cl^{2+}$ isomers may be expected to parallel those for

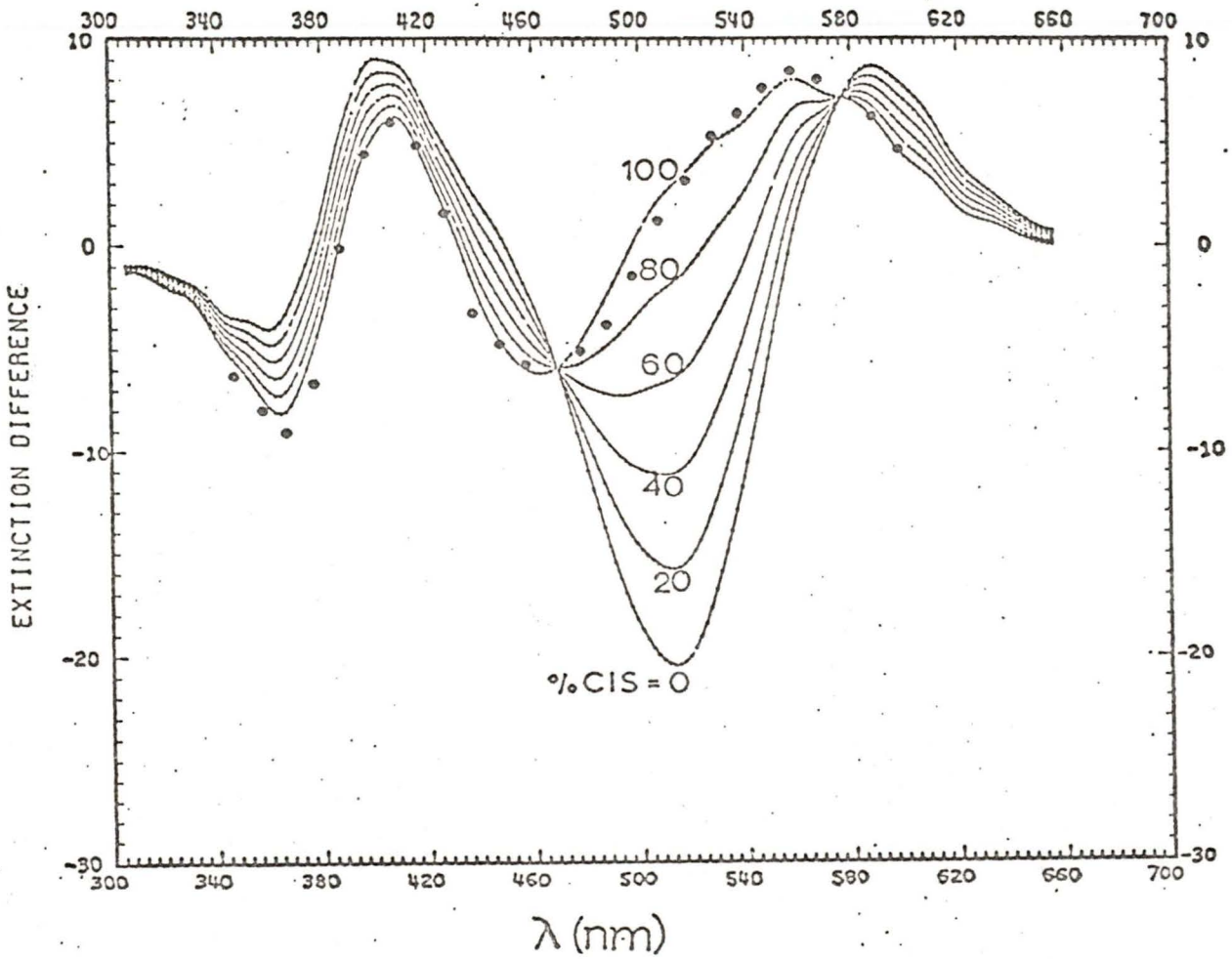

Figure 21. Comparison of the experimental difference spectrum for the photolysis of $Cr(NH_3)_5Cl^{2+}$ (••••) and the difference spectra computed for various mixtures of <u>cis</u> and <u>trans</u>-$Cr(NH_3)_4(H_2O)Cl^{2+}$ as products (from Ref. 14).

the NH_3 analogues. The spectra for cis- and trans-$Cr(NH_3)_4(H_2O)Cl^{2+}$, together with $Cr(NH_3)_5Cl^{2+}$, are displayed in Figure 22. The spectral differences between the cis and trans isomers are large. For the cis-complex, both the Q_1 and Q_2 bands are red-shifted with respect to those for $Cr(NH_3)_5Cl^{2+}$ and the maximum extinction coefficient, ε_{max}, for the Q_1 band is slightly raised while that for the Q_2 band is slightly lowered. For the trans-complex, the Q_1 band is visibly split and ε_{max} is much lower than those for either the cis-isomer or $Cr(NH_3)_5Cl^{2+}$; the Q_2 band is red-shifted and its ε_{max} is higher than that for $Cr(NH_3)_5Cl^{2+}$.

Comparison of the spectra of the photolysis products of the chloropentakis (alkylamine) chromium(III) complexes (Figures 15-18) with those of cis and trans-$Cr(NH_3)_4(H_2O)Cl^{2+}$ indicates that in each case, the product is predominately cis. However, closer examination shows that the relative differences between the spectra of the products and that of the corresponding starting materials differ from those between cis-$Cr(NH_3)_4(H_2O)Cl^{2+}$ and $Cr(NH_3)_5Cl^{2+}$. For each product/reactant pair, the red-shift of λ_{max} and decrease in ε_{max} of the Q_2 band of the product spectrum parallels the ammonia case, but in contrast to the spectral differences of the cis-$Cr(NH_3)_4(H_2O)Cl^{2+}$/$Cr(NH_3)_5Cl^{2+}$ pair, λ_{max} of the product Q_1 band seems to be slightly blue-shifted relative to that of the reactant, and ε_{max} for the Q_1 bands of (?)cis-$Cr(n\text{-}PrNH_2)_4(H_2O)Cl^{2+}$ and (?)cis-$Cr(n\text{-}BuNH_2)_4(H_2O)Cl^{2+}$ are lower than those of the corresponding reactants. The

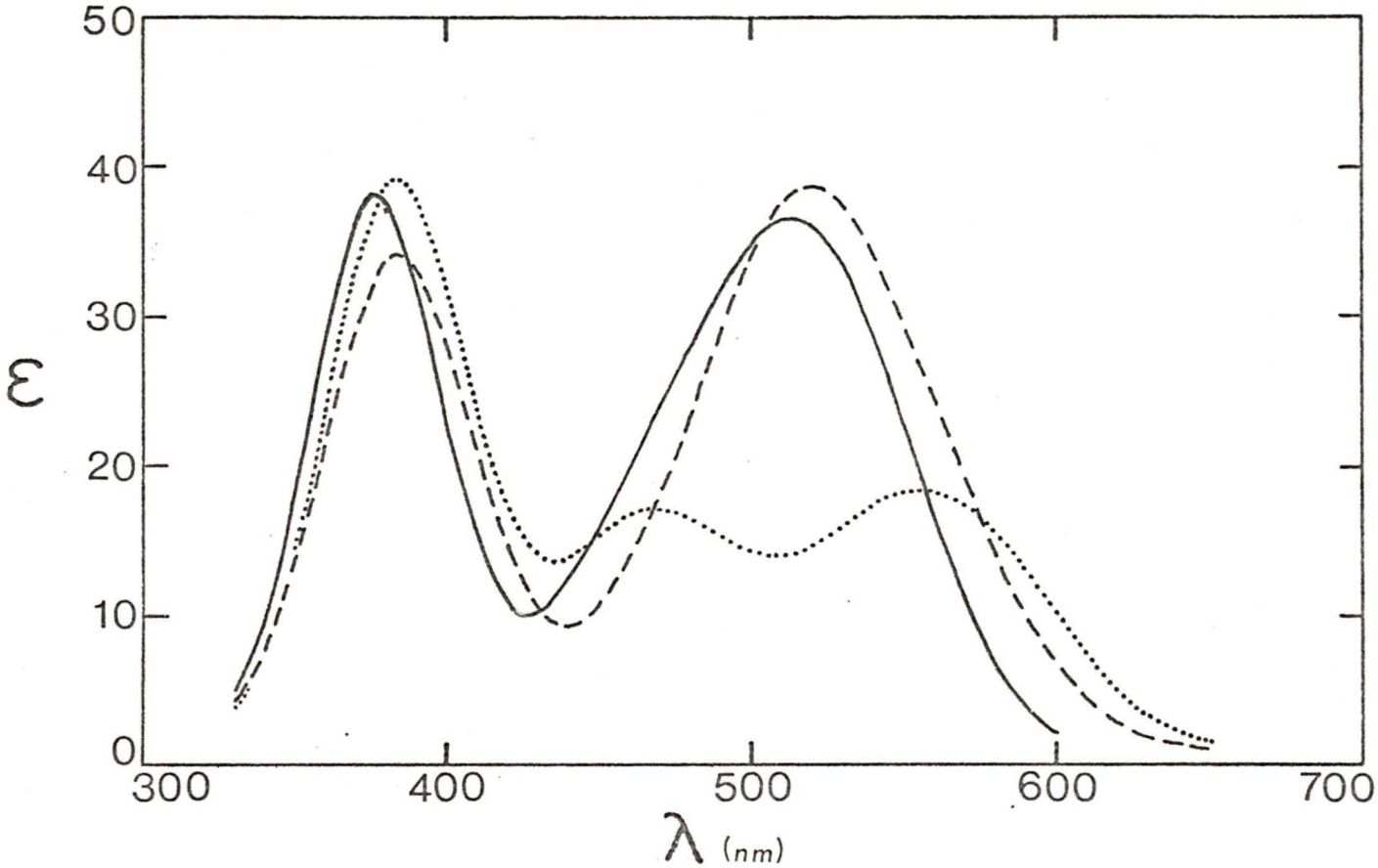

Figure 22. Absorption spectra of $Cr(NH_3)_5Cl^{2+}$ (——), <u>cis</u>-$Cr(NH_3)_4(H_2O)Cl^{2+}$ (----) and <u>trans</u>-$Cr(NH_3)_4(H_2O)Cl^{2+}$ (····).

relative differences are outside of experimental error and merit discussion.

The relative differences between the spectral characteristics of the alkylamine product/reactant pairs and those of cis-$Cr(NH_3)_4(H_2O)Cl^{2+}$ and $Cr(NH_3)_5Cl^{2+}$ might be explained by assuming various contributions of the trans-$Cr(RNH_2)_4(H_2O)Cl^{2+}$ as product. However this assumption is not necessary if careful considerations concerning the expected (or predicted) spectrum of each cis-$Cr(RNH_2)_4(H_2O)Cl^{2+}$ ion are made. Such considerations, based on extrapolation of some available spectral data on hexaaminechromium(III) and the chlorapentakis(alkylamine)chromium(III) complexes of this study, are described in what follows. It should be emphasized that the extent of predominance of the cis-product can only be finally decided when reliable spectra of the cis- and trans-isomers become available.

Table VII lists some spectral data for a number of hexaaminechromium(III) complexes and their ligand field parameters, Δ. Notable are that while the Δ values for $Cr(MeNH_2)_6^{3+}$ and $Cr(ibn)_3^{3+}$ are lower than that for $Cr(NH_3)_6^{3+}$, those for $Cr(en)_3^{3+}$ and $Cr(pn)_3^{3+}$ are higher. Since the amines are not expected to be π-donating, so that the ligand field strength should be primarily determined by the σ-bonding ability, the trend of Δ values is not the expected one. For the amines, the σ-donating ability should be in the following order,

$$NH_3 < en \simeq pn \simeq ibn \simeq MenH_2$$

since the alkyl groups are slightly electron-donating with

Table VII

Selected spectral data for some hexaaminechromium(III) complexes[a].

complex	λ_{max} ($^4T_{1g}$)	λ_{max} ($^4T_{2g}$)	$\Delta = \bar{\nu}_{max}$ ($^4T_{2g}$)[b]
$Cr(MeNH_2)_6^{3+}$	361 nm	474 nm	21,100 cm^{-1}
$Cr(ibn)_3^{3+}$	359	474	21,100
$Cr(NH_3)_6^{3+}$	350	464	21,550
$Cr(pn)_3^{3+}$	350	457	21,880
$Cr(en)_3^{3+}$	351	456	21,930

ibn = isobutylenediamine = $H_2NCH_2C(CH_3)_2NH_2$

pn = propylenediamine = $CH_3CH(NH_2)CH_2NH_2$

en = ethylenediamine = $H_2NCH_2CH_2NH_2$

[a] From Ref. 54.

[b] The lowest energy spin-allowed band directly gives Δ (or 10 Dq)[55].

respect to hydrogen. Thus the ligand field strength of the amine ligands should be in the same order:

$D_q(NH_3) < D_q(en) \simeq D_q(pn) \simeq D_q(ibn) \simeq D_q(MeNH_2)$.

In the absence of other factors, $\Delta[Cr(NH_3)_6^{3+}]$ should be smaller than Δ for all the alkyl-containing amine complexes listed in Table VII.

Space-filling models of the hexaamine complexes show that although there is little or no steric hindrance in the NH_3, en and pn complexes, it becomes important in the $MeNH_2$ and ibn analogues. The steric effect is due to the bulkiness of the amine group near the Cr-N bonding site and has been invoked in explaining the lower than expected Δ value for $Cr(MeNH_2)_6^{3+}$[56]. The same explanation appears to be satisfactory for $Cr(ibn)_4^{3+}$. Thus the relation between this steric effect and Dq may be expected to be a general one.

Space-filling models of the chloropentaaminechromium(III) complexes, $Cr(RNH_2)_5Cl^{2+}$, show that steric hindrance is also important for the alkylamine complexes (but not for $Cr(NH_3)Cl^{2+}$). Whereas the importance of steric hindrance is reflected in the smaller than expected Δ values for the octahedral (or trigonal)[57] hexaamine complexes, the interpretation is more difficult for the $Cr(RNH_2)_5Cl^{2+}$ ions, which are not octahedral. However, comparison of the spectral data for the $Cr(RNH_2)_5Cl^{2+}$ ions (Table VIII) with those for the hexaamine complexes (Table VII) suggests that for the series of chloropentaamine ions, the average ligand field strength should be proportional to the energy of the absorption maximum of the Q_1 band. For the

Table VIII

Spectral characteristics of the $Cr(RNH_2)_5Cl^{2+}$ ions.

complex	λ_{max} [a] ($^4T_1$)	λ_{min}	λ_{max} ($^4T_2$)	$\bar{\nu}_{max}$ ($^4T_2$)
$Cr(NH_3)_5Cl^{2+}$	376 (38.2)[b]	426 (10.0)	513 (36.5)	19,490 cm^{-1}
$Cr(MeNH_2)_5Cl^{2+}$	386 (55.1)	438 (15.9)	524 (49.1)	19,080
$Cr(EtNH_2)_5Cl^{2+}$	388 (62.4)	440 (16.5)	528 (55.4)	18,940
$Cr(n\text{-}PrNH_2)_5Cl^{2+}$	389 (67.8)	442 (18.2)	530 (62.0)	18,870
$Cr(n\text{-}BuNH_2)_5Cl^{2+}$	390 (72.5)	443 (25.1)	531 (65.4)	18,830

[a] Wavelengths are in nm.

[b] Figures in parentheses are the extinction coefficients (in cm^{-1} $mole^{-1}$ $liter^{-1}$) corresponding to the absorption wavelengths.

alkylamine complexes, the trend of average ligand field strength is consistent with the expectation that the σ-donating ability of the alkylamines are almost identical, and that the effect of steric hindrance increases slightly as the alkyl chain is lengthened.

Upon substitution of an amine group with a much less bulky water ligand, some relief of steric hindrance is possible. The relative ligand field strengths of the chloropentakis(alkylamine) and chloroaquotetrakis(alkylamine) complexes should thus depend on both this factor, which tends to increase the average ligand field, and the fact that $Dq(H_2O) < Dq(RNH_2)$, which tends to lower it. A small blue shift of the Q_1 band for cis-$Cr(RNH_2)_4(H_2O)Cl^{2+}$ (with respect to that for the corresponding $Cr(RNH_2)_5Cl^{2+}$) is possible if the relief of steric hindrance is more important. Thus the small blue shifts observed for the Q_1 band maximum of the photoproducts of the $Cr(RNH_2)_5Cl^{2+}$ ions (refer to Figures 15-18) is not inconsistent with the products being very predominantly cis.

Rationalization of the relative differences between the ε_{max} values of the Q_1 band of the spectra of the product/reactant pairs remains. The magnitude of ε_{max}, or more precisely, of $\int \varepsilon d\bar{\nu}$, depends on the degree to which the parity-forbiddeness of the observed d-d transitions is degraded by the coupling of electronic wavefunctions and appropriate vibrational wavefunctions, as well as the Franck-Condon and spin factors[58]. Application of theoretical treatments, based on these factors,

to predict $\int \varepsilon d\bar{\nu}$ values is not practical. Thus an empirical treatment, although it is necessarily approximate, is more appropriate.

The trend of increasing ε_{max} the Q_1 band of the $Cr(RNH_2)_5Cl^{2+}$ complexes (Table VIII), going from R=H to R=n-Bn, suggests that each amine may be empirically assigned with an effective ability to degrade the parity-forbiddeness of the d-d transitions, this ability increasing from R=H to R=n-Bn and hence increasing $\int \varepsilon d\bar{\nu}$ (and generally ε_{max}) in the same order. Referring to the ε_{max} of the Q_1 bands in question, then, whereas replacement of NH_3 by H_2O in a cis-position of $Cr(NH_3)_5Cl^{2+}$ increases ε_{max} by x units in extinction coefficient, the same replacement of $MeNH_2$ in $Cr(MeNH_2)_5Cl^{2+}$ should increase ε_{max} by y units, where $y < x$. And in general, as the alkylamine is lengthened, the change in ε_{max} upon water substitution of an in-plane amine ligand should become less positive, at some point become zero (R=n-Pr), and finally become increasingly negative. A correlation of the change in ε_{max} of the Q_1 band going from $Cr(RNH_2)_5Cl^{2+}$ to the photoproduct (Table IX) shows this trend. The correlation is rather good and the trend is consistent with the photoproducts being cis-$Cr(RNH_2)_4(H_2O)Cl^{2+}$ or at least very predominantly so. (In the calculation of $\Delta\varepsilon_{max}$ for the ammonia complexes, it is better to use $\varepsilon_{max}(2)$ of the reconstructed spectrum since $\Delta\varepsilon_{max}$ will then be compared on the same basis for the complete series.)

With the above rationalization of the relative differences (λ_{max} shifts and ε_{max} changes), between the spectra of the

Table IX

Correlation of $\Delta\varepsilon_{max}$ of the Q_1 bands of the $Cr(RNH_2)_5Cl^{2+}$ ions and their photoproducts, (?)cis-$Cr(RNH_2)_4(H_2O)Cl^{2+}$.

R	$\varepsilon_{max}(1)$[a]	$\varepsilon_{max}(2)$[a]	$\Delta\varepsilon_{max}$[b]
H	36.5	39 (42)[c]	2.5 (5.5)[d]
Me	49.1	52	3
Et	55.4	57	1.6
n-Pr	62.0	62	0
n-Bu	65.4	64	-1.6

[a] $\varepsilon_{max}(1)$ and $\varepsilon_{max}(2)$ correspond to the ε_{max} of the Q_1 bands of the $Cr(RNH_2)_5Cl^{2+}$ ions and their photoproducts, respectively.

[b] $\Delta\varepsilon_{max} = \varepsilon_{max}(2) - \varepsilon_{max}(1)$.

[c] The value in parentheses corresponds to ε_{max} of the reconstructed spectrum (not shown). This spectrum appears to have slightly higher ε_{max} values than the spectrum of an isolated sample.

[d] The value in parentheses corresponds to $\Delta\varepsilon_{max}$ obtained if $\varepsilon_{max}(2)$ of the reconstructed spectrum were used.

alkylamine product/reactant and the cis-$Cr(NH_3)_4(H_2O)Cl^{2+}$/ $Cr(NH_3)_5Cl^{2+}$ pairs, consideration of contributions of trans-$Cr(RNH_2)_4(H_2O)Cl^{2+}$ as product becomes unnecessary. Although as earlier stated, it is not really possible to establish the extent of predominance of the cis-product without reliable spectra for the cis-trans pair, a lower limit of 90% predominance seems conservative.

b. For photolysis of $Cr(MeNH_2)_5Cl^{2+}$ in practically 100% acetone

Although amine substitution by acetone rather than by water is a possibility and it would certainly be of interest to ascertain the relative importance of the two solvation modes in this solvent, this is not central to the study here. Of main concern are the stereochemistry of the photoreaction and the photolysis quantum yield. The stereochemical configuration of the product may be established by inspection of the reconstructed product spectrum (Figure 19). The spectrum is consistent with a predominance of cis-$Cr(MeNH_2)_4(S)Cl^{2+}$.

The question of the importance of acetone substitution can not be unambiguously answered. Although the spectrum of the photolysis product in practically 100% acetone (Figure 19), $\lambda_{max}(Q_2) \sim 394$, $\varepsilon_{max} \sim 47$; $\lambda_{min} \sim 458$, $\varepsilon_{min} \sim 17.5$; $\lambda_{max}(\sim Q_1) \sim 530$, $\varepsilon_{max} \sim 50$) differs noticeably from that for photolysis in water (Figure 15, $\lambda_{max}(Q_2) \sim 390$, $\varepsilon_{max} \sim 47$; $\lambda_{min} \sim 450$, $\varepsilon_{min} \sim 17$; $\lambda_{max}(Q_1) \sim 522$, $\varepsilon_{max} \sim 49$), these differences might be ascribed to a combination of uncertainty in

the spectral measurements and differences in solvent effects; in lieu of going into the details of the solvent effects, it suffices to note that the spectrum of the starting material is different in the different solvents--for example, λ_{max}'s and λ_{min} are red-shifted by 4-6 nm in the acetone solvent. However, notable is that on a relative basis, the red side of the Q_1 band of the product in 100% acetone is more red-shifted (with respect to that for the starting material) than that of the corresponding product in water. The different shifts are consistent with the presence of acetone-substituted complex in 100% acetone since Dq(acetone) < Dq(H_2O). The relative thermal stability of the acetone-substituted complex, if it is formed, cannot be predicted, but considering that complexes with similar ligands such as DMF[23, 46] and DMSO[46] have been isolated, the acetone-substituted complex may be expected to have some reasonable lifetime in the solvent used. Thus the presence of acetone-substituted species cannot be unambiguously eliminated.

However, the question of whether any acetone-substituted species are present does not make the conclusion, that the product of photosolvolysis is predominantly in the cis-configuration, less obvious. As a further comment, the question of acetone-substitution might be investigated by ion-exchange chromatography of a photolysed sample of $Cr(NH_3)_5Cl^{2+}$ (in 100% acetone) using acetone solutions as eluant. Identification of any acetone-substituted species might be made by comparison of the absorption spectrum (spectra) of the photolysis product(s)

with that of cis-$Cr(NH_3)_4(H_2O)Cl^{2+}$ in 100% acetone or, alternatively, by precipitation of the eluted fractions (by evaporation of acetone(?)) and subsequent C, H and N analysis.

3. Reaction Mode and Stereochemistry

Photolysis both in water and in 33% acetone/water should involve the solvated species discussed earlier. The smallness of the chloride aquation quantum yields, together with the predominance of the cis-aquo product (from amine aquation), for each complex, is consistent with the predictions of the photolysis mode. By analogy with other systems studied (see Section I-D), aquation of the amine ligand trans to chloride, and this occurring with stereochemical change, may be expected. Thus, photolysis of the water-solvated complex ions (in water and 33% acetone/water as solvents) obeys Adamson's proposal of weak axis labilization and aquation of the strong field ligand on this axis.

Photosolvolysis of $Cr(MeNH_2)_5Cl^{2+}$ in practically 100% acetone yields predominantly cis-$Cr(MeNH_2)_4(S)Cl^{2+}$. Whether S is water or acetone (or a mixture of both) was not unambiguously established, but the product(s) is (are) predominantly cis. The chloride quantum yield was not measured in this solvent (due to experimental difficulties) but by analogy to the photolysis in water and 40% acetone/water, solvent substitution of chloride should not be important. Thus, in this solvent, photosubstitution of amine ($\Phi \sim 0.41$) may be concluded to be the predominant photoreaction mode. Although it is not possible to determine whether the substituted ligand is the one trans to the chloride or one of the in-plane groups (since the ligands are identical), the maintenance of the

stereochemistry strongly suggests that the reaction modes in the two different solvents are the same. Thus, by analogy to the systems discussed in Section I-D, it is reasonable to conclude that photolysis of $Cr(MeNH_2)_5Cl^{2+}$ in 100% acetone obeys Adamson's proposals of weak-field axis labilization and preferential substitution of the strong field ligand on that axis.

B. Amine Quantum Yields

The investigation of the photochemistry of the series of complexes was reasonably systematic. In addition to identification of the photoproducts, the wavelength and temperature dependences of the quantum yields were considered. For $Cr(MeNH_2)_5Cl^{2+}$, quantum yields were measured in water, 40% acetone and practically 100% acetone to determine the effect of solvent on both the reaction mode and stereochemistry, and the quantum yield. The reaction modes and stereochemistries have been discussed (Section IV-A). The aspects related to the magnitude of quantum yields are considered below.

1. Wavelength Dependence

The irradiations at 401, 479 and 565 nm correspond to the low energy side of the Q_2 band, and the high and low energy sides of the Q_1 band respectively. Although the Q_2 band of C_{4v} and D_{4h} Cr(III) complexes are generally split, the energy gap between the ^4E and $^4A_2$ ($^4T_{1g}$ in O_h field) states is so small that the overlap of the corresponding absorption bands is very large and any distribution of these by selective irradiation would be practically impossible. The Q_1 band, however, often does show either observable splitting or, at least, band broadening. For most Cr(III) complexes, the lower

quartet is the ^4E, which at first approximation corresponds to promotion of a t_{2g} electron (from d_{xz} or d_{yz}) to the d_z2[18, 33], while the higher $^4B_2$ state corresponds to the promotion $d_{x^2-y^2} \leftarrow d_{xy}$[18, 24].

Irradiation of the low and high energy sides of the broadened Q_1 bands of the complexes of this study should thus lead to significantly different initial distributions of the excited quartets. Although internal conversion is believed to be fast, so that all $^4B_2$ states might be quickly converted to the ^4E state, direct reaction from the $^4B_2$ state may be possible[24] (see also Section I-D). For the complexes of this study, the observable reaction modes (substitution of RNH_2) from both of these states would be the same, although there may be differences in the quantum yields and the stereochemistries. The latter would be difficult to observe unless reaction from the $^4B_2$ state competes well with internal conversion to the ^4E state. Within experimental error, the quantum yields at 479 and 565 nm are the same for all the complexes in this study. However, notable is that the quantum yields at 401 nm are consistently lower than those for irradiations at the longer wavelengths (Table VI).

That the quantum yields are slightly wavelength dependent suggests that conversion of upper excited quartets to the lowest one via internal conversion is not complete. This implies that one or more of the following processes may be competing with internal conversion to the lowest quartet:

(a) direct internal conversion to the ground state,

(b) direct chemical reaction from an upper excited quartet, and

(c) intersystem crossing to higher levels of the doublet manifold. Determination of which of these deactivation processes is (are) important must await the results of further research developments.

2. Solvent Dependence

Since photolysis in water and in 33% aqueous acetone should involve essentially the same reacting species, any differences in the amine quantum yields should be small. The differences are small (Table IV) and could be due to experimental differences associated with the analytical determinations - for example, the volumes of water and the mixed solvent delivered by the same pipette would be slightly different.

More important is a comparison of the quantum yields of $Cr(MeNH_2)_5Cl^{2+}$ in water and practically 100% acetone. The reacting species in these two solvents should be quite different, but the quantum yield of 0.41 (±5%) in acetone is only slightly different from those in water and in 33% acetone/water (0.37 and 0.39 respectively). The relative insensitivity of the quantum yield to the change of solvent for this complex is similar to that found in the studies of $Cr(CN)_6^{3-}$ in water and DMF[23] (Φ ~ 0.12 and 0.08 respectively); trans-$Cr(NH_3)_2(NCS)_4^-$ in water, methanol and nitromethane[43] (Φ ~ 0.27, 0.20 and 0.17); $Cr(urea)_6^{3+}$ in water[43] and methanol[59] (Φ ~ 0.1 and 0.15); $Cr(NH_3)_6^{3+}$ in water and DMSO[22] (Φ ~ 0.5 and 0.6); and $Cr(NH_3)_5Cl^{2+}$ in water[18, 25], 50% aqueous ethanol[60] and DMSO[22] (Φ ~ 0.37, 0.35 and 0.29). In view of these studies, the three-fold reduction of the photoracemization quantum yield of $Cr(ox)_3^{3-}$ upon changing the solvent from water to 30 mole % ethanol/water is somewhat surprising (Φ ~ 0.09 in water)[61]. The

general insensitivity of Φ to solvent effects allows one to draw the important conclusion that the photochemical reaction is determined primarily by the nature of the reacting excited state and the properties of the substituent solvent play only a minor role.

3. Temperature Dependence

The temperature dependence of Φ was studied only at 565 nm. Irradiation at 565 nm corresponds predominantly to direct excitation to vibrational levels of the lowest excited quartet, ^4E, for each complex, and hence complications due to participation of other excited quartets are largely avoided.

The reaction quantum yield, Φ_r, is a ratio of rate constants and its temperature dependence has always been considered difficult to interpret[18]. However, as a result of recent work by Chen[48], it now appears that the temperature dependence may be identified with specific processes. According to Chen's arguments (see also Section I-E-2c), a plot of $\ln[(1/\Phi_r)-1]$ vs $1/T$ will yield the difference between the activation energies of the photochemical reaction and internal conversion, $E_r - E_{ic}$. The treatment hinges on the assumption that the efficiency of the back intersystem crossing (k_{-4}, Figure 6) is nearly unity so that essentially all $^4T_{2g}$ states are deactivated through k_3 and k_r. This assumption is now supported by very recent work by Balzani and co-workers[62], where a back intersystem crossing efficiency of 1 was found for $Cr(en)_3^{3+}$ at 15°C.

It is interesting to note that $E_r - E_{ic}$ (Table V) are all positive, generally about 2 kcal. Since E_{ic} is probably positive, E_r should be positive. Therefore reaction from the photoreactive

state is not prompt but goes through an activated intermediate.

Of additional interest would be a separation of (E_r-E_{ic}) into its components since this would allow direct comparison of E_r with the activation energies of the thermal reactions of complexes with electronic configurations which are similar to those of the excited states of Cr(III) complexes (e.g. d^2 systems such as Cr(IV) and V(III)). However, such a separation requires evaluation of E_{ic} and at present, the theory of radiationless transitions is not sufficiently well understood to allow this.

4. Φ and Average Ligand Field Strength

Since the amine quantum yields are much greater than those for chloride aquation, comparisons of the total quantum yield of the series of complexes may be made by considering the amine yields directly. Since the quantum yields are slightly wavelength, temperature and perhaps slightly solvent dependent, for convenience, comparisons should be made of values obtained at a common set of conditions. The writer chose photolyses at 565 nm, 20°C and in 33% acetone. Photolyses at 565 nm are especially suitable since the irradiation corresponds predominantly to excitation to the lowest excited quartet, which is believed to be the main reactive state.

The trends of Φ_{RNH_2} (Table IV) and $\bar{\nu}_{max}$ of the $^4T_2$ band (Table VIII), both decreasing from R=H to R=n-Bu, are qualitatively consistent with Adamson's proposal that the magnitude of Φ should vary as the average ligand field strength. However, because of lack of theoretical support for this proposal, correlation of the quantum yield with other parameters should also be considered.

For the complexes of this study, a correlation of Φ with the base strength of the amine (and hence the Cr-N bond strengths of the $Cr(RNH_2)_5Cl^{2+}$ ions) was attempted. No correlation was found and this is not surprising since the photoreaction appears to be a property of the excited state and thus should not depend largely on ground state properties. An apparent correlation between Φ and ε_{max} of the Q_1 band was found and is discussed below.

If one assumes that the return intersystem crossing ($^4T_{2g} \longleftarrow {}^2E_g$) (refer to Figure 6 and see also Section I-E-2c) is very efficient so that deactivation of the excited states occurs essentially through internal conversion and chemical reaction (as suggested by Chen[48]), then the quantum yield should depend only on the relative rates of k_3 and k_r:

$$\Phi = \frac{k_r}{k_r + k_3}$$

For a series of complexes where the k_r's are similar, then Φ should decrease with increase in k_3. From theory, k_3 should vary as the integrated intensity, $\int \varepsilon d\bar{\nu}$, of the absorption band corresponding to the decaying state, and for the complexes of this study, k_3 should be roughly proportional to ε_{max} of the Q_1 band. The trend of increasing ε_{max} from R=H to R=n-Bn (Table VIII) is thus consistent with the decreasing Φ for the same ordering of complexes. The comparison was made under the assumption that the reaction rates, k_r, are the same for the complexes. The correlation is only a qualitative one and apparently does not give the correct quantitative ordering of the quantum yields in that the observed large change in Φ is between R=Me and R=Et, whereas the expected

one (on the basis of ε_{max}) is between R=H and R=Me.

Extension of the comparison of Φ with ε_{max} of the Q_1 band to other complexes would be dangerous since the correlation observed here is probably due to the very similar properties of the complexes and their reactions. For example, the importance of the relative efficiency of the thermal repopulation of the $^4T_2$ state ($^4T_2 \longleftarrow {}^2E$) obviously depends very much on the energy spacing between the two states. For the series of complexes studied, this energy spacing should be practically constant, but this need not be so for other complexes. An extreme example is that of $Cr(CN)_6^{3-}$, where sensitization of its phosphorescence ($^2E_g \longleftarrow {}^4A_{2g}$) by $Ru(dipy)_3^{2+}$ failed to sensitize reaction[63]. Since reaction very probably occurs via the lowest quartet[23], this implies (in addition to the non-reactivity of the ^2E_g state) a zero efficiency of repopulation of the reactive state - this being consistent with the extremely large energy separation (>20 kcal/mole) between the two states in $Cr(CN)_6^{3-}$[23].

C. Chloride Quantum Yields

1. General Comments

The chloride quantum yields (Table VI) for all the complexes are rather low compared to the values reported earlier for $Cr(NH_3)_5Cl^{2+}$ (Table I). Although the values obtained for this particular ion are relatively imprecise (because the rate of the thermal chloride aquation is much larger than that for the photolytic aquation) the estimated upper limits are apparently an order of magnitude smaller than those reported by Wasgestian and

Schlafer[25] (5×10^{-3} at 546 nm) and about two orders of magnitude smaller than those by Balzani, et al[18] (4×10^{-2} at 506 nm).

The disagreement in the magnitude of the chloride quantum yields can be ascribed at least partly to errors in the earlier work. In the study by Balzani and co-workers[64], the thermal chloride aquation of the major photoproduct, cis-$Cr(NH_3)_4(H_2O)Cl^{2+}$, arising from amine loss, was not accounted for. Since the first-order chloride aquation rate for cis-$Cr(NH_3)_4(H_2O)Cl^{2+}$ is greater than that for $Cr(NH_3)_5Cl^{2+}$[7, 25] (near room temperature and at pH 3) and that for the former increases with increase in pH[7], thermal chloride release due to cis-$Cr(NH_3)_4(H_2O)Cl^{2+}$ would be very significant at the photolysis conditions (15°C and pH 7) used. However, Wasgestian and Schlafer accounted for the thermal chloride contribution in their study[25]. They treated the problem by assuming that all the light quanta were delivered instantaneously at a time t_x, taken to be $(t_s + t_e)/2$, where t_s and t_e correspond to the start and end of the photolysis period. Thus, at $t < t_x$, increase in $[Cl^-]$ is due only to thermal decomposition of the starting material (Reaction 8) and at $t_x < t < t_e$, increase in $[Cl^-]$ is due to photolytic chloride release (Reaction 7) and Reactions 8 and 9. Although the choice of t_x is not precisely correct because the increase in concentration of photoproduct (and the concurrent decrease in concentration of starting material) is not strictly linear (especially at the high conversions, ~30%, used), the error incurred would not be large (in the order of 10%). More important is that these authors used a monochromator rather than an interference filter for obtaining light of the desired energy.

Monochromators are likely to transmit some stray light so that a possible explanation for their larger chloride quantum yields is that a small fraction of the irradiating light was stray light of shorter wavelengths (<300 nm); this light results in excitation to CT states of $Cr(NH_3)_5Cl^{2+}$ where chloride aquation is very efficient (Φ = 0.23 at 250 nm)[25]. Verification of this is not possible without further details of Wasgestian and Schlafer's experimental techniques.

That the estimated upper limits for Φ_{Cl^-} for $Cr(NH_3)_5Cl^{2+}$ (3×10^{-4} at 565 nm) are reasonable can be verified by comparison with those measured for the other chloropentaamine complexes. The determinations of the photolytically released chloride are more reliable for these latter complexes since interference due to the initial dark reaction is much less severe. The generality of the smallness of the quantum yields (as compared to reported values for $Cr(NH_3)_5Cl^{2+}$) for the whole series of complexes indicates that the upper limits for $Cr(NH_3)_5Cl^{2+}$ are conservative.

It should be emphasized that even for the alkylamine complexes, the chloride yields are upper limits determined assuming no thermal chloride aquation of the major photoproduct, cis-$Cr(RNH_2)_4(H_2O)Cl^{2+}$. Although corrections may be applied for these determinations, they are not altogether warranted since the quantum yields obtained for photolysis at 565 nm are near the limits of the measuring techniques. It suffices to note that the true quantum yields, at this wavelength, are much smaller than had been believed previously.

Note that in all cases, the Φ at 401 nm is significantly

higher than that at 565 nm and a significant portion, Φ_{corr}, must be real. Therefore although the absolute quantum yields seem to differ significantly from those reported earlier for $Cr(NH_3)_5Cl^{2+}$[18, 25], the trend of increasing Φ_{Cl^-} at shorter wavelengths is the same.

2. Magnitude of Φ_{Cl^-} and the Role of Charge Transfer States

With reference to the suggestion that chloride photoaquation of $Cr(NH_3)_5Cl^{2+}$ (and similarly, bromide photoaquation of $Cr(NH_3)_5Br^{2+}$) occurs from CT state(s)[25, 26], the smaller halide (X^-) yields measured in this work are significant. Assuming chloride aquation occurs via CT states, in particular, those corresponding to X——> Cr(III), then upon irradiation in the ligand field (LF) region, the quantum yield should depend on both the intrinsic reactivity of the CT state and the relative extinction coefficients of the absorption corresponding to the CT and LF states at the irradiating wavelength. For example, if $\Phi_{X^-} = 0.2$ upon excitation solely to the CT state, then if upon LF irradiation, only one percent of the total excited molecules produced are CT states, Φ_{X^-} would be reduced to 2×10^{-3}. (Excitation to CT states upon LF irradiation is presumably due to the mixing with the tail of the intense CT band, whose absorption maximum lies at shorter wavelengths). The suggestion of X^- photoaquation of the Cr(III) complexes occurring via CT states may be compared to the case of photoreduction of Co(III) to Co(II) in Co(III) complexes, where, photoreduction (and perhaps also aquation) presumably occurs from CT states. Whereas the d-d absorption bands of analogous Cr(III) and Co(III) complexes occur at similar energies, the low energy CT

band, X ——> M(III), for halopentaamine M(III) complexes, occurs at lower energy for the Co(III) complexes (see Ref. 65) and thus overlaps with the d-d bands to a greater extent. For the Co(III) complexes, the decrease in photoreduction quantum yield, Φ_{red}, going from CT to LF irradiation is quite dramatic-- for example, for $Co(NH_3)_5Br^{2+}$, Φ_{red} is 0.15 at 370 nm and 10^{-4} at 520 nm. The earlier reported decreases in Φ_x, going from CT to LF irradiation, is much less dramatic: 0.23 at 250 nm and 5×10^{-3} at 546 nm for $Cr(NH_3)_5Cl^{2+}$[25] and; 0.26 at 250 nm and 9×10^{-3} at 546 nm for $Cr(NH_3)_5Br^{2+}$[26]. On the basis of X^- photoaquation occurring from CT states, the Φ_x's for the Cr(III) complexes should be smaller than the photoreduction quantum yields for the analogous Co(III) complexes. Thus the reported Φ_x's[25, 26] seem too large. The chloride quantum yields measured for the series of complexes in this work are more in line with the expected yields and thus lend better support to the suggestion of X^- aquation occurring via CT states.

As a further comment, although reaction from CT states requires a general decrease in Φ_{Cl^-} upon irradiation at progressively longer wavelengths for a particular complex, there is no reason to expect any trend of Φ_{Cl^-} between different complexes upon irradiation at a constant wavelength, since Φ_{Cl^-} depends on both the extent of overlap of the CT and LF bands and the intrinsic reactivity of the reacting CT state. The Φ_{Cl^-} values for each $Cr(RNH_2)_5Cl^{2+}$ ion (Table VI) are consistent with the decrease in CT population at longer wavelengths. The similarity of the quantum yields at 401 nm, for photolysis of the alkylamine complexes in 33% acetone, may be accidental.

3. Solvent Effects on Φ_{Cl^-}

The decrease in Φ_{corr} (401 nm) going from photolysis in water to 33% acetone/water as solvent, observed for both $Cr(MeNH_2)_5Cl^{2+}$ and $Cr(EtNH_2)_5Cl^{2+}$, has important implications. Langford and Tipping suggested that the large reduction in Φ_{Cl^-} of $Cr(RNH_2)_5Cl^{2+}$, R=H, Me and Et, (Φ_{Cl^-}=0.04 in water and less than 10^{-3} in DMSO for R=H) upon changing the photolysis medium from water to DMSO[23] supports their model of tetragonal distortion of the $^4T_2$ state, the extent of distortion presumably being solvent dependent. However, their comparison suffers since they assumed a value of 0.04 (506 nm) for the chloride quantum yield for $Cr(NH_3)_5Cl^{2+}$[18] in water and that Φ_{Cl^-} is similar for the analogous alkylamine complexes. Since it now seems that Φ_{Cl^-} in water is less than 10^{-3} (565 nm) for all these complexes, it is apparent that their comparison is not a fair one. Thus their Φ_{Cl^-}'s of less than 10^{-3} in DMSO (presumably upon Q_1 irradiation) are not necessarily different from those for photolysis in water. Furthermore, it should be noted that chloride substitution was assumed to occur via the excited quartet; there is no experimental proof for this.

The decrease in Φ_{Cl^-} going from water to a solvent of lower dielectric constant (of particular interest here is 33% acetone) may be qualitatively explained on the basis of reaction from the Cl ——> Cr(III) charge transfer states. Upon CT excitation, the electron distribution is changed so that formally, the metal center becomes Cr(II). The excited state molecule may be compared to the Cr(II) and Mn(III) d^4 systems which are very labile. However, since

the excitation to the CT state is allowed, the reverse non-reaction relaxation processes would be very fast. The effectiveness of the competing deactivation via chemical reaction would thus depend on the ability of the solvent to effectively displace the chloride by solvation. Generally, the solvation energy of ions decrease with a decrease in the dielectric constant of the solvent[66]. Thus solvation of chloride should be less effective in 33% acetone than in water, and the quantum yield (Φ_{Cl^-}) of reaction should be smaller. Since other factors should be approximately constant, the solvation factor would lead to reduced Φ_{Cl^-} values in the mixed solvent.

D. Summary

It has been shown that upon ligand field excitation in water and in 33% acetone/water as solvents, amine aquation to yield predominantly cis-$Cr(RNH_2)_4(H_2O)Cl^{2+}$ (a lower limit of 90% cis was estimated) is the predominant reaction mode for each of the $Cr(RNH_2)_5Cl^{2+}$ ions. Analogy to systems studied earlier indicated that the observed reaction is consistent with aquation of the strong field ligand on the weak field axis and the generally observed phenomenon of stereomobility.

Photolysis of $Cr(MeNH_2)_5Cl^{2+}$ in practically 100% acetone resulted in amine substitution (Φ= 0.41) to give a product, $Cr(MeNH_2)_4(S)Cl^{2+}$, whose configuration is predominantly cis. Whether acetone substitution occurred was not unambiguously established. The similarity of the reaction mode, quantum yield and stereochemistry to photolysis in water suggests that substitution of the strong field ligand on the weak field axis also occurs in this solvent. Since

Adamson's rules were proposed for photochemical reactions of Cr(III) complexes in water, the photochemical results of $Cr(MeNH_2)_5Cl^{2+}$ in acetone represent an extension of the validity of these rules. To the author's knowledge, this is the first observation of the stereochemistry of photoreactions in non-aqueous solvents. Thus this study serves as ground-work for further investigations. The maintenance of the stereochemistry of the reaction and the magnitude of Φ_{RNH_2} suggests that similar reaction mechanisms are operative in the different solvents. The importance is apparent since it implies that the important step in the reaction is bond-breaking (rather than bond-making).

Adamson's proposal that Φ should vary as the average ligand field strength was tested. The trend of Φ_{RNH_2} for photolysis of $Cr(RNH_2)Cl^{2+}$ in 33% acetone/water, at 565 nm and 20°C-- 0.41_4 (NH_3) 0.39_3 ($MeNH_2$), 0.23_7 ($EtNH_2$), 0.21_2 (n-$PrNH_2$) and 0.17_6 (n-$BuNH_2$)-- is consistent with this proposal. The relative magnitude of Φ_{RNH_2} was also considered in terms of the competition between reaction, k_r, and internal conversion, k_3, assuming that these two processes are the main paths of deactivation of the reacting quartet and that k_r is the same for the series of closely related complexes. Since k_3 is roughly proportional to ε_{max} of the Q_1 band, it increases from R=H to R=n-Bu (Table VIII) and is consistent with the decrease of Φ_{RNH_2} (or total quantum yield) in the same order.

The limited study of the temperature dependence showed that, for the temperature range 5-20°C, there is a general increase of Φ_{RNH_2} with temperature for all the complexes studied. Within experimental

error, all the apparent activation energies are about 1.5 kcal/mole (Table V). The temperature dependence was also considered in terms of Chen's treatment[47], where a plot of $\ln[1/(1-\Phi)]$ vs $1/T$ should yield the difference between the activation energies of the photochemical reaction and internal conversion processes of the photoreactive state (presumably the lowest excited quartet). These latter values, $E_r - E_{ic}$ (Table V), are approximately 2 kcal/mole for each of the complexes studied. E_r is apparently positive and thus suggests that photoreaction occurs via an activated intermediate.

The quantum yields for photoaquation of chloride,

$$Cr(RNH_2)Cl^{2+} + h\nu + H_2O \longrightarrow Cr(RNH_2)_5(H_2O)^{3+},$$

were determined for completeness. Generally, only upper limits were obtained, but in comparison to values reported earlier for $Cr(NH_3)_5Cl^{2+}$ (0.04[18] and 0.005[25] for Q_1 irradiation) these limits (3×10^{-4} at 565 nm) are surprisingly low. In view of the proposal that photoaquation of chloride for $Cr(NH_3)_5Cl^{2+}$ and that of bromide for $Cr(NH_3)_5Br^{2+}$ occur through CT states, a comparison of the quantum yields for these reactions with those for the photoreduction of Co(III) to Co(II) (which apparently also occurs via CT states) indicates that the lower quantum yields obtained in this work are more reasonable. Conversely, the smallness of these quantum yields supports the proposal of chloride aquation occurring from CT states.

V. SUGGESTIONS FOR FURTHER WORK

The detailed mechanistic aspects are an essential part of the study of the photoreactions. The photoaquations arising from ligand field excitation appear to occur with stereochemical change and although the extent of stereochemical change appears to be large (>90%) for a number of complexes so that proposal of an associative intermediate[30] for reaction is not unreasonable, elimination of a dissociative intermediate, such as one with a trigonal bipyramidal structure, is difficult[34]. To do so would require a 100% predominance for the product resulting from reaction with stereochemical change. Establishment of such a predominance is practically not possible using difference spectrophotometry. However quantitative measurement of the extent of predominance for the formation of a particular product is possible if the ion exchange chromatographic system described in Section II-D were used. Experiments of this type would require careful choices of complexes since problems associated with thermal decomposition and ease of separation of the photolysed complex mixture must be overcome.

One area that has not been explored is the mechanism of the photoreaction arising from CT excitation. Of particular interest would be experiments where both the reaction mode and the stereochemistry may be observed - for example with complexes such as <u>trans</u>-$Cr(en)_2XY^{n+}$ (XY= F_2, Cl_2, $(NCS)_2$, ClF, (NCS)Cl, etc.). Since CT excitation results in a significant change redistribution between the central metal atom

and a ligand, homolytic fission of the Cr-L bond is a distinct possibility. Reactions of such excited states might be expected to occur via a dissociative intermediate. It is interesting to note that complete hydrolysis of the chromium complex, as a result of excitation to L ——> Cr CT states has not been observed. This implies that the lifetime(s) of reactive CT state(s) are extremely short since the metal center is formally Cr(II) in such a state and Cr(II) complexes are extremely labile.

The question of the preferential aquation mode has been reopened since the photochemistry of trans-$Cr(en)_2FCl^{+}$[34] appears not to obey Adamson's rules. The anomalous behaviour of this complex might be considered in terms of π-bonding effects. Notice that Linck's proposed orderings of ligands, in order of leaving ability[34]

$$NH_3 > OH_2 > Cl^- \simeq NCS^- > F^-$$

$$NH_3 > Br^- > F^-$$

is consistent with an increase in π-donor ability for the same orderings. It would be interesting to study other similar complexes where such π-donation might be important (e.g. trans-$Cr(en)_2(CN)F^{+}$, trans-$Cr(en)_2(CN)Cl^{+}$, etc.).

Finally a natural extension of this work concerning solvent effects is further studies in a larger variety of solvents. Of particular interest would be studies in strong field solvents such as ammonia; however studies in other reactive solvents or even non-reactive solvents, and solvent mixtures might also yield valuable information on the nature of the reaction mechanism. Also a study of solvents effects on the photoreactions originating from CT states would

be of interest since this would directly test the proposal (Section IV-C-3) that the quantum yield decreases with the dielectric constant of the solvent.

VI. DISCUSSION OF ERRORS

The quantum yields for amine photoaquations were generally reproducible to about 2-3% for photolysis at a particular set of experimental conditions. Because reineckate actinometry was used for light flux measurements, the quantum yields are all relative to those reported for reineckate. Thus small quantum yield variations on varying the exciting wavelength may not be real. However, quite small variations in quantum yield with temperature must be real.

The accuracy of the quantum yields depend on the validity of some of the assumptions made, both for the actinometer and photolysis systems. These are discussed below.

A. Light Intensity

In the determination of light intensity by simultaneous photolysis of a reineckate solution, the following assumptions were made:

1. The changes of the absorbances of the front and actinometer solutions are small, so that $10^{-\varepsilon_a cl}$ and $10^{-\varepsilon_b cl}$ are essentially constant (refer to Section II-E).
2. The quantum yield for NCS^- release is about the same for reineckate as for its primary photoproduct, so that no correction for the decrease in concentration of reineckate ion is necessary.
3. All the light passing the front photolysis solution goes through the actinometer solution, namely, reflection of light at the water/quartz interfaces is neglected.

The first assumption is valid since the extinction coefficients of the starting material and photoproduct are not vastly different, and more important, the conversion of the starting material is usually quite small (<6% for the photolysis solution and <4% for the reineckate actinometer).

The validity of the second assumption is not directly verifiable. However, for the photoproducts of reineckate ion,

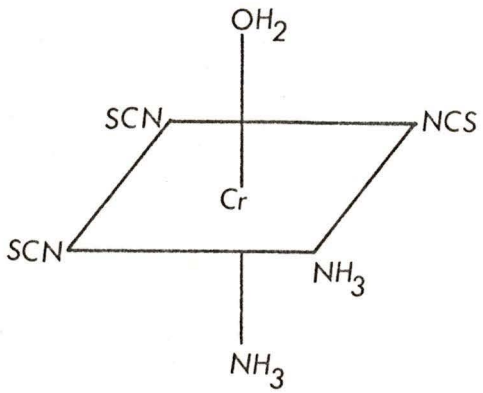

I

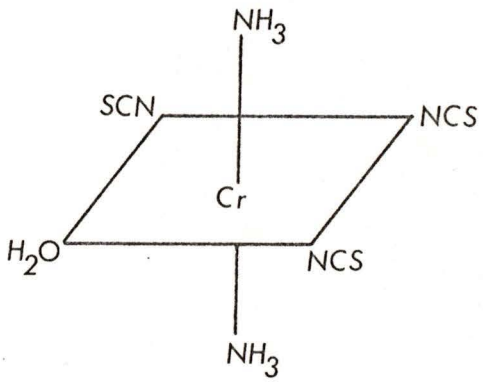

II

(assuming aquation occurs with stereochemical change), preferential aquation of the strong field ligand on the weakest field axis would result in NCS^- aquation being the predominant photoreaction, overall. Complex I would aquate NCS^- practically exclusively, but II might aquate NCS^- and/or H_2O since $Dq(NCS^-)$ is just slightly greater than $Dq(H_2O)$. In addition, assuming Adamson's rule for predicting the relative magnitude of Φ on the basis of average ligand field strength, Φ for each of the products should be about the same as for reineckate ion. Therefore the second assumption should not lead to objectionably

large errors and its use would probably result in more correct light flux values than if secondary photolysis were assumed to be negligible.

Considering the third assumption, the fraction of a beam reflected at an interface may be expressed by Fresnel's Law:

$$\frac{I_n}{I_o} = \left(\frac{n_{21} - 1}{n_{21} + 1}\right)^2$$

where n_{21} is the ratio of the refractive indices of the two media. For a quartz/water interface ($n_{quartz} \sim 1.47$ and $n_{water} \sim 1.34$ near the irradiatory wavelengths and temperatures of interest), the reflected fraction is very small (~0.2%) and is insigificant at the precision level of photochemical data. The validity of this assumption was also checked by carrying out several photolysis/actinometer runs with reineckate solutions in both cells. The light flux calculated from the photolytically released NCS^- from both solutions agreed to within 2% (5 runs).

B. The Inner Filter Effect

The inner light filter effect arises from the fact that the photoproduct, once it is formed, contributes to the absorbance of the photolysis solution and hence acts as an inner light filter[51]. The effect may become important for those cases where the extinction coefficient for the product is significantly larger than that of the reactant and when the conversion is relatively high.

When reineckate actinometry is carried out as described in the experimental section, the effect would be important whenever the absorbance of the solution changes significantly since the amount of light entering the actinometer solution is proportional to the

transmittance of the front photolysis solution. The following considerations attempt to justify the neglect of the inner filter effect in the quantum yield calculations for the complexes studied in this work.

The extinction coefficients for the reactants and the corresponding products, at the irradiating wavelengths, are not vastly different, and together with the low conversions, the absorbance of the solution and, more so the transmittance, changes very little during a photolysis experiment. Thus, the fraction of the light beam passing this solution and reaching the actinometer is practically constant. Also, since the fraction of the light beam absorbed, $(1 - 10^{-\varepsilon cl})$, is less sensitive to change than the absorbance, $A = \varepsilon cl$, the fraction of light absorbed by the reactant decreases less rapidly than the decrease in concentration due to photolysis. For example, for a complex with $\varepsilon = 30$ at the irradiating wavelength, a 1.0×10^{-2} M solution will have an absorbance of 0.30 and at 5% conversion, the absorbance of the reactant is decreased by 5%, but $(1 - 10^{-\varepsilon cl})$ decreases by only 3.6%. changing from 0.499 to 0.481. In addition, if the photoproduct is also photoreactive and if the reaction mode is the same as for the initial reactant (with respect to the analytical method)--as is expected for the complexes studied in this work--then corrections must be further diminished. In light of these considerations, the absolute errors due to the presence of photolysis products are expected to be small for low conversions--and the relative errors are even smaller-- and may be considered to be negligible at the level of precision attainable.

C. Non-Linearity of Photolysis Rate Plots

Generally, quantum yield calculations were made assuming that the change of concentration, of reactant or product, is linear with time. The assumption is valid if the extent of conversion is low (see below), but can lead to significant errors at high conversions. Two cases may be considered.

If the solution is totally absorbing and only the reactant absorbs, then photolysis is first order, and assuming no decomposition of the photoproduct,

$$C_{product} = A_o (1 - e^{-k_o t})$$

where $C_{product}$ is the concentration of photoproduct, A_o is the initial concentration of reactant, t is the photolysis time and k_o is the pseudo first order rate constant ($k_o = F_o \Phi f_a$, where f_a is the fraction of the light beam absorbed and is equal to 1 in this case). Curve A of Figure 23 is the concentration versus time plot constructed for $k_o = 5.0 \times 10^{-5}$ sec^{-1} and $A_o = 1.0 \times 10^{-2}$M (both chosen arbitrarily) and shows that linearity is approximately followed for the first 10% of photolysis.

The second case applies to solutions which are not totally absorbing, as were those in the experiments carried out in this work. For these solutions the fraction of the light beam absorbed by the reactant decreases with the photolysis time so that k decreases as photolysis progresses. Curve B of Figure 23 is the concentration versus time plot where k was chosen to decrease linearly from 5.0×10^{-5} to 4.5×10^{-5} sec^{-1} over 5000 sec ($kt = k_o t - 1.0 \times 10^{-9} t^2$). Although the choices of k, k_o and a_o are arbitrary, the example is not unlike a real case. The plot follows curve A rather closely up to 5% conversion,

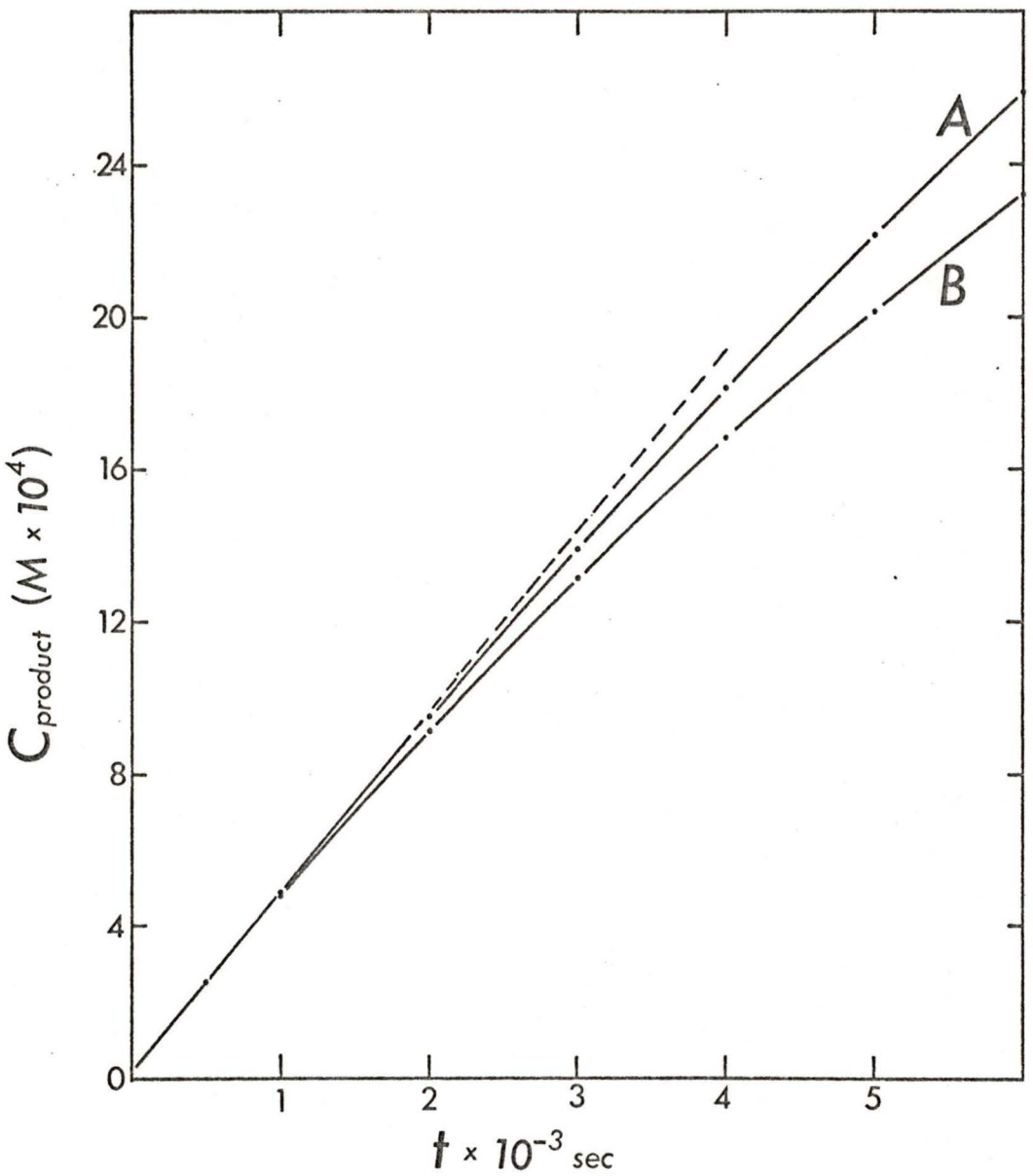

Figure 23. Plots of product concentration versus photolysis time: A, where the reactant solution is totally absorbing; B, where the solution is not totally absorbing.

deviations being greater than 2% past this point. However even for this worse situation, linearity is approximately followed for the first 8% of photolysis. Thus, since conversions were usually under 5% (for Φ_{RNH_2} determinations), the assumption of linearity for the photolysis rate was valid.

VII. BIBLIOGRAPHY

1. D. S. McClure, in *Advances in the Chemistry of Coordination Compounds*, (S. Kirsher, ed.), MacMillan, New York (1961) p. 498.

2. C. Furlani, *Coord. Chem. Rev.*, 1, 51(1966).

3. T. M. Dunn, in *Modern Coordination Chemistry*, (J. Lewis and R. C. Wilkins, ed.), Interscience, New York (1961) p. 248.

4. A. W. Adamson, *J. Inorg. Nucl. Chem.*, 28, 1955(1966).

5. H. L. Schlafer, H. Gausman and H. Witzke, *J. Chem. Phys.* 46, 1423(1967).

6. F. Basolo and R. G. Pearson, *Mechanisms of Inorganic Reactions*, John Wiley and Sons, New York (1967).

7. D. W. Hoppenjans, J. B. Hunt and C. R. Gregoire, *Inorg. Chem.*, 7, 2506(1968).

8. S. T. Spees Jr., J. R. Perumareddi, and A. W. Adamson, *J. Am. Chem. Soc.*, 90, 6626(1968).

9. N. A. P. Kane-Maguire and C. H. Langford, *J. Am. Chem. Soc.*, 94, 2125(1972).

10. S. T. Spees and A. W. Adamson, *Inorg. Chem.*, 1, 531(1962).

11. A. W. Adamson, *J. Inorg. Nucl. Chem.*, 13, 275(1960).

12. A. W. Adamson, *Advances in Chem. Ser.* No. 49, 237(1965).

13. P. Riccieri and E. Zinato, Proceedings of the XIV I.C.C.C. Toronto, 252(1972).

14. A. D. Kirk, *Mol. Photochem.*, 5, 127(1973).

15. M. R. Edelson and R. A. Plane, *J. Phys. Chem.*, 63, 327(1959).

16. H. L. Schlafer, *Z. physik Chem. Frankfurt.*, 11, 65(1957).

17. D. Valentine, Jr., *Advances in Photochemistry*, (W. A. Noyes, Jr., et al, ed.), Interscience, New York (1968) vol. 6, p. 123.

18. V. Balzani and V. Carassiti, *Photochemistry of Coordination Compounds*, Academic Press, New York (1970), Chapter 7.

19. A. W. Adamson, *J. Phys. Chem.*, 71, 798(1967).

20. A. W. Adamson, *Coord. Chem. Rev.*, 3, 169(1968).

21. S. Chen and G. B. Porter, *Chem. Phys. Lett.*, 6, 41(1970).

22. C. H. Langford and L. Tipping, *Can. J. Chem.*, 50, 887(1972).

23. H. F. Wasgestian, *J. Phys. Chem.*, 76, 1947(1972).

24. M. T. Gandolfi, M. F. Manfrin, L. Moggi and V. Balzani, *J. Am. Chem. Soc.*, 94, 7152(1972).

25. H. F. Wasgestian and H. L. Schlafer, *Z. phys. Chem. Frankfurt*, 57, 282(1968); ibid, 62, 127(1968).

26. P. Riccieri and H. L. Schlafer, *Inorg. Chem.*, 9, 727(1970).

27. E. Zinato, R. D. Lindholm and A. W. Adamson, *J. Am. Chem. Soc.*, 91, 1076(1969).

28. J. K. Zink, *J. Am. Chem. Soc.*, 94, 8039(1972).

29. M. F. Manfrin, L. Moggi and V. Balzani, *Inorg. Chem.*, 10, 207(1971).

30. A. D. Kirk, K. C. Moss and J. G. Valentin, *Can. J. Chem.*, 49, 1524(1971).

31. C. Kutal and A. W. Adamson, *J. Am. Chem. Soc.*, 93, 5581(1971).

32. P. Riccieri and E. Zinato, to be published.

33. S. C. Pyke and R. G. Linck, *J. Am. Chem. Soc.*, 93, 5281(1971).

34. G. Wirth and R. G. Linck, to be published.

35. A. D. Kirk, K. C. Moss and J. G. Valentin, *Can. J. Chem.*, 49, 375(1971).

36. A. Chiang and A. W. Adamson, *J. Phys. Chem.*, 72, 3827(1968).

37. M. R. Edelson and R. A. Plane, *Inorg. Chem.*, 3, 231(1964).

38. R. A. Plane and J. P. Hunt, *J. Am. Chem. Soc.*, 79, 3343(1957).

39. J. Valentin, M. Sc. Thesis, University of Victoria, 1970.

40. A. Rogers and P. J. Staples, *J. Chem. Soc.*, 6832(1965).

41. M. Parris and W. J. Wallace, *Can. J. Chem.*, 47, 2257(1969).

42. W. Geis and H. L. Schlafer, *Z. physik. Chem. Frankfurt*, 65, 107.

43. A. W. Adamson and E. Wegner, *J. Am. Chem. Soc.*, 88, 394(1966).

44. M. F. Manfrin, M. T. Gandolfi, L. Moggi and V. Balzani, in press.

45. J. C. Jayne and E. L. King, *J. Am. Chem. Soc.*, 86, 3989(1964); D. W. Kemp and E. L. King, ibid, 89, 3433(1967).

46. D. A. Palmer and D. W. Watts, *Australian J. Chem.*, 20, 53(1967); ibid, 21, 2895(1968).

47. C. H. Langford, *J. Chem. Educ.*, 46, 557(1969).

48. S. C. Chen, Dissertation, University of British Columbia, 1970.

49. Von M. Linhard and M. Weigel, *Z. anorg. alleg. Chemie*, 299, 15(1959).

50. V. Balzani, private communication.

51. R. C. Weast, ed., *Handbook of Chemistry and Physics*, 52nd edition, The Chemical Rubber Co. (1972), D-182.

52. J. Lee and H. H. Seliger, *J. Chem. Phys.*, 40, 519(1964).

53. H. F. Wasgestian and H. L. Schlafer, *Ber. Bunsenges, Physik, Chem.*, 71, 489(1967).

54. C. S. Garner and D. A. House, in *Transition Metal Chemistry*, (R. L. Carlia, ed.), Marcel Dekker, New York (1970), vol. 6, p. 59.

55. J. R. Perumareddi, *Coord. Chem. Rev.*, 4, 73(1969).

56. M. Parris and N. F. Feiner, *Inorg. Nucl. Chem. Letters*, 3, 337(1967).

57. Although the complexes with bidentate ligands have trigonal rather than octahedral symmetry, the ligand field symmetry is essential octahedral.

58. Ref. 18, Chapter 3.

59. D. R. Stranks and G. J. Weston, Proc. I.C.C.C. London (1959), p. 164.

60. E. Zinato, P. Tulli and P. Riccieri, *J. Phys. Chem.*, 75, 3504(1971).

61. S. T. Spees and A. W. Adamson, *Inorg. Chem.*, 1, 531(1962).

62. V. Balzani, et al, to be published.

63. N. Sabbatini and V. Balzani, *J. Am. Chem. Soc.*, 94, 7587(1972).

64. M. F. Manfrin, L. Moggi and V. Balzani, *Inorg. Chem.*, 10, 207(1971).

65. Ref. 18, Chapter 11.

66. N. A. Izmailov, *Zhur. Fiz. Khim.*, 34, 2414(1960).

VIII. APPENDIX

A. Franck-Condon Principle

The Franck-Condon Principle states that *electronic transitions are so fast (10^{-15} sec) in comparison to nuclear motions (10^{-12} sec), that the relative positions and kinetic energies of the nuclei do not change appreciably during a transition.* Thus referring to Figure 6, electronic transitions occur vertically (constant internuclear distances). If the potential energy curves for the upper and lower states have similar shapes and nuclear configurations (e.g. $^4A_{2g}$ and ^2E_g), the upward transitions, which normally occur from the zeroth vibrational level of the lower state, will be sharp. When the equilibrium configurations of the states are quite different, as for the $^4A_{2g}$ and $^4T_{2g}$, electronic excitation will result in high vibration levels of the upper state. Similar arguments are obviously also appropriate in discussing the deactivation processes.

B. Some Details of the Ion-Exchange Chromatographic Resin and Eluants

Baker analysed strong cation resin CGC 241, 200-400 mesh, was used for the chromatography work described in Section II-D. Before use, the resin was soaked in water and sifted through a 200 mesh screen. This removed all the larger beads, some of which were black, and gave a more homogeneous yellow resin. Since it was found that washing the column with strong (1-2 M) NaCl solution resulted in a slow leaching of some yellow (soluble) material, the resin was carefully washed with

strong acid, and the strong NaCl solutions (1-2 M) before using it for the chromatographic separations.

The NaCl solutions used as eluant were made up in 10^{-3}M HCl to eliminate the possibility of solutions becoming basic. For separations, the Autograd was filled, in an appropriate way, with solutions of increasing NaCl concentration to give a positive concentration gradient (usually 1-2 M). The concentration gradient depended on the volumes and the solution concentrations used and, obviously, also on the rate the eluant was pumped through the column. Although the pumping rate may be varied, it was normally kept at the maximum of 162 ml/hour.

For oxidation of the column eluant, solutions of 0.5% (0.15 M) H_2O_2 in 10^{-2}M HCl and 0.5 M NaOH were mixed with the column eluant, with added air bubbles, in volume ratios of approximately 1.3:1.3:1.0:0.4. The ratios are determined by the diameter of the pumping tubes; the corresponding tubing diameters used were 0.065, 0.065, 0.056 and 0.035 mm.

VITA

Surname: WONG Given Names: CARL FOOK CHOW

Place of Birth: CHINA Date of Birth: July 10, 1948

Educational Institutions Attended, with Dates of Entering and Leaving:

UNIVERSITY OF VICTORIA	1967 to	1973
	____ to	____
	____ to	____
	____ to	____

Degrees, Diplomas, Etc., Awarded, with Dates and Names of Institutions:

B.Sc.(Honors)	1971	University of Victoria
	____	
	____	
	____	

Honors and Awards:

Government of B.C.- Second Class Scholarships, 1970/71, 1969/70 and 1968/69

Government of B.C.- First Class Scholarship, 1967/68

Publications:

PARTIAL COPYRIGHT LICENSE

I hereby grant the right to lend my thesis or dissertation (the title of which is shown below) to users of the University of Victoria Library, and to make *single copies only* for such users or in response to a request from the library of any other university, or similar institution, on its behalf or for one of its users. I further agree that permission for extensive copying of this thesis for scholarly purposes may be granted by me or a member of the University designated by me. It is understood that copying or publication of this thesis for financial gain shall not be allowed without my written permission

Title of Thesis/Dissertation

PHOTOCHEMISTRY OF THE

CHLOROPENTAKIS(ALKYLAMINE)CHROMIUM(III) COMPLEXES

Author [redacted]

CARL WONG
Name

Date